



National Library
of Canada

Bibliothèque nationale
du Canada

Canadian Theses Service

Services des thèses canadiennes

Ottawa, Canada
K1A 0N4

CANADIAN THESES

THÈSES CANADIENNES

NOTICE

The quality of this microfiche is heavily dependent upon the quality of the original thesis submitted for microfilming. Every effort has been made to ensure the highest quality of reproduction possible.

If pages are missing, contact the university which granted the degree.

Some pages may have indistinct print especially if the original pages were typed with a poor typewriter ribbon or if the university sent us an inferior photocopy.

Previously copyrighted materials (journal articles, published tests, etc.) are not filmed.

Reproduction in full or in part of this film is governed by the Canadian Copyright Act, R.S.C. 1970, c. C-30.

**THIS DISSERTATION
HAS BEEN MICROFILMED
EXACTLY AS RECEIVED**

AVIS

La qualité de cette microfiche dépend grandement de la qualité de la thèse soumise au microfilmage. Nous avons tout fait pour assurer une qualité supérieure de reproduction.

S'il manque des pages, veuillez communiquer avec l'université qui a conféré le grade.

La qualité d'impression de certaines pages peut laisser à désirer, surtout si les pages originales ont été dactylographiées à l'aide d'un ruban usé ou si l'université nous a fait parvenir une photocopie de qualité inférieure.

Les documents qui font déjà l'objet d'un droit d'auteur (articles de revue, examens publiés, etc.) ne sont pas microfilmés.

La reproduction, même partielle, de ce microfilm est soumise à la Loi canadienne sur le droit d'auteur, SRC 1970, c. C-30.

**LA THÈSE A ÉTÉ
MICROFILMÉE TELLE QUE
NOUS L'AVONS REÇUE**

THE UNIVERSITY OF ALBERTA

PERFORMANCE EVALUATION OF A THERMOSYPHON AIR HEATING SYSTEM

by

© QIQIU ZHAO

A THESIS

SUBMITTED TO THE FACULTY OF GRADUATE STUDIES AND RESEARCH
IN PARTIAL FULFILMENT OF THE REQUIREMENTS FOR THE DEGREE
OF MASTER OF SCIENCE

DEPARTMENT OF AGRICULTURAL ENGINEERING

EDMONTON, ALBERTA

FALL 1986

Permission has been granted to the National Library of Canada to microfilm this thesis and to lend or sell copies of the film.

The author (copyright owner) has reserved other publication rights, and neither the thesis nor extensive extracts from it may be printed or otherwise reproduced without his/her written permission.

L'autorisation a été accordée à la Bibliothèque nationale du Canada de microfilmer cette thèse et de prêter ou de vendre des exemplaires du film.

L'auteur (titulaire du droit d'auteur) se réserve les autres droits de publication; ni la thèse ni de longs extraits de celle-ci ne doivent être imprimés ou autrement reproduits sans son autorisation écrite.

ISBN 0-315-32332-9

THE UNIVERSITY OF ALBERTA

RELEASE FORM

NAME OF AUTHOR QIQIU ZHAO
TITLE OF THESIS PERFORMANCE EVALUATION OF A
THERMOSYPHON AIR HEATING SYSTEM
DEGREE FOR WHICH THESIS WAS PRESENTED MASTER OF SCIENCE
YEAR THIS DEGREE GRANTED FALL 1986

Permission is hereby granted to THE UNIVERSITY OF ALBERTA LIBRARY to reproduce single copies of this thesis and to lend or sell such copies for private, scholarly or scientific research purposes only.

The author reserves other publication rights, and neither the thesis nor extensive extracts from it may be printed or otherwise reproduced without the author's written permission.

(SIGNED)

Qiqiu Zhao

PERMANENT ADDRESS:

JIAMUSI INST. OF TECHNOLOGY
JIAMUSI, HEILONGJIANG
PEOPLE'S REPUBLIC OF CHINA

DATED

OCT. 10

19 86

THE UNIVERSITY OF ALBERTA
FACULTY OF GRADUATE STUDIES AND RESEARCH

The undersigned certify that they have read and recommend to the Faculty of Graduate Studies and Research, for acceptance, a thesis entitled PERFORMANCE EVALUATION OF A THERMOSYPHON AIR HEATING SYSTEM submitted by QIQIU ZHAO in partial fulfilment of the requirements for the degree of MASTER OF SCIENCE.

[Signature]
.....
Supervisor

John Fiddle
.....
Gerald W. Sadler
.....

OCT 10, 1986
Date.....

ABSTRACT

A thermosyphon air heating system built on an inclined, south-facing wall of a farm shop was evaluated in terms of its thermal performance. The main objective of the system was to provide a suitable working environment within the shop during daytime in spring and fall seasons. Data obtained over a period of six months indicate that this criterion generally is satisfied.

Two computer models have been developed, one for a simulated direct gain system and the other for a simulated active system. Attempts have been made to see how the existing system performs in comparison with the other two options. The simulations indicate that the performance of the existing system would be enhanced by the addition of a small fan. The direct gain configuration shows more promise for future systems than the other two configurations.

The thermal balance technique and the response factor method were used to build the direct gain system model, whereas the thermal balance technique, subdivision approach and the fully-implicit finite difference scheme were employed to set up the active system model. The component model of a solar collector in the active system model also was validated and a good agreement between the measured and the calculated performance was observed.

ACKNOWLEDGEMENTS

I wish to express my sincere thanks to my supervisor, Dr. J.J. Leonard, for his guidance, advice and support throughout the research of the project and the preparation of this thesis.

I would also like to express my thanks to Mr. K. Harrold and Mr. E. Thornton for their assistance with data acquisition, and to Prof. G.W. Sadler for his valuable suggestions on the simulation approach.

Special thanks are extended to the Government of Alberta for its financial support for my study and research toward the completion of this thesis.

Finally, I would like to thank my fiancée, Miss Xu Hui, and my parents in China for their remote moral support over the duration of my study in Canada.

Table of Contents

Chapter	Page
ABSTRACT	iv
ACKNOWLEDGEMENTS	v
NOMENCLATURE	xii
1. INTRODUCTION	1
2. LITERATURE REVIEW	5
2.1 Classification of Solar Heating Systems	5
2.1.1 Solar collectors	5
2.1.2 Active systems	6
2.1.3 Passive solar heating systems	7
2.2 Response Factor Method for Calculating Heating/Cooling Load	12
2.2.1 Response Factor Method and Transfer Functions	12
2.2.2 Z-transform	13
2.3 Thermal Radiation Heat Transfer	16
2.3.1 Angle factors	16
2.3.2 Thermal radiant heat exchange	18
2.4 Convective Heat Transfer	19
2.5 Air Properties	21
2.6 Sol-Air Temperature	22
2.7 Finite-Difference Method	24
2.8 Simulation of Thermosyphon Air Systems	26
3. SOLAR RADIATION	28
3.1 Solar-Related Terminology	28
3.1.1 Determination of hour angle, sunrise and sunset time	30
3.1.2 Determination of solar-related angles	34

3.2	Solar Radiation Reaching Outer and Inner Surfaces	36
3.2.1	On outer surfaces	36
3.2.2	Solar radiation reaching interior surfaces of a direct gain building	38
3.2.3	Plastic glazing and its treatment in the simulation	40
4.	MONITORING OF THERMAL PERFORMANCE OF THE EXISTING SHOP	43
4.1	Facilities	43
4.2	Instrumentation and Monitoring System	45
4.3	Monitored Performance	47
5.	DIRECT-GAIN MODEL	54
5.1	Model Development for a Direct Gain System	54
5.1.1	Assumptions	54
5.1.2	Model development	55
5.2	Determination of Surface Heat Transfer Coefficients	60
5.2.1	Interior surfaces	60
5.2.2	Exterior surfaces	60
5.3	Solution Procedure and Sampling Time Interval ..	61
6.	ACTIVE MODEL	64
6.1	Model Development for Active Collector	64
6.1.1	Determination of heat transfer coefficients	68
6.1.2	Heat balance equations for the ith subregion	73
6.1.3	Determination of air temperature at the collector outlet	80
6.2	Calculation of Room Air Temperature	82
6.2.1	Heat gain into the structure	82

6.2.2	Collector efficiency	84
6.2.3	Calculation of room air temperature	84
6.3	Features of the Computer Model and Calculation Steps	87
7.	COMPARISON OF THE ACTUAL AND THE SIMULATED SYSTEMS ..	91
7.1	Model Validation for the Active Solar Collector ..	91
7.2	Comparison of Different Systems	96
7.3	Discussions on Model Performance	99
7.4	Discussions on Performances of Different Systems	101
8.	CONCLUSIONS AND RECOMMENDATIONS	105
	REFERENCES	107
	APPENDIX A.1: FLOOR RESPONSE FACTORS USED IN THE DIRECT-GAIN MODEL	115
	APPENDIX A.2: ROOM SURFACE ANGLE FACTORS USED IN THE DIRECT-GAIN MODEL	116
	APPENDIX A.3: FLOWCHART FOR THE DIRECT-GAIN MODEL	117
	APPENDIX A.4: PROGRAM LISTING OF THE DIRECT-GAIN MODEL ..	118
	APPENDIX A.5: FORMAT OF INPUT FILE #1 FOR THE DIRECT-GAIN MODEL	137
	APPENDIX A.6: A SAMPLE OUTPUT FILE FROM THE DIRECT-GAIN MODEL	140
	APPENDIX B.1: FLOWCHART OF THE ACTIVE SYSTEM MODEL	146
	APPENDIX B.2: PROGRAM LISTING OF THE ACTIVE SYSTEM MODEL ..	147
	APPENDIX B.3: FORMAT OF INPUT FILE #1 FOR THE ACTIVE SYSTEM MODEL	180
	APPENDIX B.4: A SAMPLE OF OUTPUT FILE FROM THE ACTIVE SYSTEM MODEL	183
	APPENDIX C.1: SPECIFICATIONS OF TWO FLAT-PLATE COLLECTORS BUILT BY ALBERTA AGRICULTURE	189

List of Tables

Table	Page
3.1 Local standard time meridian	34
4.1 Thermocouples and their locations	46
4.2 Daily energy collection & collector efficiency	48
7.1 Measured & predicted energy collection for the single-glazed collector	95
7.2 Measured & predicted energy collection for the double-glazed collector	95
7.3 Comparison of active and thermosyphon systems	100
7.4 Savings of an active system against electric heaters	104

List of Figures

Figure	Page
2.1 A simplified direct gain system	9
2.2 A simplified thermosyphon system	9
2.3 Pulses output from a sampler of a continuous function	14
2.4 Configuration for radiant interchange between two finite surfaces	17
2.5 Discrete points for one-dimensional heat conduction	25
3.1 Solar declination	29
3.2 Solar angles for a tilted surface (adapted from ASHRAE, 1981)	31
3.3 Hour angle (adapted from ASHRAE, 1971)	32
3.4 Sunrise and sunset times (adapted from ASHRAE, 1971)	32
3.5 Direction cosines of solar beam	35
3.6 Radiation on horizontal and tilted surfaces	37
3.7 Morning illuminations of room interior surfaces	39
4.1 A view of the shop and the solar collector	44
4.2 Monitored performance for Oct. 18, 1985	49
4.3 Monitored performance for Dec. 21, 1985	49
4.4 Monitored performance for Feb. 6, 1986	50
4.5 Monitored performance for Feb. 7, 1986	50
4.6 Monitored performance for Feb. 9, 1986	51
4.7 Measured air flow velocity for Oct. 17-19, 1985	51
4.8 Measured thermal stratification of room air (Feb. 6, 86)	53
5.1 A sketch of the simplified direct-gain ^o system	57

Figure

Page

6.1 A subdivision for the collector67

6.2 Detail of the *i*th region67

6.3 A subregion and its thermal network for a single-glazed collector69

6.4 A double-glazed system72

6.5 A triple-glazed system72

6.6 Air temperature at the outlet of the collector82

6.7 Heat gain into the room from the collector83

6.8 Interior and boundary nodes for the floor slab86

7.1 Measured and calculated outlet temperatures of a single-glazed, one-path collector on a cloudy day92

7.2 Measured and calculated outlet temperatures of a single-glazed, one-path collector on a clear day92

7.3 Measured and calculated outlet temperatures of a double-glazed, one-path collector on a cloudy day93

7.4 Measured and calculated outlet temperatures of a double-glazed, one-path collector on a clear day93

7.5 Performances of measured and simulated systems for Dec. 21, 198597

7.6 Performances of measured and simulated systems for Dec. 22, 198597

7.7 Performances of measured and simulated systems for Feb. 5, 198698

7.8 Performances of measured and simulated systems for Feb. 7, 198698

NOMENCLATURE

Symbols	Descriptions	Units
A	area in Chap.2	m ²
A	apparent solar irradiation beyond the atmosphere in Chap.3	Wm ⁻²
A's	matrix coefficients in Chap.4 & 5	
AST	Apparent solar time	hours
a,b,c	response factors	
B	atmospheric extinction coefficient in Chap.3	
B's	matrix right-hand terms in Chap.4 & 5	
COS(E)	direction cosine of solar beam	
COS(S)	direction cosine of solar beam	
COS(Z)	direction cosine of solar beam	
Cp	specific heat	Jkg ⁻¹ °C ⁻¹
D	hydraulic diameter	m
ET	Equation of time	hours
F	angle factor	
F _g	ground view factor	
F _y	sky view factor	
f	weighting factor in Chap.2	
f(Δ)	pulse output of a function	
G	transfer function	
g	gravitational acceleration	ms ⁻²

H_b/H	ratio of beam to global solar radiation	
H_d/H	ratio of diffuse to global solar radiation	
h	heat transfer coefficient	$Wm^{-2}C^{-1}$
hr	radiant heat transfer coefficient	$Wm^{-2}C^{-1}$
I	input to a system in Chap.2	
I	solar radiation	Wm^{-2}
I_{DN}	direct normal solar radiation	Wm^{-2}
k	thermal conductivity	$Wm^{-1}C^{-1}$
L	characteristic length	m
LG	local longitude	deg.
LSM	local standard meridian	deg.
LT	local latitude	deg.
\dot{m}	mass flow rate	$kg s^{-1}$
Nu	Nusselt number	
n	day of a year	
nr	No. of response factors	
ns	No. of surfaces	
O	output of a system in Chap.2	
P	atmospheric pressure	Pa
Pr	Prandtl number	
Q	rate of heat transfer	W
EQ	total energy collection	KJm^{-2}
R	ideal gas constant	$Jkg^{-1}C^{-1}$
Ra	Rayleigh number	

R_b	beam correction factor	
Re	Reynolds number	
Ro	ratio of total radiation on a tilted surface to that on a horizontal surface	
ΔR	radiation difference	Wm^{-2}
r	length of connecting line in Chap.2	m
S	area	m^2
S'	illuminated area	m^2
SRT	sunrise time	Hour
SST	sunset time	Hour
s	spacing	m
T	temperature	$^{\circ}C$
\bar{T}	mean temperature	$^{\circ}C$
T	temperature at previous time	$^{\circ}C$
ΔT	temperature difference	$^{\circ}C$
TU	total heat transfer coefficient	Wm^{-2}
t	time	s
Δt	time increment	s
U	velocity of fluid	ms^{-1}
V	volume	m^3
X, b	coefficients of an equation	
Δx	grid size	m
x	coordinate along a collector	
α	thermal diffusivity	m^2s^{-1}

α	absorptance	
β	angle between a line & a surface normal in Chap.2	deg.
β	coefficient of thermal expansion	$^{\circ}\text{K}^{-1}$
γ	surface-solar azimuth	deg.
Δ	time interval	s
δ	solar declination	deg.
ϵ	emittance	—
η	efficiency	
Θ	surface inclination	deg.
θ	angle of incidence	deg.
μ	dynamic viscosity	Nsm^{-2}
ν	kinematic viscosity	m^2s^{-1}
ρ	density	kgm^{-3}
ρ	ground reflectance in Chap.3	
σ	Stefan-Boltzmann constant	
τ	transmittance	
ϕ	solar azimuth	deg.
ψ	surface azimuth	deg.
ω	hour angle	deg.

1. INTRODUCTION

Energy consumption in today's world is enormous, and is growing rapidly (Rapp, 1981), partly due to the progressive rate of increase in world population and partly due to the greater energy demands of increasingly sophisticated lifestyle. In the United States, for example, an increase of around 3% per year in energy consumption was predicted by Rapp (1981). Approximately, 4.0% of total commercial energy is being used for agricultural purposes (Stout, 1979).

The large energy requirements around the world have been met with several major developed energy sources which include coal, oil, natural gas (these three are also called fossil fuels), hydroelectric power and nuclear power.

However, as is being realized by more and more people, the fossil fuels are limited in quantity and will become short in supply at some point in the future. People have been upset by the fluctuating oil prices. Nuclear energy is a promising alternative substitute for the fossil fuels. However, nuclear fusion and nuclear materials, are hard to handle and pose safety problems (Fisk and Anderson, 1982). This argument is strengthened by the melt-down of a nuclear power plant recently in the Soviet Union. The adverse effects of radioactive pollution to the global environment caused by such accidents could last for many years to come.

In contrast, solar radiation is safe, pollution-free and available in large quantities in almost every part of the earth. Solar energy requires no transportation and no

maintenance, and is free in terms of its availability (Halacy, 1973). These attractive features of solar energy have made it one of a number of important alternative energy sources that have been constantly studied over the past 20 years.

The distribution of incoming solar energy is best suited for relatively low-temperature agricultural applications. Therefore, full advantage should be taken of the possibilities for converting solar energy into useful forms on farms.

Interest in solar energy as a heating source for agricultural applications began in the 1950's (Stout, 1978), and renewed interest was caused in the 1970's by the 1973 oil embargo.

Brewer (1981) gives a detailed discussion on solar energy applications in agriculture. These include:

- food processing
- grain and crop drying
- heating of livestock shelters and workshops
- heating and cooling of green houses

Both active and passive solar systems can be found in grain drying, in green house applications and in the heating of livestock buildings. Green houses take advantage of the spectrum difference between solar radiation (mainly visible and near infrared) and the reradiation from objects on the earth (mainly far infrared) (Thorndike, 1976), and have been used for centuries (Walls, 1973). Grain drying with solar

energy has been studied by many researchers (Thompson and Pierce, 1981; Chau and Baird, 1981; Calderwood, 1981; Converse *et al.*, 1981; Feddes *et al.*, 1980). Heating of livestock buildings with solar energy also has been investigated (Hellickson, 1982; Waddell *et al.*, 1982; Ellis and Phillips, 1982). However, few studies have been found on the solar heating of farm service buildings such as farm shops.

A thermosyphon air system was built onto the south-facing wall of a farm shop on the Halford farm near Lamont, Alberta, with the aim of providing sufficient space heating during late fall and early spring when the shop is used for machinery maintenance. For a farm shop, a suitable working temperature is assumed to be about 10°C during daytime.

The absorbing surface of the collector was made of the original steel siding painted black and covered with one layer of glazing. Vents were cut at the bottom and the top of the collector for air to enter and to exit. An unusual feature of the system was that it had two air passages, one on each side of the absorbing plate. Heat is collected by the collector and is carried into the shop by the air movement through the collector which is caused by the difference in density between the heated air and the cooler air entering the collector.

To evaluate the thermal performance of this thermosyphon air system is the major thrust of the project.

Data were collected from the existing shop and analyzed for the heating season of 1985-1986.

The evaluation of the existing system would, perhaps, be more meaningful if its performance were compared to other options such as a fan-forced flow (active system) and a south-facing window (direct gain system). Since full-scale physical systems were not available for such a comparison, a secondary aim was to develop two computer models that could simulate these alternatives. The models could be used to evaluate possible modifications to the existing system and to investigate the effects of changing design parameters on the performance of an active system.

The existing shop was used as the basis of the two models. The collection area (14.6 m by 4.3 m) of the actual system was taken as the collector area for the active model and as the window area for the direct gain model.

2. LITERATURE REVIEW

2.1 Classification of Solar Heating Systems

2.1.1 Solar collectors

Solar energy reaching the earth's surface is not continuous due to the shift of day and night, and due to the change of clear and cloudy days. Solar collectors are designed to convert solar radiation, when it is available, into heat at a desired temperature with a high efficiency.

The essential part of a solar heating system is the solar collector (A south-facing window is a type of solar collector in direct gain systems.) which transforms solar radiation energy into other useful forms. Solar collectors with radiation concentration are called *FOCUSING* collectors, whereas those without radiation concentration (i.e., those for which the area absorbing solar radiation is the same as the area intercepting it) are called *FLAT-PLATE* collectors (Duffie and Beckman, 1974).

Maximizing the absorbed solar energy and minimizing heat losses of a collector are the important considerations in the collector design since they affect the collector efficiency directly. The absorbing surface of a flat-plate collector commonly is blackened to enhance its absorptivity and usually is covered with glazing on the top to reduce heat losses. The various schemes for reducing radiative losses by use of covers all make use of the difference

between the spectrum of the incident solar energy (mainly the visible and near infrared) and the spectrum of the reradiated energy (the far infrared in most cases). Glass or some other materials (e.g., some types of plastics as discussed later) that are transparent to solar radiation but opaque to far infrared radiation are used as covers. Thus, the solar radiation can enter easily but the infrared reradiation has difficulty escaping. This phenomenon is discussed in detail by Thorndike (1976), and is referred to as the *HEAT TRAPPING EFFECT*.

Flat-plate collectors are ideal for applications requiring energy delivery at moderate temperatures. They have the advantages of using both beam and diffuse solar radiation, not requiring accurate orientation toward the sun and requiring little maintenance. Furthermore, as pointed out by Duffie and Beckman (1974), they are simple and less expensive to construct than focusing collectors.

Solar heating systems can be classified broadly into two categories: active and passive systems. Some systems, however, have both active and passive features and, hence, are called hybrid systems by some researchers.

2.1.2 Active systems

Active solar systems require electrically or mechanically powered pumps or blowers to circulate the thermal transport fluids (either air or water) in the system. An active solar heating system generally consists of

a solar radiation collecting device (solar collector), heat transport fluid, heat storage, a control system and a circulation system. Active systems have the advantage of removing heat from collectors in a controlled way, and heat may be sent to places of need or stored for later use when required.

2.1.3 Passive solar heating systems

Passive solar heating systems collect and utilize solar energy by natural means, and do not involve the use of mechanical or electrical power for the circulation of the heat transport fluid. Control elements such as vents and dampers often are incorporated into passive designs to regulate the flow of thermal energy. Passive systems may or may not have specially designed and constructed collectors and storage units. Major advantages of such systems are the easy construction, easy operation and low cost.

Various forms of passive systems include (Williams, 1983):

- direct gain systems
- thermal storage walls or Trombe walls
- thermal storage roofs
- attached greenhouses
- convective loop or thermosyphon systems

In direct gain systems the solar radiation enters through a window and directly strikes the floor and other objects in the room. The heated surfaces of those objects in

turn store energy and heat the air inside the room. Thermal inertia of the conditioned space helps to store this heat for nighttime usage. Figure 2.1 is a simplified illustration of a direct gain system.

Direct gain systems are very effective in gaining heat during daytime hours and high temperatures may be reached during sunny days. However, they are also very effective in losing heat during winter night hours.

In a thermosyphon system (Figure 2.2), solar energy is collected by a collector which closely resembles an active solar collector. Heated fluid (air or water) rises in the collector in a natural way due to buoyancy effects. The difference in density between the heated air and the cooler air entering the collector is equivalent to a pressure head and causes air to flow through the collector (Kohler, 1981).

If, for a Northern hemisphere system, the induced air flow is directed from a collection area on the South wall, through ducting in the ceiling and the North wall to a storage area located in the crawl space below the floor, and back to the collector, the system is called an *AIR THERMAL ENVELOPE* or *DOUBLE SHELL HOUSE*. Marshall et al. (1981) studied an air thermal envelope system with a rock storage in the North wall, and reported that the low flow velocities measured did not allow heat to be transferred effectively to the thermal mass, and that a large thermal stratification between lower level and upper level rooms existed during the monitoring period. The air thermal envelope houses have been

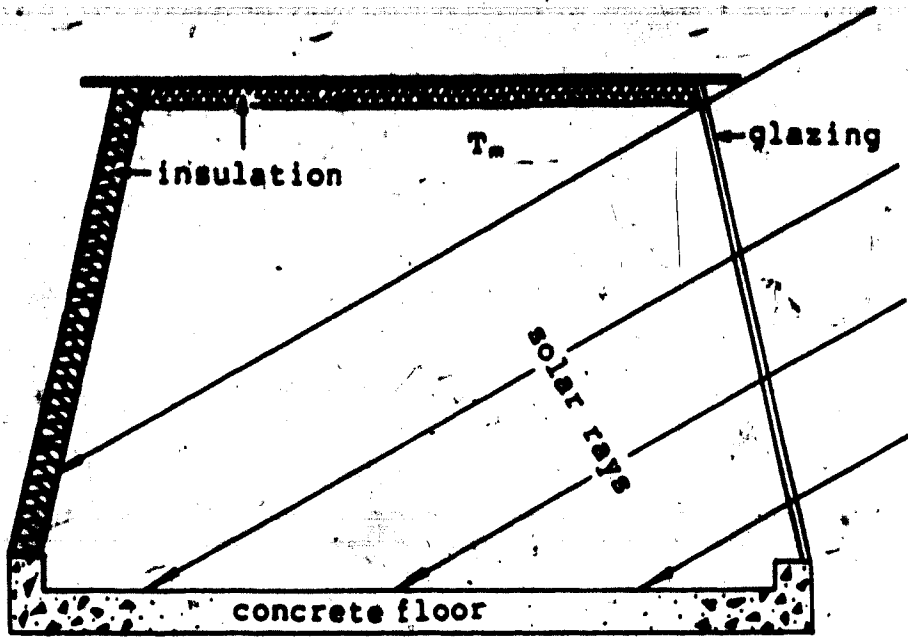


Figure 2.1 A simplified direct gain system

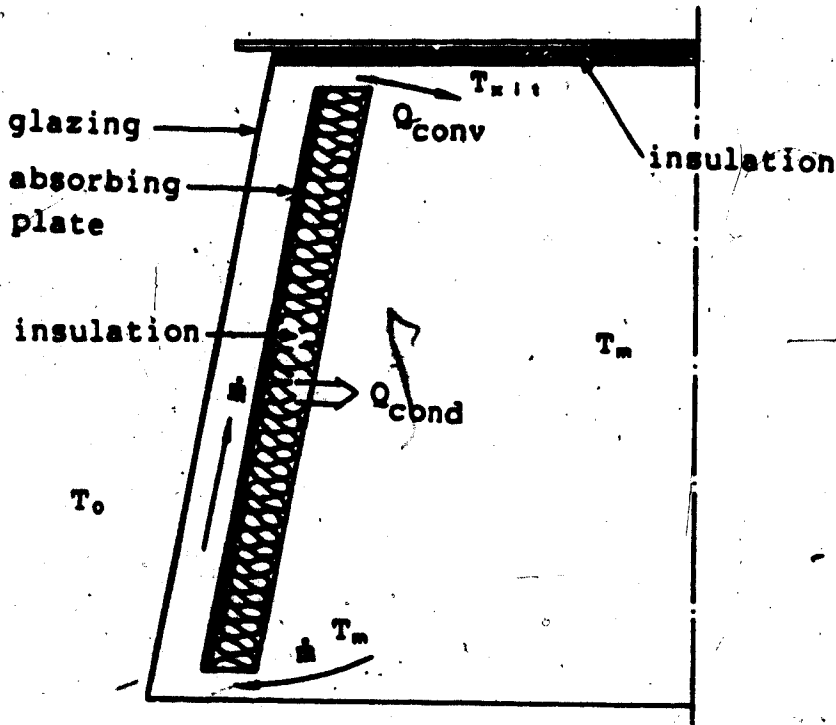


Figure 2.2 A simplified thermosyphon system

seen to have lower thermal performance than either a Trombe wall or a direct gain system (Marshall et al., 1980).

If the collecting plate is made of metal sheet and the collected energy flows directly into the room space in a thermosyphon system, the system is referred to as a THERMOSYPHON AIR PANEL (TAP). A TROMBE WALL uses concrete or massive masonry built on the South wall to collect solar energy, to store heat and to conduct heat into the room. Carter (1980) studied Trombe walls in four typical Canadian climates and found that the most effective method of reducing heating loads in Canada is by improving insulation and that the simplest way to use solar energy is with south facing windows, using the inherent thermal capacity of the building as storage.

Hagan et al. (1980) investigated two thermosyphon air panels (TAPS), one with air moving above the collecting plate (Front-path) and the other with air moving under the collecting plate (Back-path). A thermal anemometer located at the lower vent was reported as recording maximum velocities of under 0.15 m/s. The conclusion of these authors was that, with a massive masonry wall behind the collecting plate, the conductive portion of the collector heat gain was greater than the convective portion.

Reif. (1980) calculated the material costs for construction of TAPS as \$8.00 (U.S.) per square foot of collector surface. The cost was considered low compared to that for active systems.

Reno (1981), in examining the effects on the thermal performance of inlet and outlet port geometry, the air channel depth and the length of the TAP, found that back draft dampers were extremely restricting. He suggested that an air channel depth of 25.4 mm would give optimum performance, and that the performance would increase with the increase of the TAP length to a limit of about 4.6 m. Finally, he indicated that fan-forced flow might be a viable option to TAPS.

Stetzel (1983) described a workshop with a thermosyphon air system built on the south-facing wall, which was similar to the case studied in this project in terms of building construction. The thermal performance of the building was monitored and positive conclusions about the structure were reached. However, no details were given of measurement of its thermal performance.

Jones and Morris (1980) analyzed two passive air thermosyphon-heated homes designed and built by the Mark Jones Corporation in Santa Fe, CA. One home was built with a vertical rockbed in the North wall, and the other with a rockbed under the floor. The thermosyphon/rock storage systems were observed to deliver quite high solar fractions (ratios of the total solar heat collected to the total heating load), even in large houses, using radiant heat transfer to living spaces, without the use of fans.

Chen and Jones (1981) compared a thermosyphon water heating system with an active solar water heating system

built in Ontario over the summer of 1980. They reported that the thermosyphon system was more efficient and more reliable than the active system for the summer test.

Despite the work by other researchers described above, the performance of thermosyphon systems is not yet well defined and there is some uncertainty associated with the design of such systems.

2.2 Response Factor Method for Calculating Heating/Cooling Load

2.2.1 Response Factor Method and Transfer Functions

The response factor method for calculating heating and cooling loads of a building was first developed by Stephenson and Mitalas (1967) and then was accepted as a new procedure of heating/cooling load calculation by ASHRAE (1971).

The response factor method is based on the assumption that the heat transfer processes occurring in a room can be described by linear equations and, thus, that the superposition principle can be used for the calculation of heating or cooling load. If a disturbance or an excitation is given to a system as input, then the corresponding component of heating load can be expressed in terms of system transfer functions. Transfer functions of a system relate the input (disturbances) to the output (responses) of the system as follows:

$$O(s) = G_1(s) \cdot I_1(s) \quad (2.1)$$

where $O(s)$ = output of the system

$G_1(s)$ = transfer functions of the system, and

$I_1(s)$ = input of the system.

The above equation is in the frequency domain (s-domain), which is obtained simply by taking the Laplace transform of system equations in the time-domain (t-domain).

Transfer functions contain all the characteristics of a system and are independent of external conditions. Once all the system transfer functions have been defined, the system's response to any excitation can be determined easily by equation 2.1.

2.2.2 Z-transform

The Z-transform of a function is based on the Laplace transform of the function. When a continuous signal $f(t)$ is sampled at a regular time interval of Δ , the output signal of the sampling device is a train of pulses as shown in figure 2.3.

The Laplace transform of the output pulses is:

$$f(0) + f(\Delta)e^{-s\Delta} + f(2\Delta)e^{-2s\Delta} + \dots \quad (2.2)$$

The Z-transform of the output from the sampler is obtained by substituting Z for $e^{s\Delta}$ in equation 2.2, i.e. let $Z = e^{s\Delta}$, then equation 2.2 becomes:

$$f(0) + f(\Delta)Z^{-1} + f(2\Delta)Z^{-2} + \dots + f(n\Delta)Z^{-n} + \dots \quad (2.3)$$

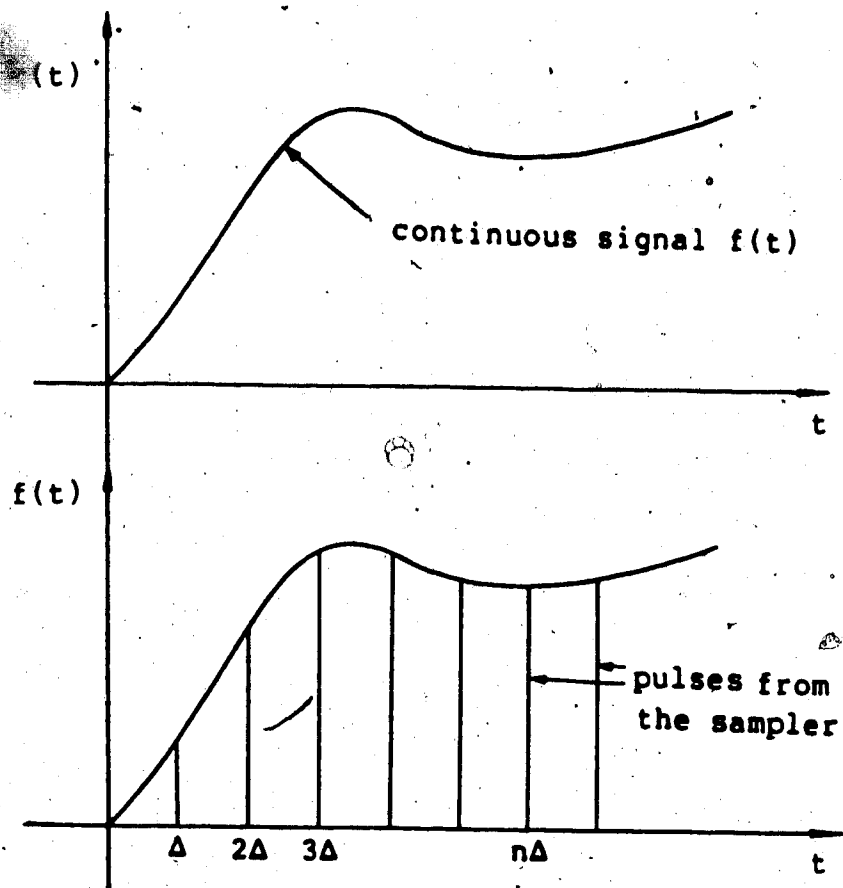


Figure 2.3 Pulses output from a sampler of a continuous function

This polynomial in Z^{-1} has the advantage that it can be obtained just by sampling the function at regular time intervals. The successive outputs are the coefficients of successive powers of Z^{-1} in the Z-transform polynomial.

A Z-transfer function for a system is the ratio of the output to input expressed in terms of their Z-transforms.

$$\text{Let } G(Z) = \frac{a_0 + a_1 Z^{-1} + a_2 Z^{-2} + \dots}{b_0 + b_1 Z^{-1} + b_2 Z^{-2} + \dots} \quad (2.4)$$

be the transfer function for a system. Then

$$O(Z) = G(Z) * I(Z) \quad (2.5)$$

where $O(Z)$ = output Z-transform and

$I(Z)$ = input Z-transform.

If both $O(Z)$ and $I(Z)$ are expressed as polynomials, then:

$$O(Z) = O_0 + O_1 Z^{-1} + O_2 Z^{-2} + \dots \quad (2.6)$$

and

$$I(Z) = I_0 + I_1 Z^{-1} + I_2 Z^{-2} + \dots \quad (2.7)$$

The coefficients of various powers of Z^{-1} must be the same on both sides of equation 2.5. Thus, the output or response of the system at any time $t = n\Delta$ is the coefficient of Z^{-n} . Equating the coefficients of Z^{-n} gives:

$$\begin{aligned} O_n b_0 &= I_n a_0 + I_{n-1} a_1 + I_{n-2} a_2 + \dots \\ &\quad - \{O_{n-1} b_1 + O_{n-2} b_2 + \dots\} \end{aligned} \quad (2.8)$$

or,

$$O_n b_0 = \sum a_j I_{n-j} - \sum b_j O_{n-j} \quad (2.9)$$

This expression relates the output at any time $t = n\Delta$ to the input at that time and the values of output and input at the previous times. The coefficients a_j and b_j contain the characteristics of the system, i.e., they describe how a particular system behaves under external disturbances. They are called *RESPONSE FACTORS* when referred to heat conduction through walls and ceilings, and *WEIGHTING FACTORS* when referred to space heating & cooling load calculations (ASHRAE, 1971).

2.3 Thermal Radiation Heat Transfer

Thermal radiant heat transfer occurs by means of electromagnetic waves between two surfaces having different temperatures, and does not depend upon the presence of an intermediate material for energy exchange. The net energy transfer rate depends on the absolute temperatures and the spatial relationships of the surfaces involved. In engineering calculations assumptions often are made to simplify the determination of radiation heat transfer. Gebhart (1971) summarizes the assumptions as:

- all surfaces are considered to be either gray or black.
- radiation and reflection processes will be diffuse.
- each surface will have uniform properties over its whole extent.
- absorptivity of a surface is equal to its emissivity and independent of its temperature.
- all surfaces are considered opaque, i.e., $\tau = 0$, where τ is the transmissivity of the surfaces.
- material occupying the space between radiating surfaces will neither emit nor absorb radiation.

2.3.1 Angle factors

Angle factor is defined, according to ASHRAE (1981) and Sparrow and Cess (1978), as follows:

"In terms of two surfaces, i and j , the angle factor from surface i to surface j , F_{i-j} , is the fraction of diffuse radiation energy leaving surface i , which falls directly

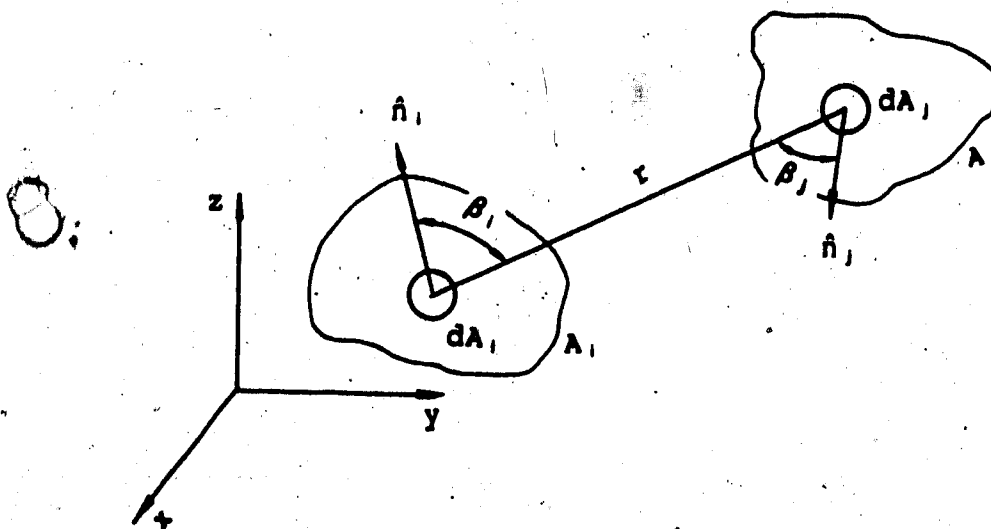


Figure 2.4 Configuration for radiant interchange between two finite surfaces

upon (i.e., is intercepted by) surface j." Figure 2.4 illustrates the configuration for interchange between two finite surfaces. The mathematical formula for evaluating the angle factor is:

$$F_{1 \rightarrow j} = \frac{1}{A_1} \iint \frac{\cos \beta_1 \cos \beta_2}{\pi r^2} dA_1 dA_2 \quad (2.10)$$

where β_1 , β_2 are angles formed by the respective normals (\hat{n}_1, \hat{n}_2) and the connecting line between two elements dA_1 , dA_2 , and r is the length of the connecting line.

The angle factors provide information on the fraction of the diffusely distributed radiant energy leaving one surface that arrives at another surface. As seen in equation

2.10 the angle factor is, in fact, dependent only on the geometry and positions of two surfaces involved.

Since the integration for angle factors between two surfaces is difficult to perform, charts are given in many references (e.g., Sparrow and Cess, 1978; ASHRAE, 1981; Sucec, 1975). These charts were obtained originally by performing the exact integration for each different spatial configuration of the surfaces with respect to one another.

There are two useful relationships that can be helpful in determination of angle factors (Eckert and Drake, 1972).

i. Reciprocal law: For two surfaces 1 and 2,

$$A_1 F_{1-2} = A_2 F_{2-1} \quad (2.11)$$

where A_1 and A_2 are the areas of two surfaces (m^2), respectively, and F_{1-2} and F_{2-1} are the angle factors (F_{1-2} from surface 1 to surface 2).

ii. When surface A_1 is completely surrounded by n other surfaces the following relation holds:

$$\sum_{k=1}^n F_{1-k} = 1 \quad (2.12)$$

2.3.2 Thermal radiant heat exchange

The heat transfer (Q_1 or Q_2) by thermal radiation between two arbitrary surfaces is determined by:

$$Q_1 = -Q_2 = \frac{\sigma(T_2^4 - T_1^4)}{(1-\epsilon_1)/\epsilon_1 A_1 + 1/A_1 F_{1-2} + (1-\epsilon_2)/\epsilon_2 A_2} \quad (2.13)$$

where σ = Stefan-Boltzmann constant

ϵ_1, ϵ_2 = emittances of surface 1 and 2, respectively

A_1, A_2 = areas (m^2) of surface 1 and 2, respectively

T_1 = temperature ($^{\circ}K$) of surface 1

T_2 = temperature ($^{\circ}K$) of surface 2, and

F_{1-2} = angle factor from surface 1 to 2.

For radiation between two infinite parallel plates, the areas A_1 and A_2 are equal and F_{1-2} is unity, then equation 2.13 becomes (Duffie and Beckman, 1974):

$$Q = \frac{\sigma A (T_2^4 - T_1^4)}{1/\epsilon_1 + 1/\epsilon_2 - 1} = Ahr(T_2 - T_1) \quad (2.14)$$

$$\text{where } hr = \frac{\sigma (T_2^3 + T_2^2 T_1 + T_2 T_1^2 + T_1^3)}{1/\epsilon_1 + 1/\epsilon_2 - 1}$$

and is often called the *RADIANT HEAT TRANSFER COEFFICIENT*.

2.4 Convective Heat Transfer

Convection is the mode of heat transfer in which heat is carried along by moving fluid particles (Eckert and Drake, 1972). Convective heat transfer may be classified by the potential that drives the fluid flow. When the flow is mechanically driven by a fan or a pump and pressure gradients other than the hydrostatic gradient are present, heat is transferred by forced convection. Free or natural convection occurs when only density differences and, hence, buoyancy forces are present to drive the flow. Internal convection arises when the flowing medium is completely bounded by solid walls, whereas external convection

describes a flowing medium only partially bounded by walls or surfaces.

The heat transfer due to the wind acting on the outer surfaces of a collector is, according to the above definitions, external forced convection and so is the heat transfer from collecting plates to the working fluid in active systems. Heat losses through the enclosed spaces between the covers or between the innermost cover and the absorbing plate of a flat-plate collector are due to internal free convection.

The heat transfer rate due to fluid motion depends primarily on the nature of the fluid flow process, on the flow velocity and the properties of the fluid. The state of fluid flow can be either laminar or turbulent depending upon the Reynolds Number (Re) (Gebhart, 1971), which is expressed as:

$$Re = \frac{U \cdot D}{\nu} \quad (2.15)$$

where Re = Reynolds Number

U = velocity of fluid (ms⁻¹)

D = hydraulic diameter of flow passage (m), and

ν = kinematic viscosity of fluid (m²s⁻¹).

For different states of flow, the heat transfer coefficients, often expressed in terms of the Nusselt Number (Nu), are different. The Nusselt Number is one of the dimensionless quantities that are important in the study of convective heat transfer. The Nusselt Number is defined as:

$$Nu = \frac{L \cdot h}{k} \quad (2.16)$$

where L = characteristic length (m)

h = heat transfer coefficient ($\text{Wm}^{-2}\text{°C}^{-1}$), and

k = thermal conductivity of fluid ($\text{Wm}^{-1}\text{°C}^{-1}$).

Many empirical correlations have been found that relate Nu to Re and/or the Rayleigh Number (Ra), as well as the Prandtl Number (Pr) (Sucec, 1975). These correlations are used mostly in engineering calculation of heat transfer. The definitions of the Rayleigh Number and the Prandtl Number are as follows:

$$Ra = \frac{\beta g \Delta T L^3}{\nu \alpha} \quad (2.17)$$

$$Pr = \frac{\nu}{\alpha} \quad (2.18)$$

where β = coefficient of thermal expansion (°K^{-1})

($=1/T$ where T is in °K)

ΔT = temperature difference (°C), and

α = thermal diffusivity (m^2s^{-1}).

2.5 Air Properties

Properties of air are functions of air temperature, pressure and humidity. Often in heat transfer, air is assumed to be dry and the pressure is assumed to be that of a standard atmosphere (Chapman, 1984). The ideal gas law is used for estimating the air density, as follows:

$$\rho = \frac{P}{RT} = \frac{353}{T} \quad (2.19)$$

where ρ = air density (kgm^{-3})

P = atmospheric pressure (101325Pa)

R = ideal gas constant ($287 \text{ Jkg}^{-1}\text{°K}^{-1}$), and

T = air temperature (°K).

Expressions for viscosity (μ), specific heat (C_p) and thermal conductivity (k) of air are suggested by ASHRAE (1976a) as:

$$\mu(10^{-4} \text{Nsm}^{-2}) = \sqrt{T}/(0.6717 + 85.2297/T - 2111.475/T^2 + 106417/T^3) \quad (2.20)$$

$$k(\text{Wm}^{-1}\text{K}^{-1}) = \sqrt{T}/(385.859 + 9.1144 \cdot 10^4/T - 2.6867 \cdot 10^6/T^2 + 5.526 \cdot 10^7/T^3) \\ \text{for } 80^\circ\text{K} < T < 300^\circ\text{K} \quad (2.21)$$

$$k(\text{Wm}^{-1}\text{K}^{-1}) = \sqrt{T}/(328.052 + 1.6732 \cdot 10^4/T - 3.0295 \cdot 10^7/T^2 + 3.586 \cdot 10^9/T^3) \\ \text{for } 300^\circ\text{K} < T < 600^\circ\text{K} \quad (2.22)$$

$$C_p(\text{KJkg}^{-1}\text{K}^{-1}) = 1.032 - 0.001225T \\ \text{for } 90^\circ\text{K} < T < 260^\circ\text{K} \quad (2.23)$$

$$C_p(\text{KJkg}^{-1}\text{K}^{-1}) = 1.04466 - 3.1597 \cdot 10^{-4}T + 7.07907 \cdot 10^{-7}T^2 - 2.7034 \cdot 10^{-10}T^3 \\ \text{for } 250^\circ\text{K} < T < 600^\circ\text{K} \quad (2.24)$$

The solar-related terminology is discussed in detail in the next chapter.

2.6 Sol-Air Temperature

ASHRAE (1981) defines the sol-air temperature as:

$$T_{s,a} = T_{o0} + \alpha_o I_t / h_o - \epsilon_o \Delta R / h_o \quad (2.25)$$

where α_o = absorptance of the exterior surface

I_t = intensity of total solar radiation incident on the exterior surface (Wm^{-2})

T_{o0} = ambient temperature ($^\circ\text{C}$)

h_o = coefficient of heat transfer by longwave

radiation and convection at the outer surface

($\text{Wm}^{-2}\text{C}^{-1}$).

ϵ_0 = emittance of the surface, and

ΔR = difference between long wave radiation incident on the surface from the sky and surroundings, and the radiation emitted by a blackbody at outdoor air temperature (Wm^{-2}).

Sol-air temperature is that temperature of the outdoor air which, in the absence of all radiation exchanges, would give the same rate of heat entry into the surface as would exist with the actual combination of incident solar radiation, radiant energy exchange with the sky and other outdoor surroundings, and convective heat exchange with the outdoor air (ASHRAE, 1981).

For the roof surface that receives longwave radiation from the sky only, an appropriate value of ΔR is suggested as 63 Wm^{-2} . Vertical surfaces receive longwave radiation from both the foreground and the sky, so the values for their ΔR are difficult to determine. When solar radiation intensity is high, surfaces of terrestrial objects usually have a higher temperature than the ambient air. Thus their longwave radiation compensates to some extent for the sky's low emittance. Because of this, $\Delta R = 0$ is commonly assumed for vertical surfaces (ASHRAE, 1981).

2.7 Finite-Difference Method

The method of solution of differential problems in which differential operators are replaced by their approximate values expressed in terms of functions at individual discrete points is called the *FINITE-DIFFERENCE METHOD* (Nogotov, 1978). The method is illustrated below.

A general equation of unsteady one-dimensional heat conduction is expressed as:

$$\rho C_p \frac{\partial T}{\partial t} = \frac{\partial}{\partial x} \left(k \frac{\partial T}{\partial x} \right) \quad (2.26)$$

With reference to Figure 2.6, equation 2.26 is approximated with the finite-difference method as (Patankar, 1980):

$$\rho C_p \frac{T_i - \hat{T}_i}{\Delta t} = f \frac{k(T_{i+1} - T_{i-1})}{\Delta x^2} + (1-f) \frac{k(\hat{T}_{i+1} - \hat{T}_{i-1})}{\Delta x^2} \quad (2.27)$$

where ρ = density, (kgm^{-3})

C_p = specific heat ($\text{Jkg}^{-1}\text{°C}^{-1}$)

Δx = grid size (m)

k = thermal conductivity ($\text{Wm}^{-1}\text{°C}^{-1}$)

\hat{T}_i = temperature of node i at previous time (°C)

T_i = temperature of node i (°C), and

f = weighting factor.

The grid size (Δx) and the thermal conductivity (k) are assumed to be constant in the above equation, although they can be varying or temperature-dependent.

When the weighting factor f is chosen to be zero (i.e., $f = 0$), equation 2.27 becomes:

$$\rho C_p \frac{T_i - \hat{T}_i}{\Delta t} = k \frac{\hat{T}_{i+1} - \hat{T}_{i-1}}{\Delta x^2} \quad (2.28)$$

and is referred to as the *FULLY-EXPLICIT* scheme since the temperature at node i can be determined explicitly from the

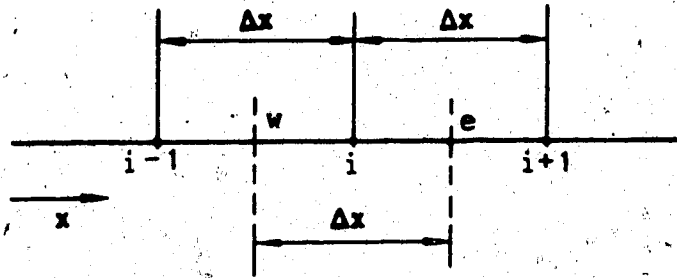


Figure 2.5 Discrete points for one-dimensional heat conduction

temperatures at nodes $i-1$, i and $i+1$ at the previous time.

When $f = 1$, equation 2.27 then takes the form of:

$$\rho C_p \frac{T_i - T_i}{\Delta t} = k \frac{T_{i+1} - T_{i-1}}{\Delta x^2} \quad (2.29)$$

Equation 2.29 is referred to as the *FULLY-IMPLICIT* scheme, since the temperature at node i can not be determined based on the old temperatures of the three nodes. A new temperature at node i can only be determined simultaneously with new temperatures at all other nodes by solving a set of matrix equations, provided that boundary conditions are adequate.

The advantage of the fully-explicit scheme is the simplicity of the solution procedure necessary to find a new temperature of a node, whereas the shortcoming of it is the small grid size and the small time increment required for convergence to be maintained. The fully-implicit scheme always gives stable solutions (convergence guaranteed)

regardless of the grid size or the time increment used.

Any other scheme (where $0 < f < 1$) has the characteristics of both the fully-explicit scheme and the fully-implicit scheme. And the selection of f is total up to the user.

2.8 Simulation of Thermosyphon Air Systems

An attempt has been made to investigate developments in modelling thermosyphon air systems. No satisfactory models which could simulate a thermosyphon air system have been found in the literature. This may be due to the complex nature of the system or due to the lack of empirical correlations that are available to relate the induced air flow to the temperature gradient which causes the flow.

A thermosyphon air system virtually does not have boundary conditions that are known or can be specified. The air flow in a thermosyphon system is induced by buoyancy forces which are due to the existence of temperature gradients. The air is heated by the heated surface of an absorbing plate which converts solar radiation into thermal energy. The induced air flow in turn affects the heat transfer coefficients between the absorbing plate and the air in the collector, resulting in the temperature of the absorbing plate varying from time to time. These unknowns are not independent.

Akbari and Borgers (1979) set up a finite difference model to study the free convective laminar heat transfer

between the channel surfaces of a Trombe wall. The calculation was done, however, with assumed known constant uniform temperatures of the two surfaces forming the channel. With a similar approach, Borgers and Akbari (1984) studied the case of free convective turbulent heat transfer between parallel plates. The grid size along the channel was reported to be in the order of 10^{-7} m to 10^{-10} m, which is extremely small and would not be practical to use. Marshall *et al.* (1981) investigated the performance of a thermosyphon air system with a computer model. Their model, however, requires the measured data, such as the collector outlet temperature, as input. Kohler (1981) developed a mathematical model for quantitatively examining the performance of thermosyphon air systems, but no validation was provided for the model. Later, Reno (1981) used the model to simulate a thermosyphon air system and reported that the agreement between the measured and calculated temperatures was good only for one case.

Until some better correlations between the induced fluid flow and the driving temperature gradients become available, the possibility of an accurate simulation model for thermosyphon air systems seems remote.

3. SOLAR RADIATION

3.1 Solar-Related Terminology

The solar constant is defined as the intensity of solar radiation on a surface normal to the sun's ray beyond the earth's atmosphere at the mean earth-sun distance of 149,504,000±100 km. According to ASHRAE (1981), the currently accepted value of the solar constant is 1353 Wm⁻². Direct normal solar intensity at the earth's surface on a clear day, I_{DN} , is, however, varying constantly and is expressed as:

$$I_{DN} = \frac{A}{\text{EXP}(B/\text{SIN}\beta)} \quad (3.1)$$

where A = apparent solar irradiation beyond atmosphere (Wm⁻²)

B = atmospheric extinction coefficient, and

β = solar altitude above the horizon (°).

Solar altitude, β , is the angle formed by the sun's rays and their projection on a horizontal plane. Solar azimuth, ϕ , is the angle between the solar ray projection on a horizontal plane and South, and is considered positive when measured east of South and negative when measured west of South. Solar declination, δ , is the angle formed by the line from the centre of the earth to the centre of the sun on a particular day, and the plane containing the earth's equator, as shown in Figure 3.1.

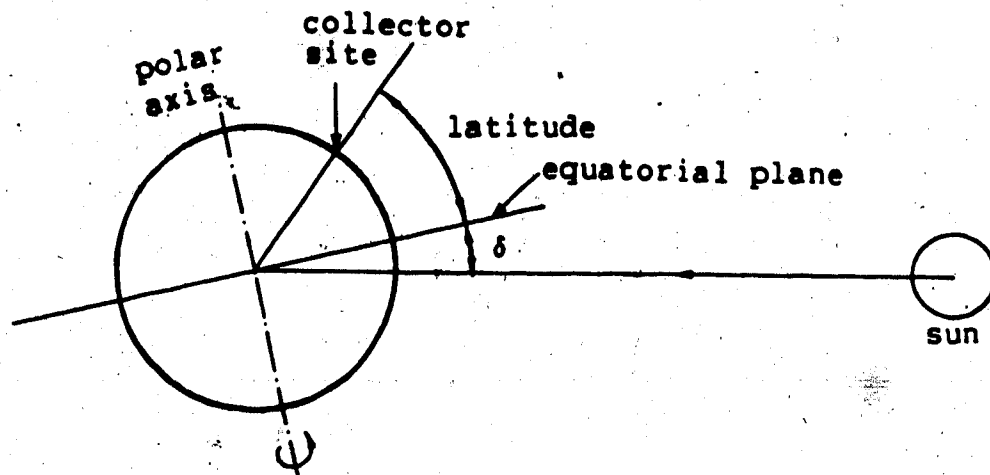


Figure 3.1. Solar declination (adapted from ASHRAE, 1971)

Solar declination is defined as positive when the sun-earth connecting line is in the northern latitudes and negative when the sun is in the southern latitudes.

As the earth progresses along its orbit about the sun, solar declination changes due to the tilt of the earth's polar axis with regard to its orbital plane. Therefore, δ depends on the earth's position in its orbit, i.e. the day of the year.

Williams (1983) suggests the following equation for the calculation of solar declination, δ , with an accuracy of 1 minute.

$$\delta = 0.36 - 22.96\cos(0.9856n) - 0.37\cos(2*0.9856n)$$

$$- 0.15\cos(3 \cdot 0.9856n) + 0.4\sin(0.9856n) \quad (3.2)$$

where n is the day of the year.

The angle of incidence, θ , for a surface is the angle between the incoming solar rays and a line normal to the surface under consideration.

Figure 3.2 shows the angles discussed above.

Apparent solar time (AST) is the time determined by sundial, whereas mean time is the time kept by a clock running at a uniform rate. Equation of time is defined as the variation of apparent time from the mean time due to the earth elliptical orbit and is expressed as ET. Williams (1983) recommends the calculation of ET as follows:

$$\begin{aligned} ET &\approx -14.2\sin\{(n + 7)180/11\} && \text{for } 1 \leq n \leq 106 \\ &= 4 \sin\{(n - 106)180/59\} && \text{for } 107 \leq n \leq 166 \\ &= -6.5\sin\{(n - 166)180/80\} && \text{for } 167 \leq n \leq 246 \\ &= 16.4\sin\{(n - 247)180/113\} && \text{for } 247 \leq n \leq 365 \end{aligned} \quad (3.3)$$

3.1.1 Determination of hour angle, sunrise and sunset time

Hour angle: Hour angle, ω , is shown in figure 3.3. It is the angular displacement of the sun measured as the angle between the projection of the sun's ray on the equatorial plane and the meridional axis in the earth-centered coordinate system. At solar noon on the meridian of the observer, ω is zero degrees. For each hour away from solar noon, ω changes by 15° . Hour angles are, as a convention, positive in the morning and negative in the afternoon. The

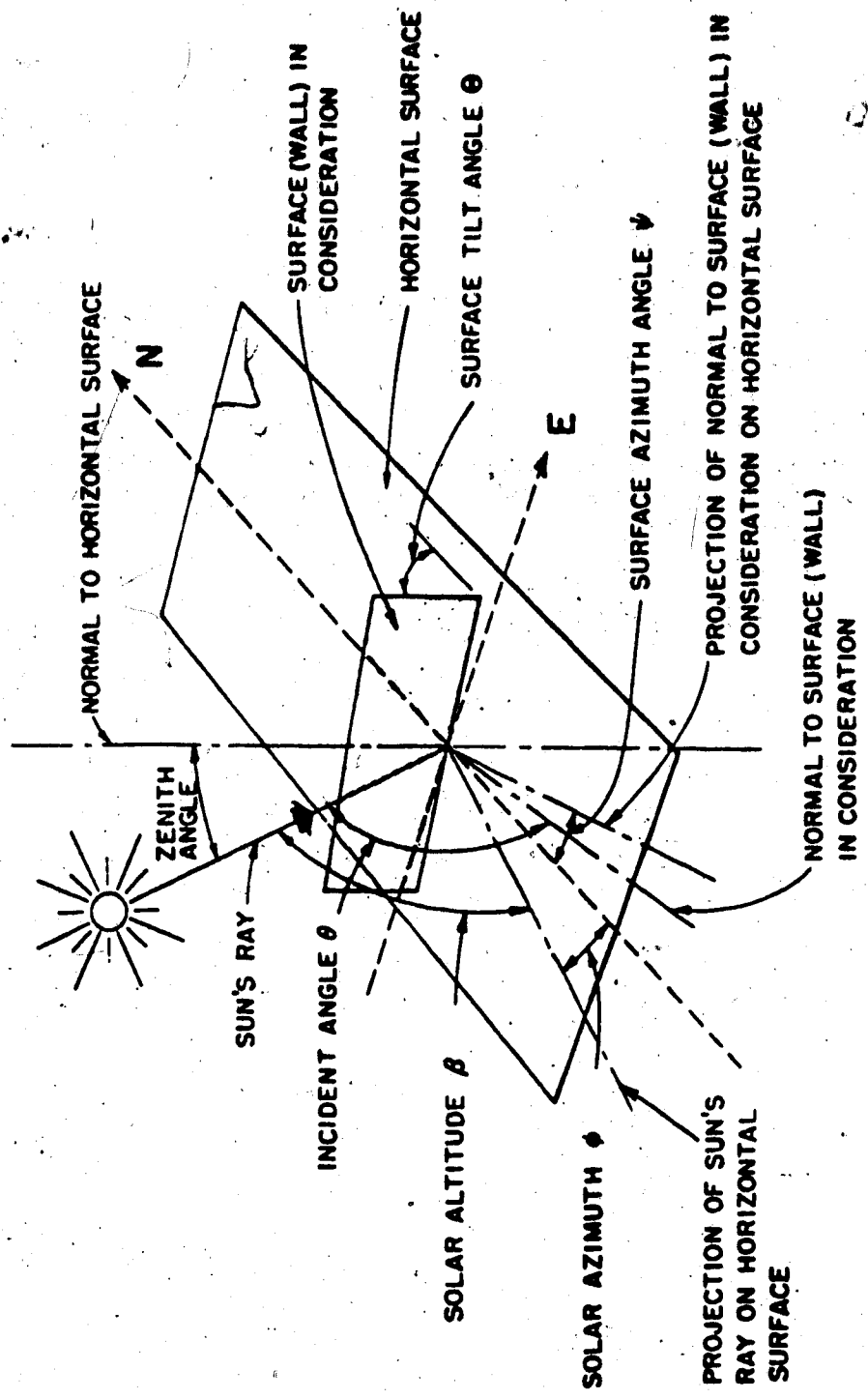


Figure 3.2 Solar angles for a tilted surface (adapted from ASHRAE, 1981)

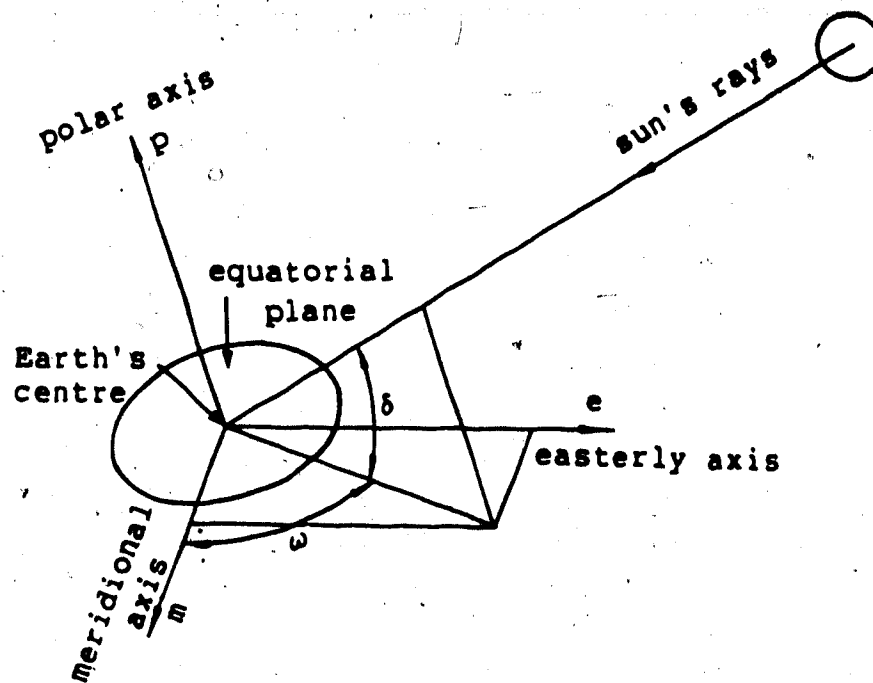


Figure 3.3 Hour angle (adapted from ASHRAE, 1971)

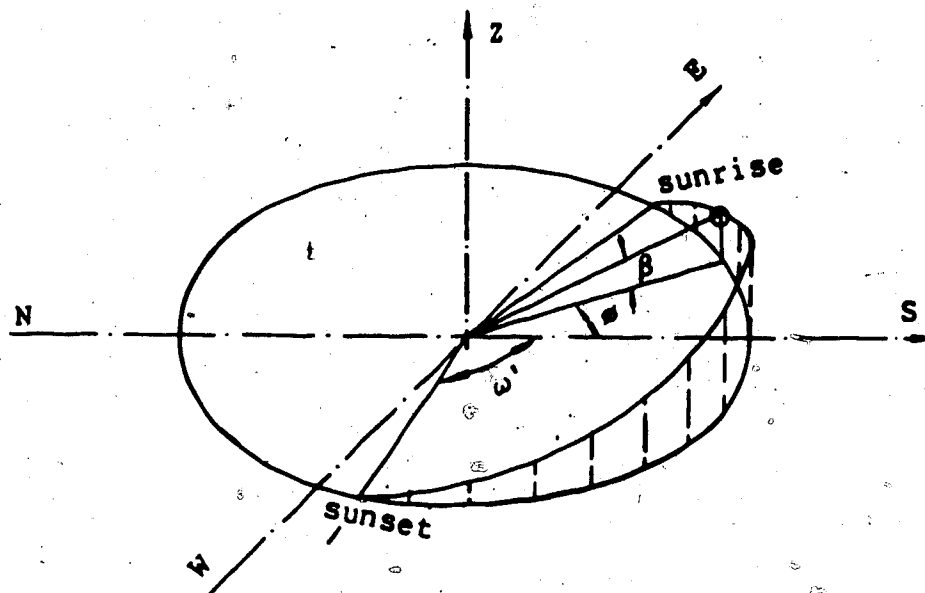


Figure 3.4 Sunrise and sunset times
(adapted from ASHRAE, 1971)

expression for the hour angle is:

$$\begin{aligned}\omega &= 0.25(720 - \text{AST}) \\ &= 180 - 15t - \text{ET}/4 - \text{LSM} + \text{LG}\end{aligned}\quad (3.4)$$

where t = local standard time (hours)

LSM = local standard time meridian (degree) and

LG = local longitude (degree).

For different locations, ASHRAE (1981) gives the values for LSM as in table 3.1.

Sunrise and Sunset Time: Sunrise and sunset times vary from day to day as a result of the motion of the earth in its orbit about the sun. Thus daytime is longer in summer than in winter.

In order to determine the sunrise time and sunset time, the following approach is taken from ASHRAE (1976b).

$$\omega' = \text{COS}^{-1}\{-\text{TAN}(\text{LT})\text{TAN}(\delta)\} \quad (3.5)$$

$$Y = \omega' * 12/\pi \quad (3.6)$$

where ω' and Y are two intermediate parameters and LT is the latitude of the location (degree), positive for north and negative for south.

Sunrise time is then:

$$\text{SRT} = 12 - \text{ET}/60 - (\text{LSM} - \text{LG} + \omega')/15 \quad (3.7)$$

and the sunset time is:

$$\text{SST} = \text{SRT} + 2Y \quad (3.8)$$

Figure 3.4 shows the sunrise time and sunset times, as well as ω' for a location.

Hour angle, ω , as determined by equation 3.4, may be compared with ω' . If $|\omega| \geq |\omega'|$, then the sun is beyond the

Table 3.1. LOCAL STANDARD TIME MERIDIAN

Local Time Zone	LSM, Degrees
Atlantic	60
Eastern	75
Central	90
Mountain	105
Pacific	120
Yukon	135
Alaska-Hawaii	150

horizon, therefore no solar radiation is available.

3.1.2 Determination of solar-related angles

i. Direction cosines of direct solar beam

With reference to Figure 3.5, the direction cosines of the solar beam can be determined as (ASHRAE, 1981):

$$\cos(E) = \cos(\delta)\sin(\omega) \quad (3.9)$$

$$\cos(S) = \cos(\delta)\cos(\omega)\sin(LT) \quad (3.10)$$

$$\cos(Z) = \cos(\delta)\cos(\omega)\cos(LT) + \sin(\delta)\sin(\omega) \quad (3.11)$$

Axis E is pointing east, axis S south and axis Z vertically up.

ii. Solar altitude, β

$$\beta = \sin^{-1}(\cos(Z)) \quad (3.12)$$

iii. Solar azimuth, ϕ

$$\phi = \sin^{-1}\left(\frac{\cos(E)}{\cos(\beta)}\right) \quad \text{for } \cos(S) > 0$$

$$\phi = \pi - \sin^{-1}\left(\frac{\cos(E)}{\cos(\beta)}\right) \quad \text{for } \cos(S) < 0$$

(3.13)

iv. Incidence angle, θ

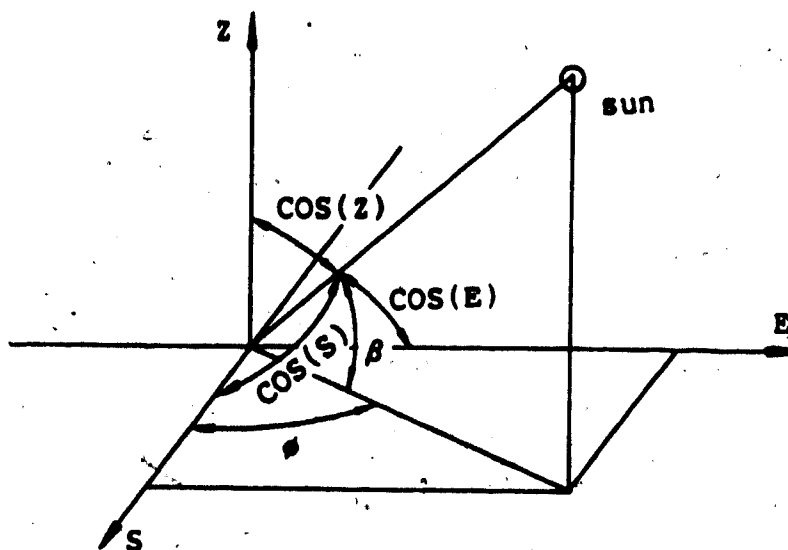


Figure 3.5 Direction cosines of solar beam
(adapted from ASHRAE, 1971)

$$\gamma = \phi - \psi \text{ a.m.}$$

$$\gamma = \phi + \psi \text{ p.m. for surfaces facing east of south,}$$

and

$$\gamma = \phi + \psi \text{ a.m.}$$

$$\gamma = \phi - \psi \text{ p.m. for surfaces facing west of south.}$$

where γ is the surface-solar azimuth (degree), and ψ is the surface azimuth (degree) measured from South.

If γ is greater than 90° the surface is in shade. The incidence angle, θ , then is calculated as:

$$\text{COS}(\theta) = \text{COS}(\beta)\text{COS}(\gamma)\text{SIN}(\Theta) + \text{SIN}(\beta)\text{COS}(\Theta) \quad (3.14)$$

where Θ = tilt angle of the surface from horizontal, (degrees).

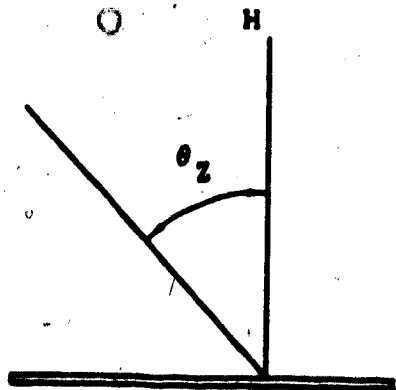
3.2 Solar Radiation Reaching Outer and Inner Surfaces

3.2.1 On outer surfaces

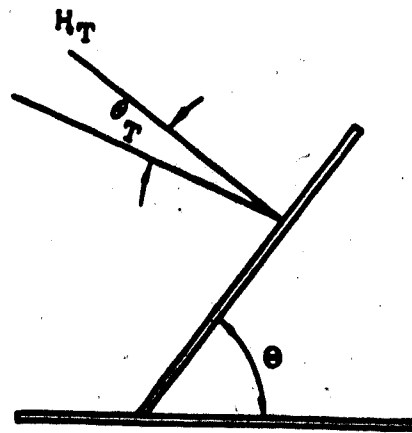
Solar radiation on its way to the earth encounters the atmosphere, clouds and dust. Some portion of the radiation from the sun is reflected or scattered by these clouds and dust at least once. This part of solar radiation reaching the earth's surface is termed as diffuse solar radiation. The portion directly reaching the earth's surface is called direct solar radiation. On a clear day, the solar radiation reaching the earth is typically 90% direct and 10% diffuse. On cloudy days, all of the solar radiation reaching the ground may be diffuse.

The intensity of solar radiation on a fixed surface on the earth's surface varies since such a surface is not always perpendicular to the solar rays. The area of a flat surface, when projected perpendicular to the solar beams, is the product of the actual surface area and the cosine of the angle between the solar rays and the surface normal.

In order to use horizontal total radiation data, the ratio, R_o , of total radiation on a tilted surface to that on a horizontal surface needs to be determined. Liu and Jordan (1963) have derived a model for calculating the ratio by considering the radiation on the tilted surface to be made up of three components: the beam radiation, diffuse solar radiation and solar radiation reflected from the ground which the tilted surface "sees". A surface tilted at slope θ



(a) on a horizontal plane



(b) on a tilted plane

Figure 3.6 Radiation on horizontal and tilted surfaces

from the horizontal sees a portion of the sky dome given by a sky view factor, F_v , and a portion of the foreground given by a ground view factor, F_g . F_v and F_g are determined with the following equations:

$$F_v = \frac{1 + \cos\theta}{2} \quad (3.15)$$

and

$$F_g = \frac{1 - \cos\theta}{2} \quad (3.16)$$

The ratio, R_o , of total radiation on a tilted surface to that on a horizontal surface (Figure 3.6) is:

$$R_o = (H_b/H)R_b + (H_d/H)F_v + F_g\rho \quad (3.17)$$

where R_b , the beam correction factor is given by:

$$R_b = \cos\theta_T / \cos\theta_Z \quad (3.18)$$

where H_b/H = ratio of beam to global solar radiation

H_d/H = ratio of diffuse to global solar radiation

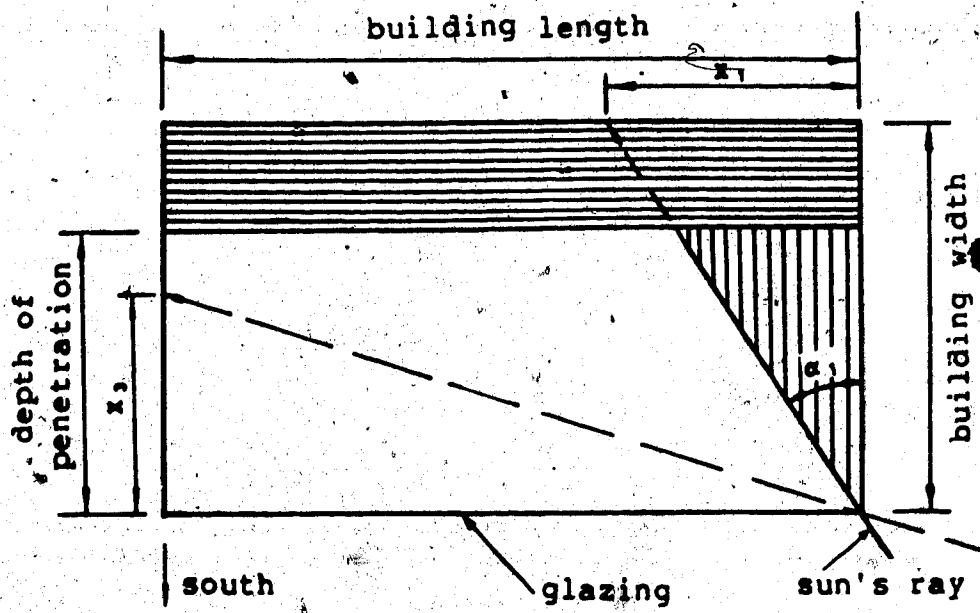
ρ = ground reflectance (0.7 for snow cover and 0.2 for no snow), and

θ_T, θ_Z = angles (degrees) of incidence for horizontal and tilted surface respectively.

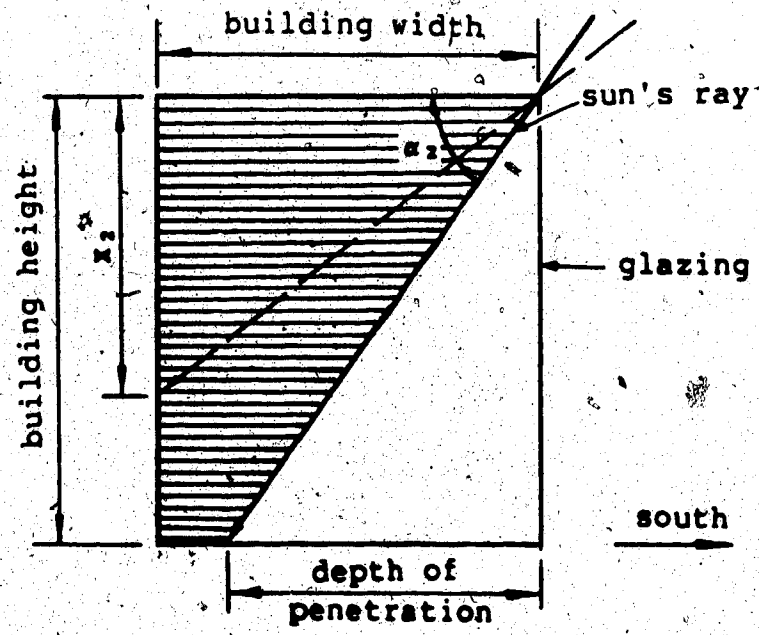
The intensity of solar radiation received by each of the outer surfaces of a building can, therefore, be determined with equations 3.17 and 3.18, once the global solar radiation on a horizontal surface at the same location is known.

3.2.2 Solar radiation reaching interior surfaces of a direct gain building

For a building with the entire south wall being glazed and facing due south, the direct solar radiation reaching interior surfaces is a function of the sun's position in the sky. The length of the area of an interior surface illuminated by the solar rays is termed *DEPTH OF PENETRATION* (Lebens, 1979). Figure 3.7 shows the possible patterns of illumination in the morning. In Figure 3.7, α_1 and α_2 are two angles that are used to calculate the illuminated areas of the interior walls, together with x_1, x_2 and x_3 , which are the lengths on different walls associated with the solar



(a) plane view.



(b) section view

Figure 2.7 Morning illuminations of room interior surfaces

illumination. Similar patterns may be found for the afternoon hours. The illuminated areas of the interior wall surfaces change and may be determined at each time instant. Once the sun is above the horizon, the ceiling of the room receives only diffuse and ground reflected solar radiation that enters the room in all possible directions through the glazed area.

The total amount of solar radiation reaching an interior surface, for example the floor surface, is calculated as:

$$H_{\text{floor}} = I_{\text{beam}} \tau \cos \theta S'_{\text{floor}} + I_{\text{diff}} \tau S_{\text{floor}} \quad (3.19)$$

where I_{beam} = beam solar radiation intensity (Wm^{-2})

τ = transmittance of glazing

θ = incidence angle of solar beam ($^{\circ}$)

S'_{floor} = illuminated floor area (m^2)

I_{diff} = diff. solar rad. intensity (Wm^{-2}), and

S_{floor} = total floor area (m^2).

3.2.3 Plastic glazing and its treatment in the simulation

The transmittance of glass for long-wave radiation, for all practical purposes, is considered to be zero, whereas that of most plastics is not. The assumption of only gray surfaces being involved in the radiant heat transfer inside the room seems not to be justified, since a plastic window on the South wall is not totally opaque to long-wave

radiation. However, according to Whiller (1963), Tedlar is completely opaque to radiation between wavelengths of 0.9 - 13 microns and about 45% of radiation by surfaces in the temperature range 0 to 200°C lies in this wavelength region. A constant value of 30% is suggested for transmittance of 0.102 mm Tedlar for long-wave radiation. Normal transmittance of fibreglass-reinforced polyester is, according to O'Brien-Bernini and McGowan (1984), 7.6% for long wave radiation and 87% for short wave radiation.

According to the manufacturer (Lasco Industries, 1982), the glazing material used in the Harrold farm shop is made of fibreglass-reinforced polyester with surfaces painted with Tedlar. The combined transmittance for longwave radiation therefore may be considered to be negligible. Although this assumption may lead to overestimating of the performance of the system, it allows the calculation of radiant heat transfer within the room to be simplified a great deal. Thus the trapping effect discussed previously for glass glazing can be applied directly to the case for the plastic glazing.

More than one layer of glazing may be used in the design of direct gain systems or active systems to minimize the heat losses through the glazing. In order to determine the amount of solar radiation transmitted, reflected and absorbed by each layer of glazing, an algorithm derived by Edwards (1977) was integrated into the computer model. For the direct gain system, the room, in place of an absorber

plate, is assumed to have a reflectance of 0.05 and an absorptance of 0.95.

4. MONITORING OF THERMAL PERFORMANCE OF THE EXISTING SHOP

4.1 Facilities

The structure, located at 54° N. latitude and 113° longitude, is 14.64 m long and 4.88 m high, with bottom width of 9.76 m and top width of 5.63 m. The windowless building is steel-framed, has steel siding on the outer surfaces and is oriented with one of its inclined walls (long dimension) facing due south, on which the thermosyphon air panels were constructed. The slope of the south side wall is 67° from horizontal. The walls and ceiling are insulated with 152.4 mm fibreglass batts (RSI=3.5) with plywood sheathing on the interior surfaces. One overhead door (double sliding) facing west is insulated with 38 mm extruded polystyrene (RSI=7.5), and the uninsulated floor is poured concrete. The roof slope is only 5° measured from horizontal (Figure 4.1). The building is not air tight. Major air leakage is around the overhead door facing West.

The absorbing surface of the collector is made of steel siding painted black with Tremclad Rust Paint, covered with fibreglass reinforced, clear plastic panels (Lascolite) and has a total collection area of 4.27 x 13.42 m². Two air channels were formed, one between the absorbing plate and the glazing (front-path) and the other between the absorbing plate and the back insulation (back-path). The spacing for the front-path is 63.5 mm and that for the back-path is 50.8 mm. There are 44 air inlets at the bottom of the collector

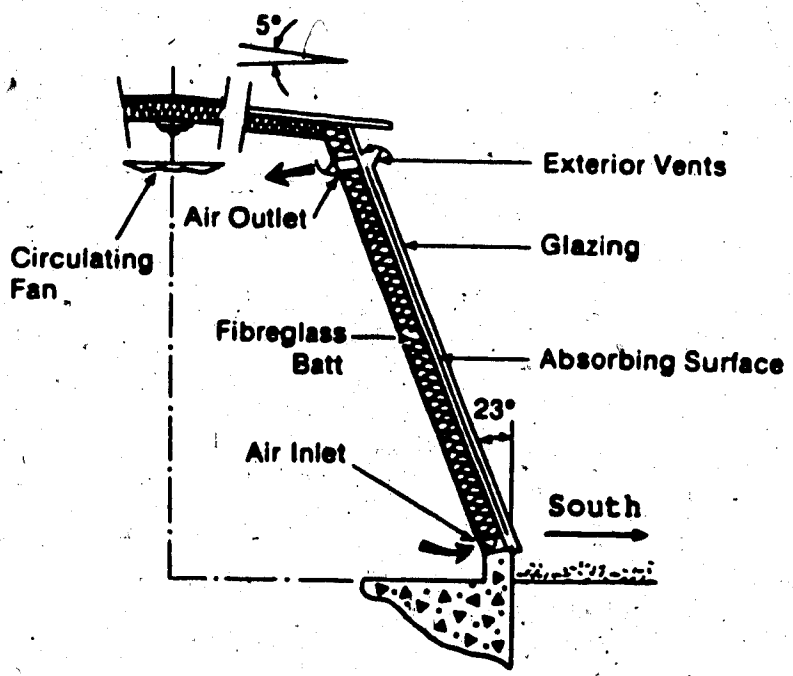
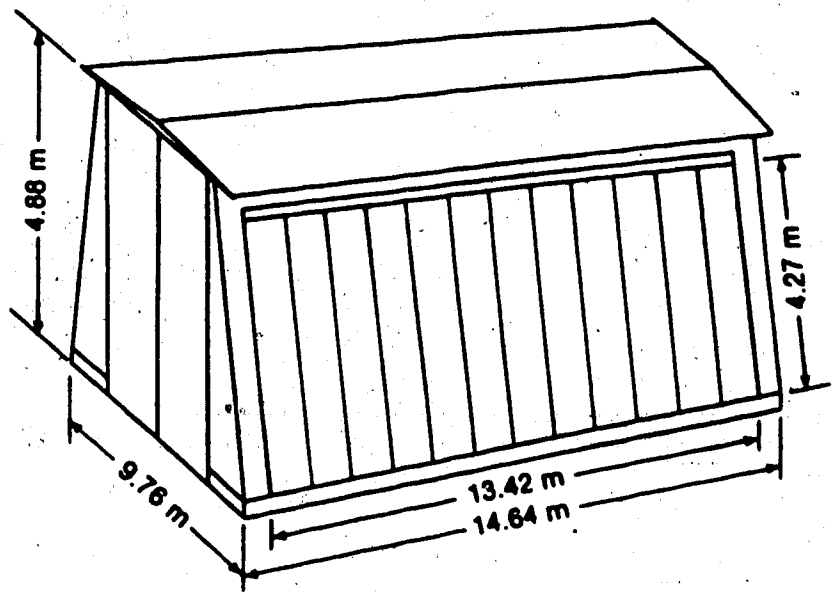


Figure 4.1 A view of the shop and the solar collector

and corresponding 44 air outlets at the top, each $\phi 76$ mm by 205 mm, spaced horizontally at 300 mm on center. One-way dampers consisting of "chicken wire" mesh and plastic film (Saran Wrap), are installed at the air inlets and outlets to restrict back draft that may occur at night. There are exterior vents at the top of the collector that can be opened manually in summer to let out excess heat collected in order to keep the room air from overheating and to prevent the build-up of high temperature in the collector. Two ceiling-mounted circulation fans are installed for destratification of the room air but were not used during the monitoring periods. There is a furnace with a capacity of 29.3 kW installed in the shop but, according to the owner, this was never used to heat the entire shop.

During the monitoring periods, the shop was in use, full of lumber, farm tools and machinery. The eastern end of the shop was partitioned into two rooms to a height of about 2.5 m and is heated with the furnace when used.

4.2 Instrumentation and Monitoring System

Global solar radiation was measured by a pyranometer (Model MR-5, Hollis Observatory, Nashua, NH) mounted horizontally on the roof of the shop immediately above the collector. The amount of solar radiation falling on the inclined solar collecting surface then was estimated with the equations suggested by Duffie and Beckman (1974). Ten thermocouples (type T) were used to measure temperatures at

Table 4.1. THERMOCOUPLES AND THEIR LOCATIONS

sensor #	description of location
1	outside temp, sheltered on the northside of the shop
2	temp at the top of absorbing plate
3	air temp at the inlet, east bottom
4	air temp at the outlet, east top
5	air temp at the outlet, west top
6	air temp at the inlet, west bottom
7	room air temp, 0.6 m from ceiling
8	room air temp, 1 m from floor
9	air temp in front-path, 1.5 m up from bottom
10	air temp in front-path, 1.5 m down from the top

different locations. Table 4.1 lists these thermocouples and their locations for the monitoring of the building thermal performance. Two thermocouples, one east and one west, were placed at the top air outlets and, similarly, two at the bottom air inlets in order to get mean temperatures at those points. Two more thermocouples were placed along the front-path of the collector so that the temperature distribution of the front-path could be determined. Lower level and upper level room air temperatures were sensed to detect thermal stratification.

The air flow velocity was measured with a thermal anemometer (hot thermistor type; Model TA3000, Airflow Development Ltd., High Wycombe, England) located at the bottom air inlet on the center of the collector. By continuity, the amount of air flowing into the collector was expected to be equal to that flowing out. This was checked *in situ* with two anemometers (Model TA3000) and the

difference of air velocities at the top and bottom was seen to be negligible. This measured air velocity was taken as the average velocity for the whole collector and was used in the calculation of energy collection.

Wind speed and direction were measured also during the monitoring periods. A light-weight cup anemometer and a light-weight wind vane (Models 1005-DC and 1010-360, Sierra Instruments, Redlands, CA.) were mounted on a pole 3 meters above the roof. The outputs from all these sensors were recorded by a data logger (Model CR21, Campbell Scientific, Edmonton, AB.) at 15 minute intervals. Each monitoring cycle lasted about one week. At the end of a monitoring cycle, data were down-loaded from the data logger memory to magnetic disk on a microcomputer for further analysis.

4.3 Monitored Performance

The monitoring of the thermal performance of the building was done for about one week in every month from October, 1985 to March, 1986. The summer performance also was monitored in July, 1985, when the exterior vents were open. The monitoring system, however, was found to be malfunctioning under severe cold conditions (about -30°C) in November, 1985, and, therefore, the data for that month were not used in the analysis that follows. The data logged for March 1986 were not used either since the monitoring system was not set up and adjusted appropriately.

Table 4.2. DAILY ENERGY COLLECTION & COLLECTOR EFFICIENCY

mm/dd/yy	ΣQ , KJ/m ²	I_0 , KJ/m ²	η , %
10/18/85	4,445.0	13,212.1	33.6
10/19/85	1,726.9	10,497.6	16.5
10/20/85	2,747.6	12,056.6	22.8
10/21/85	2,540.0	13,339.7	19.0
12/20/85	3,060.5	9,182.3	33.3
12/21/85	2,876.4	11,020.7	26.1
12/22/85	1,311.4	7,282.7	18.0
02/05/86	886.7	8,172.3	10.9
02/06/86	4,195.5	13,458.8	31.2
02/07/86	457.9	6,765.6	6.8
02/08/86	1,239.8	9,966.3	12.4
02/09/86	2,069.6	10,779.7	19.2
02/10/86	3,080.2	12,559.8	24.5
mean	2,356.7	10,638.0	21.1

Table 4.2 shows the daily energy collection (ΣQ) by the collecting system, the total available solar radiation incident (I_0) on the inclined collector surface and the calculated daily efficiency (η) of the collector for typical days over the monitoring period. (The half-day data were not used.) More heat is seen to have been collected and transported into the shop during sunny days such as Oct. 18, Dec. 20 and Feb. 6. The daily collector efficiency for those days was above 30%. On cloudy days, on the other hand, the daily efficiency could be as low as 6.8%.

Figures 4.2, 4.3 and 4.4 show the measured temperatures on three typical sunny days (Oct. 18, 1985; Dec. 21, 1985; Feb. 6, 1986). High temperatures of 52 - 58°C at the air outlet were observed at mid-day for those three days, while the room mean temperature rose less than 10°C and remained relatively uniform throughout the day. The thermal behavior of the building during two cloudy days is plotted in Figures

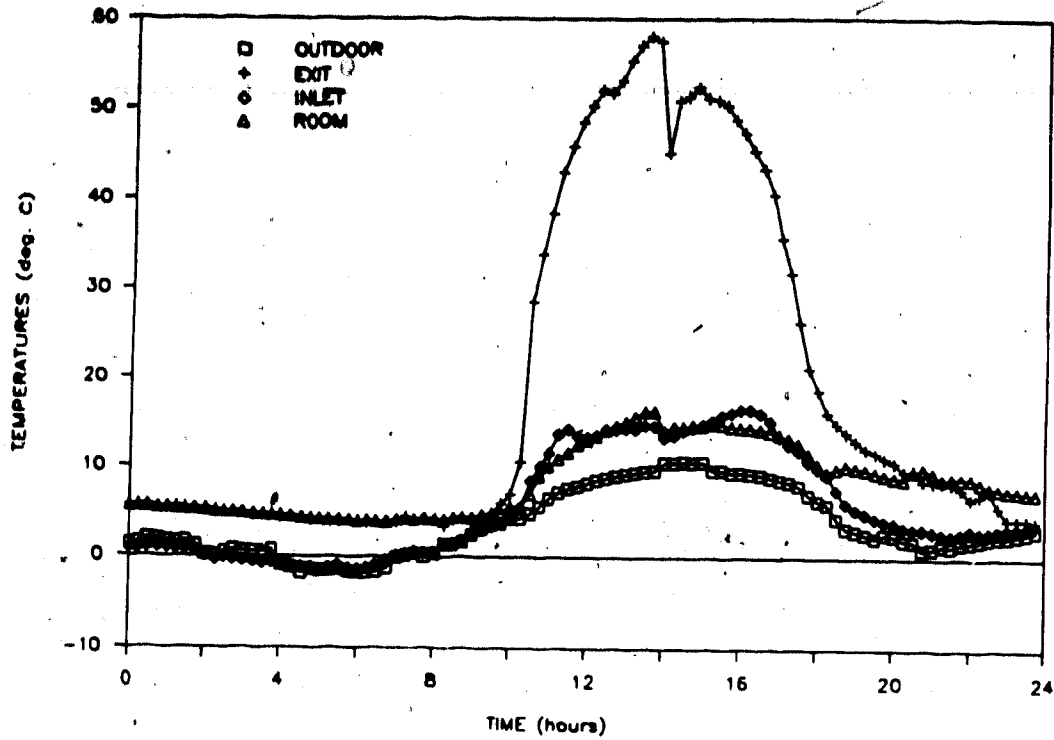


Figure 4.2 Monitored performance for Oct. 18, 1985

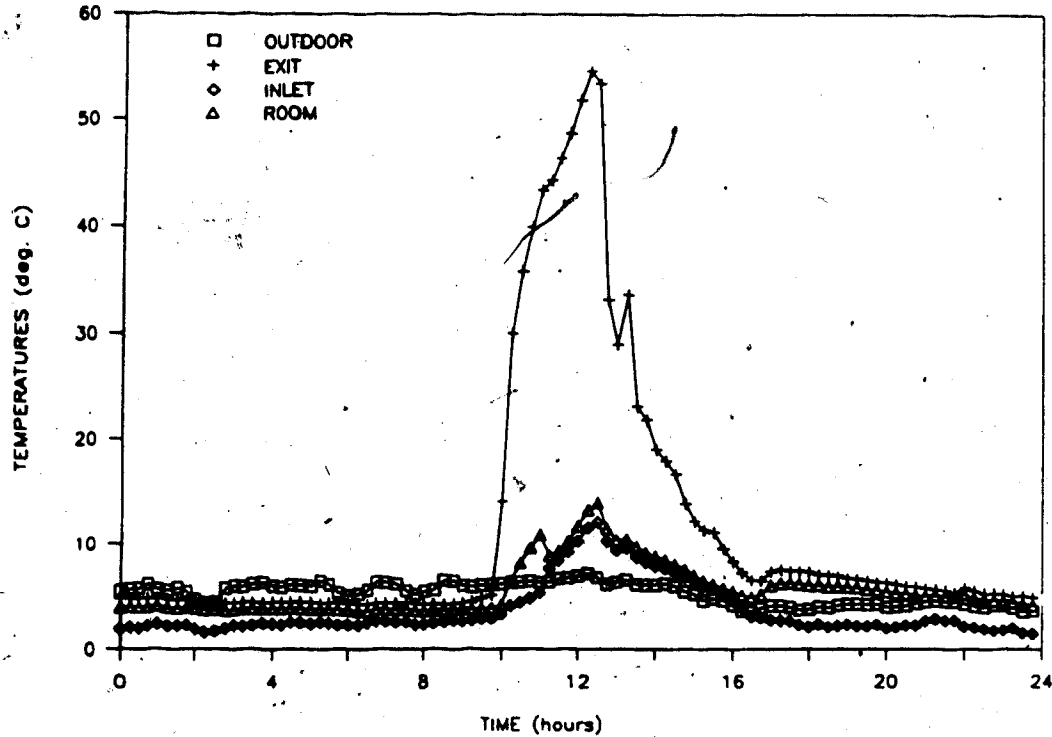


Figure 4.3 Monitored performance for Dec. 21, 1985

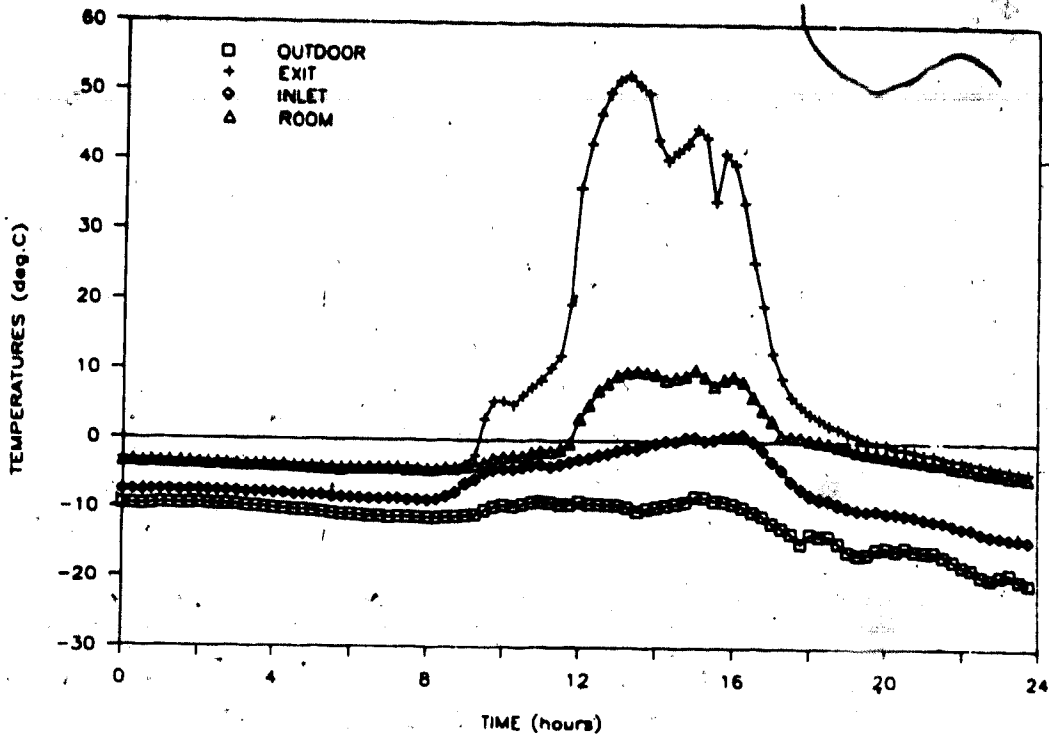


Figure 4.4 Monitored performance for Feb. 6, 1986

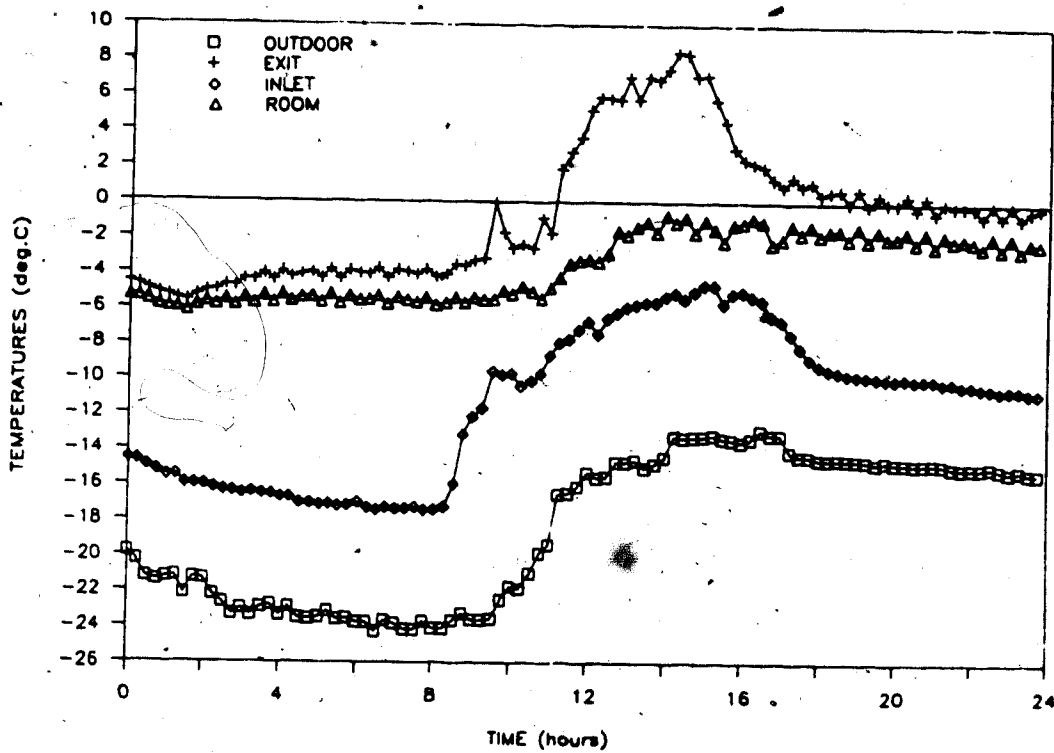


Figure 4.5 Monitored performance for Feb. 7, 1986

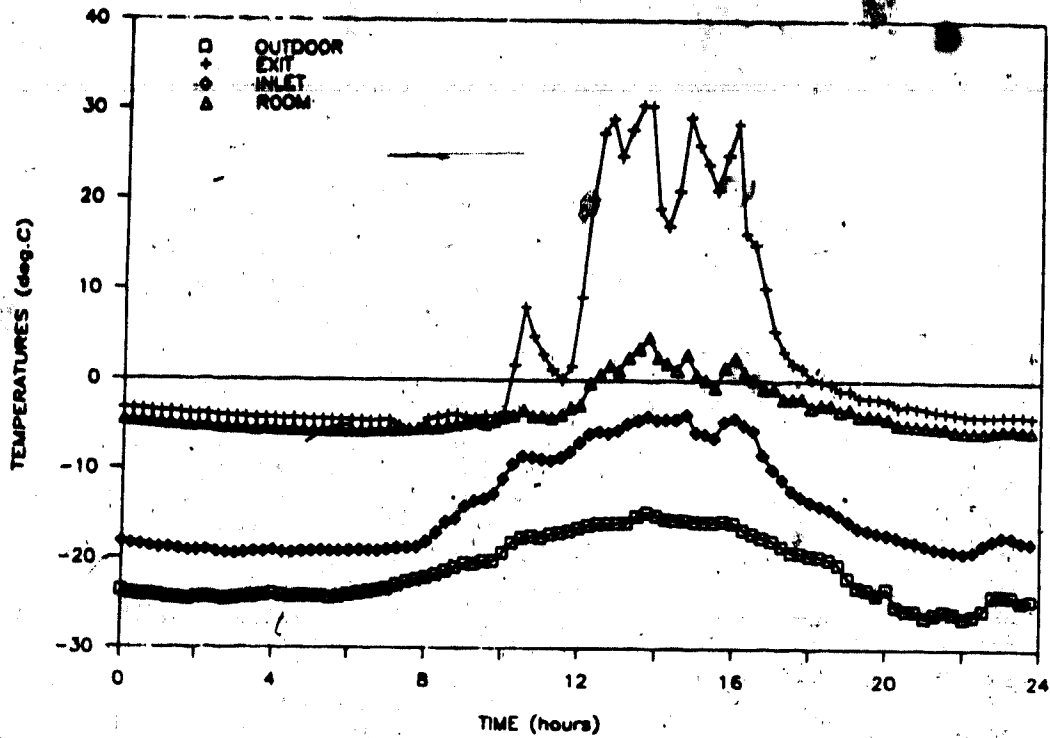


Figure 4.6 Monitored performance for Feb. 9, 1986

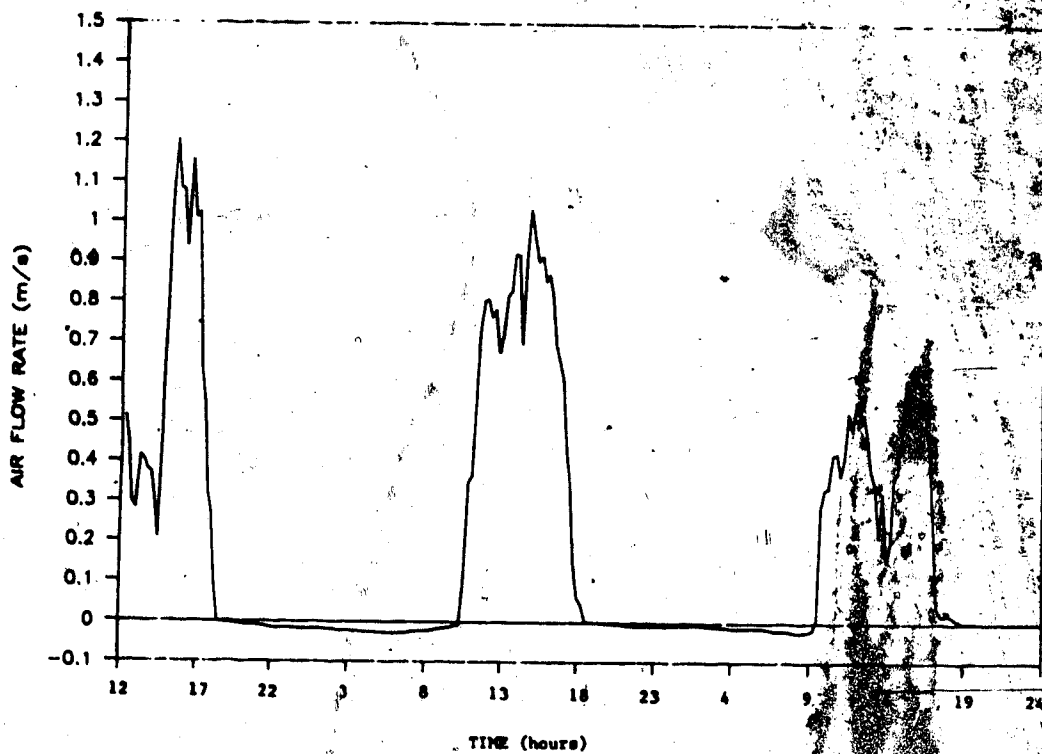


Figure 4.7 Measured air flow velocity for Oct. 17-19, 1985

4.5 and 4.6. The air temperature at the outlet is seen to have fluctuated with the varying availability of solar radiation. The room temperature was observed to be about 20°C higher than outdoor temperature during cold days (Figures 4.5 and 4.6). The measured air flow velocity (Figure 4.7) varied dramatically from day to day, depending upon the temperature difference between the inlet and outlet air temperatures. In spite of the presence of the back draft dampers, reverse air flow did exist, although the velocities were quite small. Figure 4.8 is a typical plot showing the thermal stratification in the shop (circulation fans not operating). The maximum difference in temperature between the upper and the lower levels of the shop was approximately 16°C.

As mentioned above, the summer performance of the building also was observed in July, 1985. No overheating was found either inside the shop or in the collector. During this period the exterior vents on the collector were open day and night and the door was open during the daytime.

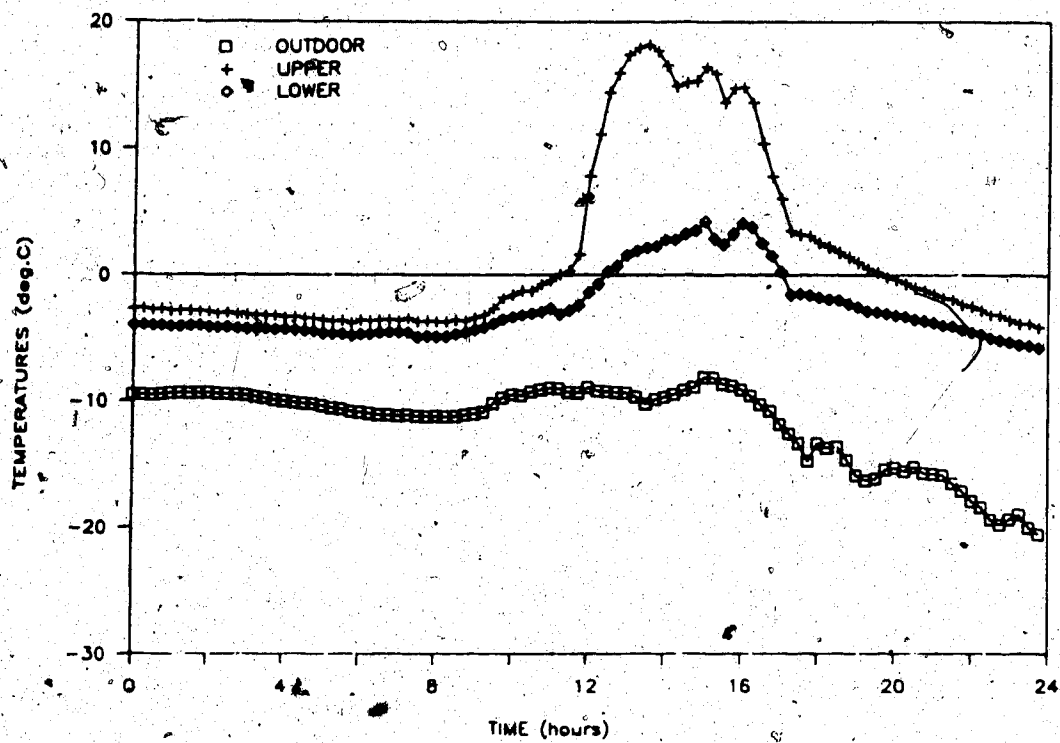


Figure 4.8 Measured thermal stratification of room air
(Feb. 6, 1986)

5. DIRECT-GAIN MODEL

The thermal balance method used in the development of the direct gain model in this study is one of the methods often employed in the calculation of the thermal performance of direct-gain systems (Williams, 1983). The thermal effect of floor concrete of a building is taken into account by its thermal response factors (Stephenson and Mitalas, 1967). A computer program developed by Mitalas and Arseneault (1972) was used to find these response factors, which are given in Appendix A.1.

5.1 Model Development for a Direct Gain System

5.1.1 Assumptions

There are some assumptions in the development of the model that actually are associated with the theory of the thermal balance approach. Assumptions, however, are not uncommon in simulation studies (Duffie, 1978) since, in many cases, they simplify the calculation procedure while not invalidating the simulation results.

The following assumptions were used in the formulation of the direct gain model.

1. Room air temperature is uniform everywhere inside the building.
2. Latent heat is not significant due to low moisture content of the room air.
3. Amount of heat added to the room due to lights and other

equipment is negligible.

4. Linear equations are adequate to describe the heat transfer processes in the building. This allows the use of response factor techniques.
5. The interior and exterior surfaces of the building envelope are gray, and all radiation properties of the surfaces are independent of wavelength.
6. The surface temperature of any wall is uniform.
7. Incident solar beam radiation, if any, is uniformly received by a surface, and diffuse solar radiation is in every direction.
8. The ground temperature is constant, and the thermal effects of the building components, except for the floor, are small and negligible.

5.1.2 Model development

In order to simplify the equations that are derived in this chapter, the following numbers and letters are used as subscripts to carry specific meanings (valid only in this chapter).

- 1 --- floor surface
- 2 --- interior surface of the rear wall
- 3 --- interior surface of the West wall (overhead door)
- 4 --- interior surface of the ceiling
- 5 --- interior surface of the East wall
- 6 --- interior surface of the South wall (glazing)
- 00 -- ambient air (outdoor)

d --- ground underneath the building

m --- room air

s --- solar radiant heat gain

x --- conductive heat transfer

y --- convective heat transfer

z --- radiant heat transfer

A general equation of a heat balance at surface i of the simulated building (Figure 5.1), at any time t is given below:

$$Q_{x,i}(t) + Q_{y,i}(t) + Q_{z,i}(t) + Q_{d,i}(t) = 0 \quad (5.1)$$

For the floor surface the conductive heat gain is:

$$Q_{x,i}(t) = \sum_{j=0}^{nr} a_j T_i(t-j) - \sum_{j=0}^{nr} b_j T_d + \sum_{j=0}^{nr} c_j Q_{x,i}(t-j) \quad (5.2)$$

where a_j , b_j and c_j = response factors of the floor slab

$Q_{x,i}(t-j)$ = conductive heat gain history, and

nr = number of response factors to be used.

The convective heat gain is:

$$Q_{y,i}(t) = h_i(T_m(t) - T_i(t)) \quad (5.3)$$

where h_i is the surface heat transfer coefficient of the floor ($Wm^{-2}C^{-1}$), and is determined according to ASHRAE (1971).

Radiant heat gain from other surfaces inside the building can be estimated as:

$$Q_{z,i}(t) = \sum_{k=1}^{ns} G_{ik}(T_k(t) - T_i(t)) \quad (5.4)$$

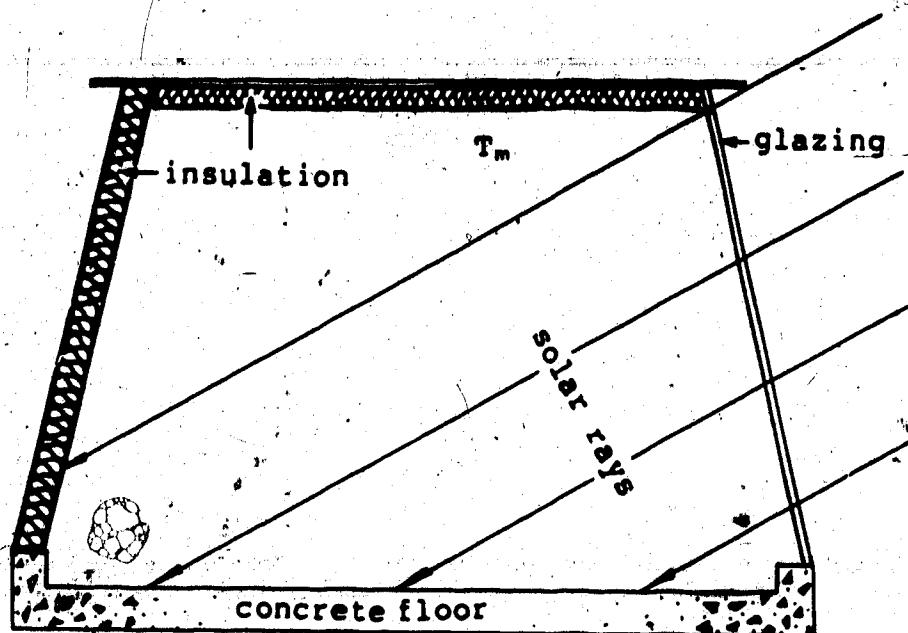


Figure 5.1 A sketch of the simplified direct-gain system

where n_s = number of surfaces within the room space

$$G_{1,k} = 4\sigma\epsilon_1 F_{1,k} (T_0 + 273)^4$$

T_0 = reference temperature ($^{\circ}\text{C}$)

(often room temperature is used as T_0 .)

$F_{1,k}$ = angle factor between surface 1 and k, and

σ = Stefan-Boltzmann constant.

The evaluation of angle factors was discussed in chapter 2. The specific values of the angle factors used for the simulated direct gain system are listed in Appendix A.2. Solar radiant heat gain of the floor surface can be written as:

$$Q_{s,1}(t) = \alpha_1 I_1(t) S'_{1,1}(t) / S_1 \quad (5.5)$$

where α_1 = absorptance of the floor surface

$I_1(t)$ = intensity of solar radiation reaching

the floor (Wm^{-2})

$S'_1(t)$ = floor area illuminated (m^2), and

S_f = total floor area (m^2).

$I_1(t)$, $S'_1(t)$ are time-dependent variables and can be determined as outlined in chapter 2. Substituting equations 5.2 through 5.5 into equation 5.1 and rearranging terms result in:

$$A_{1,1}T_1 + A_{1,2}T_2 + A_{1,3}T_3 + A_{1,4}T_4 + A_{1,5}T_5 + A_{1,6}T_6 = B_1 \quad (5.6)$$

where $A_{1,1} = a_0 + h_1 + \sum_{k=1}^{n_1} G_{1,k}$

$$A_{1,j} = -G_{1,j}, \quad (j = 2, 3, \dots, 6) \text{ and}$$

$$B_1 = Q_{s,1}(t) + h_1 T_m - \sum_{j=1}^{n_1} a_j T_1(t-j) + \sum_{j=0}^{n_1} b_j T_4 - \sum_{j=0}^{n_1} c_j Q_{x,1}(t-j).$$

The energy balance equations for the wall surfaces and for the ceiling surface may be similarly obtained. The conductive heat gain, however, is determined for each of the surfaces with the assumption that the wall is of small thermal mass. For surface j ($j=2, 3, \dots, 6$), the equation of the thermal balance is identified as:

$$A_{j,1}T_1 + A_{j,2}T_2 + A_{j,3}T_3 + A_{j,4}T_4 + A_{j,5}T_5 + A_{j,6}T_6 = B_j \quad (5.7)$$

where $A_{j,1} = h_j + TU_j + \sum_{k=1}^{n_1} G_{j,k}$

$$A_{j,k} = -G_{j,k} \quad (k = 1, 2, \dots, 6)$$

$$B_j = h_j T_m + TU_j T_{s,1,j} + Q_{s,j}$$

$$G_{j,k} = 4\sigma\epsilon_j F_{j,k} (T_0 + 273)^2$$

$F_{j,k}$ = angle factor between surface j and surface k

TU_j = total heat transfer coefficient of wall j from its interior to its exterior surface ($Wm^{-2}C^{-1}$)

$T_{s,j}$ = sol-air temperature for wall j ($^{\circ}\text{C}$), and

$Q_{s,j}$ = solar radiation reaching surface j (Wm^{-2}).

From equations 5.6 and 5.7, a general matrix equation is obtained as follows:

$$[A]\{T\} = \{B\} \quad (5.8)$$

The above matrix equation is solved to determine the unknown temperatures of the interior wall surfaces, only when the room air temperature is known. An iterative solution is required since the room air temperature is an unknown and, in fact, is what is required to be determined.

From an energy balance on the entire room air, the following equation is obtained based on the newly-calculated temperatures of the interior surfaces of the building.

$$\sum_{j=1}^{n_s} S_j h_j (T_j - T_m) + \rho_m C_p \dot{w}_{xx} (T_{o,o} - T_m) = \rho_m C_p V_m \frac{dT_m}{dt} \quad (5.9)$$

where ρ_m = density of room air (kgm^{-3})

C_p = specific heat of room air ($\text{Jkg}^{-1}\text{ }^{\circ}\text{C}^{-1}$)

V_m = volume of room air (m^3), and

\dot{w}_{xx} = rate of air leakage (m^3s^{-1}).

The first derivative of the room air temperature with respect to time on the right-hand side of equation 5.9 can be approximated by the finite-difference method as:

$$\rho_m C_p V_m \frac{dT_m}{dt} = \rho_m C_p V_m \frac{T_m - T_m}{\Delta t} \quad (5.10)$$

where T_m is the room air temperature at the previous time

and Δt is the time increment. Combining equations 5.9 and 5.10 and rearranging terms results in:

$$T_m = \frac{W_1 T_m + W_2 T_{oo} + \sum S_j h_j T_j}{W_1 + W_2 + \sum S_j h_j} \quad (j=1, 2, \dots, 6) \quad (5.11)$$

where $W_1 = \rho_m C_{p_m} V_m / \Delta t$ and $W_2 = \rho_m C_{p_m} \dot{V}_{x,x}$.

5.2 Determination of Surface Heat Transfer Coefficients

5.2.1 Interior surfaces

Heat transfer to or from an interior surface is mainly by natural convection and thermal radiation. In general, the surface heat transfer coefficients for convection and radiation are temperature-dependent variables. In many thermal dynamic calculations, however, the surface film transfer coefficients are assumed independent of the surface temperatures (Winn, 1982; Subbarao *et al.*, 1983; Mehta and Woods, 1980). ASHRAE (1971) propose a method of estimating an interior surface heat transfer coefficient according to the state of room air adjacent to the surface. For moving air (due to natural convection) the heat transfer coefficient for the surface is:

$$h = 11.0 \text{ (Wm}^{-2}\text{°C}^{-1}\text{)} \quad (5.12)$$

5.2.2 Exterior surfaces

The convective heat transfer occurring at the exterior surfaces of a building is a mixture of natural and forced

convection. Whenever wind blows onto or across a heated surface, the film coefficient of heat transfer will depend on many factors, such as the wind attack angle with respect to the surface and the surface geometry. ASHRAE (1977) recommend the following correlations for the average coefficients of heat transfer for all orientations of building surfaces:

$$h_o = 5.5 + 2.7U_{oo} \quad \text{for glass} \quad (5.13)$$

$$h_o = 10.21 + 4.57U_{oo} \quad \text{for brick} \quad (5.14)$$

$$h_o = 11.35 + 11.7U_{oo} \quad \text{for stucco} \quad (5.15)$$

where h_o is in $\text{Wm}^{-2}\text{C}^{-1}$ and U_{oo} is the wind velocity in ms^{-1} .

Equation 5.13 was used for the glazing and for the metal sheets of the shop walls.

5.3 Solution Procedure and Sampling Time Interval

Matrix equation 5.8 is solved in the program using the Gaussian elimination method (Leon, 1980) for each step of calculation. A value of the room air temperature, T_m , is assumed, then the interior surface temperatures are computed. Afterwards, a new room air temperature is calculated based on the newly-computed temperatures of the interior surfaces, and is compared with the assumed T_m . The new T_m replaces the assumed T_m for the next iteration if a prescribed accuracy is not met. If the difference between the new and the assumed T_m is within the given accuracy, the solution to the set of unknown surface temperatures and the

room air temperature is found. Then, the time is advanced by one increment. The flowchart for the direct-gain model can be found in Appendix A.3.

The time interval used for the calculation of transient heat transfer through buildings with response factor techniques usually is one hour (ASHRAE 1981; Stephenson and Mitalas, 1967). Many tabulated response factors for different types of wall structures are based on the one-hour interval (ASHRAE 1977). In this study, however, a 1/4 hour time interval was used, since, the existing shop was monitored on a 1/4 hour basis. Therefore, a one-to-one comparison can be made between the simulated direct-gain system and the existing farm shop.

The program developed by Mitalas and Arseneault (1972) is capable of calculating Z-transfer coefficients (response factors) for different time intervals.

The simulation program of the direct-gain system (see Appendix A.4 for the program listing) requires two input files. The first contains information on the building's physical dimensions, the thermal properties of the building materials, the orientation of the building surfaces, and the location of the building. Simulation run control parameters, floor response factors, initial temperatures and an estimated cloudiness factor also must be included in the file. The format of the first file and a sample input file used for the simulation runs are shown in Appendix A.5.

The second input file is the data file containing the measured solar radiation, wind velocity and outdoor temperature, as well as the monitored room temperature of the real structure.

The output file of the program contains detailed information that is fed to the model through the first file. In addition, the effective thermal properties of the cover system, the day of the year and the sunrise and sunset times of the day are printed. Then, five-columns of data are printed. They are, in sequence, time of the day, global solar radiation, outdoor temperature, measured room air temperature, and calculated room air temperature. The output file can be easily modified to a format suitable for plotting. Appendix A.6 shows a sample of the output file.

6. ACTIVE MODEL

6.1 Model Development for Active Collector

The modelling of the collector in a solar heating system is the crucial step in the whole modelling procedure, since an accurate calculation of the collector's performance is required to provide information for the assessment of the collecting system such as collector efficiency and the heat gain into the building. Currently, the most common approach used in modelling an active solar collector is called the Hottel-Whillier-Bliss model (Duffie and Beckman, 1974). The Hottel-Whillier-Bliss model assumes a steady-state condition, a uniform temperature across the collecting surface. A collector heat removal factor is used to correct these assumptions. The collector heat removal factor, however, is a function of a collector efficiency factor and an overall collector heat loss coefficient, which includes the effects of convection and long-wave re-radiation losses from the top of the collector. The radiant heat transfer coefficients are temperature-dependent, and iterations are necessary in the solution procedure (Shewen *et al.*, 1980).

Compared with the Hottel-Whillier-Bliss model, the method developed below seems simpler, more straight-forward and physically more meaningful. The model works under transient conditions and does not require the assumption of constant fluid properties. The radiant heat exchanges between surfaces in the collector and between the outermost

glazing surface and the ambient air are calculated in each of the computational steps.

The algorithm is derived from the basic energy balance laws that govern the heat exchanges between the fluid and the surfaces in contact with the fluid, and between surfaces that "see" each other. The collector is divided, along its flow passage, into a number of subregions (Figure 6.1) analogous to the treatment in the finite-element theory (Cook, 1981). The temperature within each subregion is assumed to be uniform (this is true if the number of the subregions approaches infinity.), and a node at the center of the region is used to perform a regional energy balance. The time interval used can be small or big (a commonly-used time interval is one hour). The temperature distributions, along the collector, of the cover plates, of the absorbing plate and of the insulation surface, as well as of the fluid can be determined at each time instant. Therefore, the heat gain into the building can be determined from the air outlet temperature and the air flow rate.

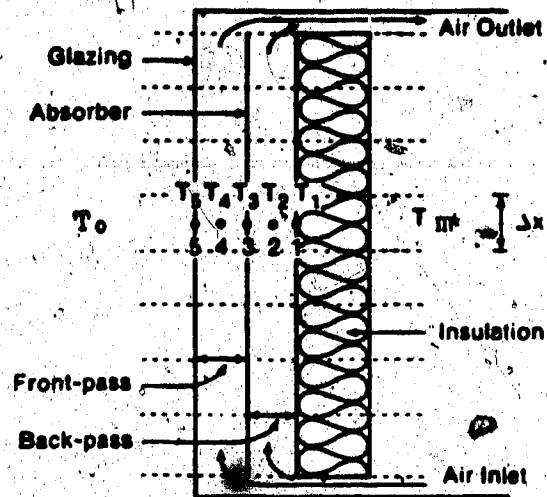
The model derived here is based on the following assumptions:

1. Heat transfer is two-dimensional in the collector and one-dimensional in the floor slab.
2. Since the metal sheet is thin (a few millimeters), temperatures on the two surfaces of, as well as inside the absorbing plate are assumed to be identical. The same assumption applies to the cover glazing.

3. Radiation heat loss to the ambient air can be adequately estimated by using a mean radiant temperature of the surroundings suggested by Shewen *et al.* (1980).

Referring to Figure 6.2, the following numbers and letters are used as subscripts in the equations derived in this chapter:

- 1 -- insulation surface
- 2 -- air moving in back-path
- 3 -- absorbing plate
- 4 -- air moving in front-path
- 5 -- innermost cover
- 6 -- outermost cover in double-glazing, and 2nd cover in triple-glazing
- 7 -- outermost cover plate in triple-cover system
- 0 -- ambient air
- + -- fluid flow
- d -- ground
- i -- *i*th region of the collector
- m -- room air
- r -- radiant heat transfer
- s -- solar radiation
- st -- stored energy in a control volume
- y -- sky
- z -- floor



- T_1 : surface temp. of insulation
- T_2 : air temp. in back-pass
- T_3 : absorbing plate temp
- T_4 : air temp. in front-pass
- T_5 : cover temp.
- T_m : room air temp.
- T_o : outdoor temp.

Figure 6.1 A subdivision for the collector

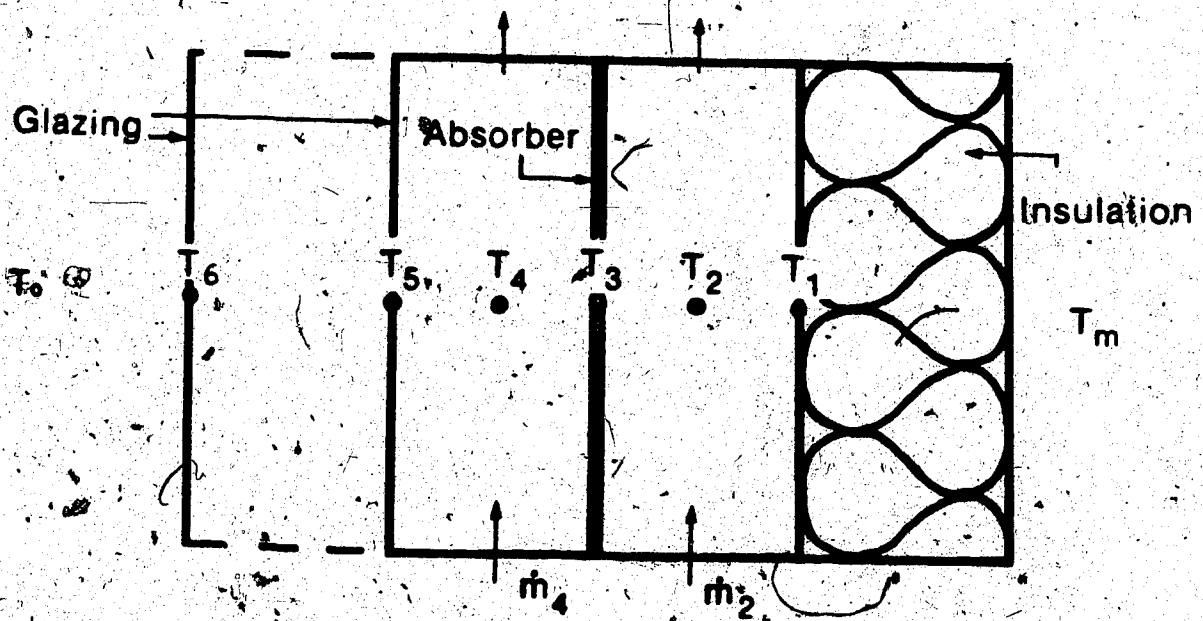


Figure 6.2 Detail of the i th region

6.1.1 Determination of heat transfer coefficients

The process of heat exchange in the collector involves conduction, convection and radiation. In a broad sense, each mode of heat transfer can be written as:

$$Q = hSAT \quad (6.1)$$

where Q = amount of heat transferred (W)

h = heat transfer coefficient ($Wm^{-2}^{\circ}C^{-1}$)

S = heat transfer area (m^2), and

ΔT = temperature difference ($^{\circ}C$).

The heat transfer coefficient, h , is referred to as the conductive heat transfer coefficient in conduction processes, as the convective heat transfer coefficient in convection processes and as the radiant heat transfer coefficient in radiation processes. Subscript "r" is supplied to h as an indication of the mode of radiant heat transfer, whereas no distinctions are made between convection and conduction heat transfer processes.

The conductive heat transfer coefficient, h_{m1} , (Figure 6.3) is the reciprocal of the insulation resistance (RSI) from the inner surface of the insulation to the room air. The RSI can be determined easily from the properties and thickness of the insulation on the back of the collector and an estimated room air film coefficient of heat transfer.

The convective heat transfer coefficient (h_{21}) between the air in the back-path and the insulation surface is assumed to be identical to that (h_{23}) between the air and the lower surface of the absorbing plate. The state of the

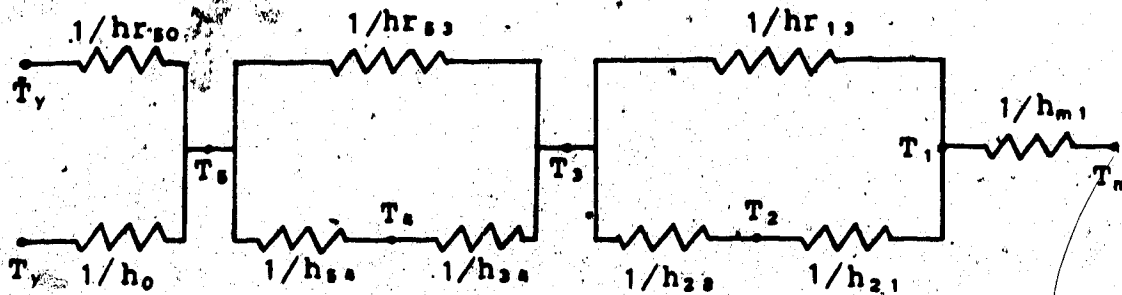


Figure 6.3 Thermal network for a single-glazed two-path collector

fluid flow determines which empirical correlation is to be used. For turbulent flow ($Re \geq 2300$), the following correlation suggested by Duffie and Beckman (1974) is used to estimate the Nusselt number:

$$Nu = 0.0158 Re^{0.8} \quad (6.2)$$

where $Nu = \frac{h_{2,1} L}{k}$

Re = Reynolds number

k = thermal conductivity of fluid ($Wm^{-1}C^{-1}$)

L = 2s, characteristic length (m) and

s = spacing in the back-path (m).

For laminar flow ($Re < 2300$), the Nusselt number is estimated by the following equation (Mercer et al., 1967):

$$Nu = 3.77 + \frac{0.0606 (Re Pr s / 2x)^{1/2}}{1 + 0.1 Pr^{0.4} (Re s / 2x)^{0.7}} \quad (6.3)$$

where x is the coordinate along the collector with the bottom edge being the origin, and Pr is the Prandtl number of air. Therefore,

$$h_{2,1} = \frac{kNu}{L} \quad (6.4)$$

As detailed in Chapter 2, the radiant heat transfer coefficient ($hr_{3,1}$) between the insulation surface and the lower surface of the absorbing plate is determined from:

$$hr_{3,1} = \frac{\sigma}{1/\epsilon_1 + 1/\epsilon_3 - 1} (T_1^3 + T_1^2 T_3 + T_1 T_3^2 + T_3^3) \quad (6.5)$$

Similarly, the convective heat transfer coefficients on the front-path and the radiant heat transfer coefficient between the inner surface of the glazing and the absorbing surface can be determined.

Radiation heat loss from the front glazing surface to the ambient air is approximated with an approach after Shewen *et al.* (1980). A mean radiant temperature of the surroundings is defined as:

$$\bar{T}_0 = (F_v T_v^4 + F_d T_d^4)^{1/4} \quad (6.6)$$

where $T_v = 0.0552 T_0^{1.5}$, and $T_d = T_0$.

Then the radiant heat transfer coefficient is computed as:

$$hr_{5,0} = \sigma \epsilon_5 (T_5^3 + T_5^2 \bar{T}_0 + T_5 \bar{T}_0^2 + \bar{T}_0^3) \quad (6.7)$$

The convective heat transfer coefficient due to wind blowing onto or across the collector surface can be estimated with the correlations suggested by Ramsey and Charmchi (1980) or by ASHRAE (1976b), depending on the direction of the wind. The study of Sparrow *et al.* (1979) shows that the wind-related heat transfer coefficients were quite insensitive to the angle of attack and to the aspect

ratio of the plate (which is defined as the ratio of plate length to height), when the angle of attack falls in the range of $90^\circ - 25^\circ$. Hence, when the angle of attack is in this range, the correlation to be used is (Ramsey and Charmchi, 1980):

$$h_o = 0.86 \frac{k}{L_c} Re_o^{1/2} Pr^{1/2} \quad (6.8)$$

where $L_c = Ac/C$, characteristic length (m)

$$Re_o = U_o L_c / \nu$$

ν = kinematic viscosity of air ($m^2 s^{-1}$)

C = perimeter of the collector (m), and

U_o = wind velocity (ms^{-1}).

When the angle of attack is out of the range given above, the collector surface is essentially leeward. The equation for estimating h_o is then (ASHRAE, 1976b):

$$h_o = 3.28(0.3 + 0.05U_o)^{0.805} \quad (6.9)$$

For a double (Figure 6.4) or a triple-glazed (Figure 6.5) system (or a single-glazed back-path system), the heat transfer occurring across the enclosed space between two layers of glazing is by conduction or by natural convection. Hollands *et al.* (1976) studied the free convective heat transfer across inclined air layers and suggested a critical value for the Rayleigh number:

$$Ra' = \frac{1708}{\cos \theta} \quad (6.10)$$

Rayleigh number (Ra) is temperature-dependent and is evaluated as:

$$Ra = \frac{g \beta \Delta T_s^3}{\nu \alpha} \quad (6.11)$$

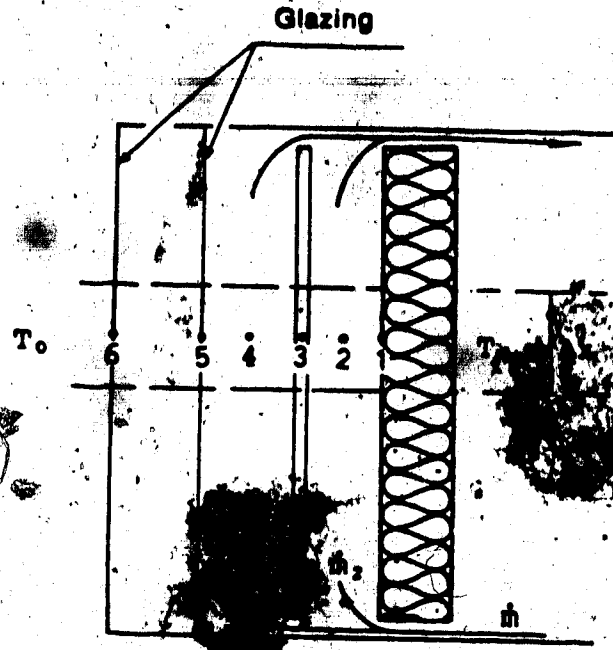


Figure 6.4 A double-glazed system

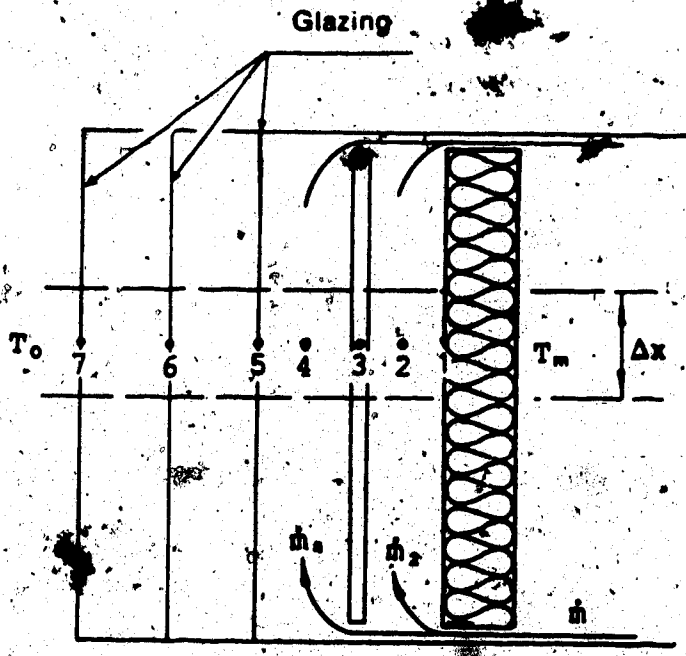


Figure 6.5 A triple-glazed system

where g = gravitational acceleration (ms^{-2})

β = coefficient of thermal expansion ($^{\circ}\text{K}^{-1}$)

α = thermal diffusivity (m^2s^{-1}).

ΔT = temperature difference ($^{\circ}\text{C}$), and

s = spacing of the enclosure (m).

If $Ra < Ra'$, the air in the enclosure is essentially stagnant and heat transfer occurs by conduction, (i.e., $Nu = 1$).

If $Ra = Ra'$, the heat transfer is said to be in the immediate postconductive regime, and the Nusselt number is determined as:

$$Nu = 1.44 \left(1 - \frac{1708}{Ra \cos \theta}\right) \quad (6.12)$$

When $Ra > Ra'$, the following correlation is used:

$$Nu = 1 + 1.44 \left[1 - \frac{1708}{Ra \cos \theta}\right] \left(1 + \frac{1708 (\sin 1.8 \theta)^{1/4}}{Ra \cos \theta}\right) + \left[\left(\frac{Ra \cos \theta}{1708}\right)^{1/3} - 1\right] \quad (6.13)$$

where θ is the inclination of the enclosed space, and the terms in the square brackets are defined by $[X] = (|X| + X)/2$.

6.1.2 Heat balance equations for the i th subregion

The heat balance for node 1 on the insulation surface can be obtained by noting that the sum of heat gains at the node must be equal to zero since there is no thermal storage there. Heat gains at node 1 can be identified as:

the convective heat gain from the fluid in the back-path,

$$Q_{2,1} = h_{2,1} (T_{2,1} - T_{1,1}) S_1 \quad (6.14)$$

where $T_{2,1}$ is the temperature at node 2 for the i th region,

the radiant heat gain from the back surface of the absorber plate,

$$Q_{r31} = hr_{31}(T_{3,1} - T_{1,1})S_1 \quad (6.15)$$

and the conduction heat gain from the room air,

$$Q_{m1} = h_{m1}(T_m - T_{1,1})S_1 \quad (6.16)$$

Then the heat balance is found as:

$$Q_{2,1} - Q_{r31} - Q_{m1} = 0 \quad (6.17)$$

Combining equations 6.14, 6.15, 6.16 and 6.17 results in an equation of the form:

$$A_{11}T_{1,1} + A_{12}T_{2,1} + A_{13}T_{3,1} = B_1 \quad (6.18)$$

where $A_{11} = S_1(h_{21} + hr_{31} + h_{m1})$

$$A_{12} = -S_1 h_{21}$$

$$A_{13} = hr_{31}, \text{ and}$$

$$B_1 = S_1 h_{m1} T_m$$

The heat balance for node 2 involves energy transport due to the fluid flow. Each subregion is a control volume for the fluid flowing in the back-path. Therefore, the temperature of the preceding region is the temperature at which the fluid flows into the control volume for the current region. The heat gains are:

the convective heat gain from the insulation surface,

$$Q_{12} = h_{12}(T_{1,1} - T_{2,1})S_1 \quad (6.11)$$

the convective heat gain from the back surface of the absorber,

$$Q_{32} = h_{32}(T_{3,1} - T_{2,1})S_1 \quad (6.20)$$

and the heat gain due to the fluid flow,

$$Q_2 = \dot{m}_2 C_p (T_{2,r-1} - T_{2,1}) \quad (6.21)$$

Then the heat balance can be written as:

$$Q_{12} + Q_{32} + Q_2 = 0 \quad (6.22)$$

Combining equations 6.19, 6.20, 6.21 and 6.22 gives:

$$A_{21}T_{1,1} + A_{22}T_{2,1} + A_{23}T_{3,1} = B_2 \quad (6.23)$$

where $A_{21} = \epsilon_1 S_1 (h_{12} + h_{32}) + \dot{m}_2 C_{p2}$

$$A_{22} = \dot{m}_2 C_{p2} - S_1 h_{12}$$

$$A_{23} = S_1 h_{32}$$

$$B_2 = \dot{m}_2 C_{p2} T_{2,1}$$

\dot{m}_2 is flow rate in back-path (kgs⁻¹), and

$T_{2,1}$ temperature at previous region (°C).

Node 2 is on the absorbing plate. It receives solar radiation and has thermal radiant heat exchanges with both the innermost cover surface and the insulation surface, in addition to the convective heat transfer occurring on both sides of the plate. The thermal mass effect also is taken into consideration, so that the temperature of the same region at the previous time can have an effect on the temperature of the region at the present time. These heat gains are detailed as follows:

the solar radiant heat gain,

$$Q_{r,1} = I(\tau\alpha)S_1 \quad (6.24)$$

where I is the intensity of the solar radiation reaching the collector surface.

the radiant heat gain from the insulation surface,

$$Q_{r,2} = hr_{13}(T_{1,1} - T_{3,1})S_1 \quad (6.25)$$

the convective heat gain from the fluid in the back-path,

$$Q_{c,2} = h_{23}(T_{2,1} - T_{3,1})S_1 \quad (6.26)$$

the convective heat gain from the fluid in the front-path,

$$Q_{4,3} = h_{4,3}(T_{4,1} - T_{3,1})S_1 \quad (6.27)$$

and the radiant heat gain from the innermost glazing surface,

$$Q_{r5,3} = hr_{5,3}(T_{5,1} - T_{3,1})S_1 \quad (6.28)$$

The change of energy stored in the control volume i of the metal plate can be approximated by the finite-difference method, and is expressed as:

$$Q_{s,i} = \rho_3 Cp_3 V_3 (T_{3,i} - T_{3,i-1}) / \Delta t \quad (6.29)$$

where $T_{3,i-1}$ = plate temperature at previous time ($^{\circ}\text{C}$)

ρ_3 = density of metal plate (kgm^{-3})

Cp_3 = specific heat of metal plate ($\text{Jkg}^{-1}\text{C}^{-1}$)

V_3 = volume of plate in the i th region (m^3), and

Δt = time increment (s).

For energy balance at node 3, the sum of heat gains at node 3 must equal the change of energy stored in node 3. Thus,

$$Q_{s,3} + Q_{r1,3} + Q_{2,3} + Q_{4,3} + Q_{r5,3} = Q_{s,i} \quad (6.30)$$

Substituting equations 6.24 to 6.99 into equation 6.30 and rearranging terms result in the following equation:

$$A_{31}T_{1,1} + A_{32}T_{2,1} + A_{33}T_{3,1} + A_{34}T_{4,1} + A_{35}T_{5,1} = B_3 \quad (6.31)$$

where $A_{33} = S_1(hr_{1,3} + h_{2,3} + h_{4,3} + hr_{5,3}) + \Omega$

$$A_{31} = -S_1 hr_{1,3}$$

$$A_{32} = -S_1 h_{2,3}$$

$$A_{34} = -S_1 h_{4,3}$$

$$A_{35} = -S_1 hr_{5,3}$$

$$B_3 = I(\tau\alpha)S_1 + \Omega T_{3,i-1}, \text{ and}$$

$$\Omega = \rho_3 Cp_3 V_3 / \Delta t.$$

The heat balance on node 4 for the fluid in the front-path can be performed in a similar way to that for the fluid in the back-path and results in the following equation:

$$A_{43}T_{3,i} + A_{44}T_{4,i} + A_{45}T_{5,i} = B_4 \quad (6.32)$$

where $A_{44} = S_1(h_{34} + h_{54}) + \dot{m}_4 C_p$

$$A_{43} = -S_1 h_{34}$$

$$A_{45} = S_1 h_{54}$$

$$B_4 = \dot{m}_4 C_p T_{4,i-1}, \text{ and}$$

\dot{m}_4 = mass flow rate in front-path (kgs^{-1}).

For a single-glazed system the energy balance on node 5 includes the radiant heat exchange between the glazing and the ambient sky. For a double or a triple-glazed system, only the outermost glazing is considered to have radiant heat exchange with the ambient sky, while inner glazings are considered to have radiant heat transfer with adjacent glazings or surfaces, and to have natural convection heat transfer. A portion of the solar radiation passing through the cover system is absorbed by each layer of glazing. For a single-glazed system, heat gains for the glazing are identified as:

the solar radiation absorbed by the glazing,

$$Q_{s,5} = \alpha_s I S_1 \quad (6.33)$$

the radiant heat gain from the absorbing surface,

$$Q_{r,5} = h_{r,5}(T_{3,i} - T_{s,i}) S_1 \quad (6.34)$$

the convective heat gain from the fluid in the front-path,

$$Q_{c,5} = h_{c,5}(T_{4,i} - T_{s,i}) S_1 \quad (6.35)$$

the convective heat gain from the ambient air,

$$Q_{05} = h_0(T_0 - T_{s,1})S_1 \quad (6.36)$$

and the long-wave radiant heat loss to the ambient air,

$$Q_{r50} = hr_{50}(T_{s,1} - \bar{T}_0)S_1 \quad (6.37)$$

Then the heat balance is stated as:

$$Q_{s,5} + Q_{r35} + Q_{45} + Q_{05} - Q_{r05} = 0 \quad (6.38)$$

Combining equations 6.33 to 6.38 gives:

$$A_{53}T_{3,1} + A_{54}T_{4,1} + A_{55}T_{s,1} = B_5 \quad (6.39)$$

where $A_{55} = S_1(hr_{35} + h_{45} + hr_{50} + h_0)$

$$A_{53} = -S_1 hr_{35}$$

$$A_{54} = -S_1 h_{45}$$

$$B_5 = S_1(\alpha_s I + h_0 T_0 + hr_{50} \bar{T}_0)$$

α_s = effective absorptance of 1st glazing, and

\bar{T}_0 = mean radiant temperature of ambient ($^{\circ}K$).

For a double and a triple-glazed system there will be one and two more nodes, respectively, added to the system. The following discussion treats each case separately.

For a double-glazed system, the energy balance equation for node 5 may be written as:

$$A_{53}T_{3,1} + A_{54}T_{4,1} + A_{55}T_{s,1} + A_{56}T_{6,1} = B_5 \quad (6.40)$$

where $A_{55} = S_1(hr_{35} + h_{45} + h_{65} + hr_{65})$

$$A_{53} = -S_1 hr_{35}$$

$$A_{54} = -S_1 h_{45}$$

$$A_{56} = -S_1(h_{65} + hr_{65})$$

$$B_5 = S_1(\tau'\alpha_s)I, \text{ and}$$

$(\tau'\alpha_s)$ = effective transmittance-absorptance
of 1st glazing.

The equation for node 6 is:

$$A_{66}T_{6,i} + A_{60}T_{6,e} = B_6 \quad (6.41)$$

where $A_{66} = S_1(hr_{66} + h_{66} + hr_{60} + h_0)$

$$A_{60} = -S_1(hr_{66} + h_{66})$$

$$B_6 = S_1(\alpha_6 I + h_0 T_0 + hr_{60} T_0), \text{ and}$$

α_6 = effective absorptance of 2nd glazing.

For a triple-glazed system, node 7 will be added as one more layer of glazing is included in the system. Node 6, therefore, has no direct contact with the ambient and thus is classified as an inner node. The formulation for node 6 now becomes:

$$A_{66}T_{6,i} + A_{65}T_{6,e} + A_{67}T_{7,i} = B_6 \quad (6.42)$$

where $A_{66} = S_1(hr_{66} + h_{66} + hr_{76} + h_{76})$

$$A_{65} = -S_1(hr_{66} + h_{66})$$

$$A_{67} = -S_1(hr_{76} + h_{76})$$

$$B_6 = S_1(r'\alpha_6)I, \text{ and}$$

$(r'\alpha_6)$ = effective transmittance-absorptance of 2nd glazing layer.

And the formulation for node 7 will be similar to that for node 6 of the double-glazed system:

$$A_{77}T_{7,i} + A_{76}T_{7,e} = B_7 \quad (6.43)$$

where $A_{77} = S_1(hr_{77} + h_{77} + hr_{76} + h_0)$

$$A_{76} = -S_1(hr_{77} + h_{77})$$

$$B_7 = S_1(\alpha_7 I + h_0 T_0 + hr_{76} T_0), \text{ and}$$

α_7 = effective absorptance of 3rd glazing.

The formulation of energy balance equations for the case where there is only air flow in a back-path in an

active system may be considered in a similar way. To avoid needless repetition, details of this derivation are omitted. The equation, however, can be seen easily in the computer program which is listed in Appendix B.2.

6.1.3 Determination of air temperature at the collector outlet

The energy equations derived above, if combined, take the matrix form:

$$[A]\{T\} = [B] \quad (6.44)$$

The number of simultaneous equations in equation 6.44 depends upon the number of layers of glazing in the system. There will be five equations for a single-glazed two-path system, six for a double-glazed two-path system, and seven equations for a triple-glazed two-path system. For a single-glazed one-path (back-path) system, four equations will be sufficient, since the node in the front-path is eliminated.

For each subregion there will be a set of simultaneous equations in the form of 6.44 which may be solved with the Gaussian elimination method. After assuming an initial room air temperature, the calculation starts from the lowest subregion where the air enters the collector, and proceeds up the collector based on the calculated air temperature for the previous subregion. Finally, the air temperatures calculated for the top subregions for both the front and the back paths, are used to determine air outlet temperature as

the two air flows merge and exit to the room in a state of uniform temperature.

According to mass conservation (Figure 6.6), the following equation is obtained:

$$\dot{m} = \dot{m}_2 + \dot{m}_4 \quad (6.45)$$

where \dot{m} is the total mass flow rate (kgs^{-1}).

Energy conservation requires that the total amount of energy carried into the room by mass flow rate \dot{m} is the sum of the amounts of energy carried in by the component mass flow rates \dot{m}_2 and \dot{m}_4 , i.e.,

$$\dot{m}C_p(T_{x_{1,t}} - T_m) = \dot{m}_2C_p(T_{x_{1,t,2}} - T_m) + \dot{m}_4C_p(T_{x_{1,t,4}} - T_m) \quad (6.46)$$

where $T_{x_{1,t}}$ is the air temperature at the collector outlet.

Combining equations 6.45 and 6.46 gives the air temperature at the collector exit:

$$T_{x_{1,t}} = T_m + W1(T_{x_{1,t,2}} - T_m) + W2(T_{x_{1,t,4}} - T_m) \quad (6.47)$$

where $W1 = \frac{\dot{m}_2}{\dot{m}_2 + \dot{m}_4}$, and $W2 = \frac{\dot{m}_4}{\dot{m}_2 + \dot{m}_4}$.

The size of each subregion is identical, although they can be different if so desired, and can be set by the user at the start of each simulation run. The time interval, or step, for the calculation is arbitrary and also is set at the start of a simulation run.

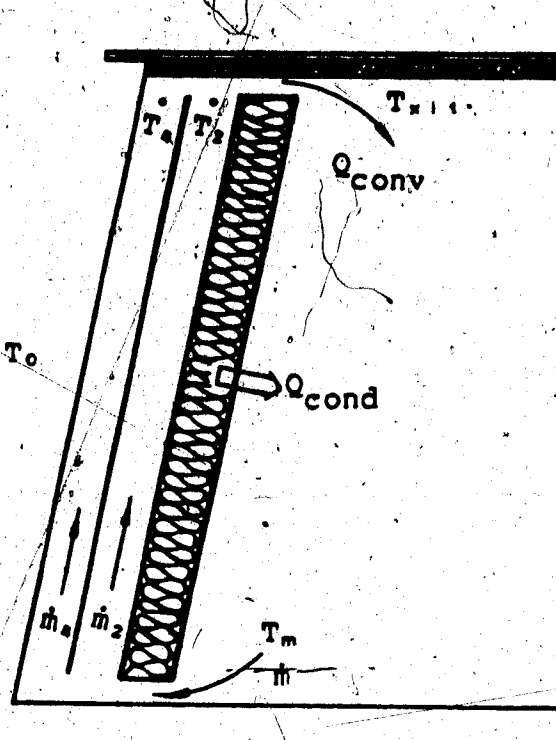


Figure 6.6 Air temperature at the outlet of the collector

6.2 Calculation of Room Air Temperature

6.2.1 Heat gain into the structure

The heat gain into the room from the collector consists of two parts (Figure 6.7). The first is the part (Q_{conv}) transported by the moving air and the second (although it may be small) is the part (Q_{cond}) conducted into the room through the collector's back insulation. The total heat gain into the building can be expressed as:

$$Q_{gain} = Q_{conv} + Q_{cond} \quad (6.48)$$

The convective heat gain, Q_{conv} , is readily obtained with the mass and energy conservations as discussed in the previous section. That is:

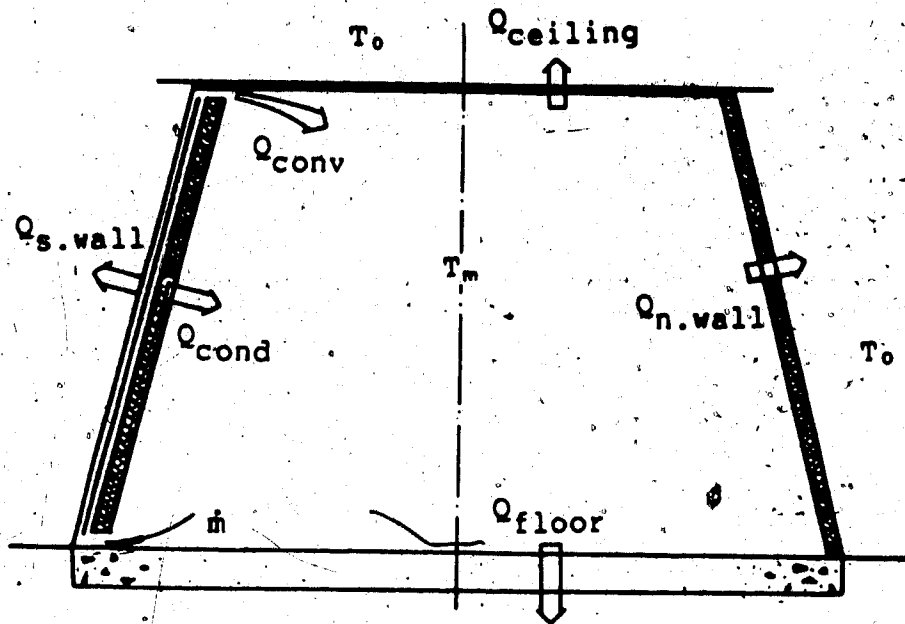


Figure 6.7 Heat gain into the room from the collector

$$Q_{\text{conv}} = \dot{m}C_p(T_{x_{11}} - T_m) \quad (6.49)$$

The conductive heat gain, Q_{cond} , can be determined by integrating portions of the heat conducted from each subregion of the collector after the inner surface temperature of the insulation is computed. The equation takes the form of:

$$Q_{\text{cond}} = \sum S_i h_{i,m} (T_{i,m} - T_m) \quad (6.50)$$

6.2.2 Collector efficiency

The collector efficiency is defined by ASHRAE (1978) as the ratio of the total useful heat gain to the total available solar radiation in a certain duration of time. In this study, the duration of time is set as a 24-hour period (a diurnal cycle), so the collector efficiency is actually the daily efficiency. In addition, the conduction part of the heat gain is not included in the calculation of the daily collector efficiency, since the function of the collector is to collect and to transport heat through the motion of air only. This is also the basis for comparison of active collectors of the same type. The efficiency equation is:

$$\eta = \frac{\text{daily total useful heat gain via convection (kJ)}}{\text{daily total available solar radiation (kJ)}} \quad (6.51)$$

6.2.3 Calculation of room air temperature

The calculation of the room air temperature is based on the heat balance on the entire building envelope. The heat gains are mainly from the collector as outlined in the previous section. Heat losses occur through all the walls, ceiling and floor. The south-side collector wall is considered to contribute to the heat gain through conduction during daytime, but to heat loss at night. The room air temperature is determined simultaneously with the calculation of the floor temperature distribution.

The floor is divided into a number of horizontal layers that are assumed to be isothermal. This means that heat transfer through the floor into the ground is taken as one dimensional. The general equation governing the one-dimensional heat conduction is:

$$\rho C_p \frac{\partial T}{\partial t} = \frac{\partial}{\partial x} \left(k \frac{\partial T}{\partial x} \right) \quad (6.52)$$

In the following, equation 6.52 is discretized with a fully implicit scheme according to Patankar (1980). Figure 6.8 shows the interior and boundary nodes associated with their respective control volumes for the floor slab.

The discretization equation for each of the interior nodes takes the form:

$$X_P T_P = X_N T_N + X_S T_S + b \quad (6.53)$$

where $X_S = \frac{k}{\Delta x}$

$$X_N = \frac{k}{\Delta x}$$

$$X_P^o = \frac{\rho_z C_{p_z} \Delta x}{\Delta t}$$

$$b = X_P^o T_P$$

$$X_P = X_S + X_N + X_P^o$$

$$T_P = \text{temperature at previous time } (^{\circ}\text{C})$$

$$C_{p_z} = \text{specific heat of the floor } (\text{Jkg}^{-1}\text{ }^{\circ}\text{C}^{-1})$$

$$\rho_z = \text{density of the floor } (\text{kgm}^{-3}), \text{ and}$$

$$\Delta x = \text{length of grids (m).}$$

On the boundaries, the control volume for each node is only half of that for the interior nodes. The equation for a node on the boundary is found to be:

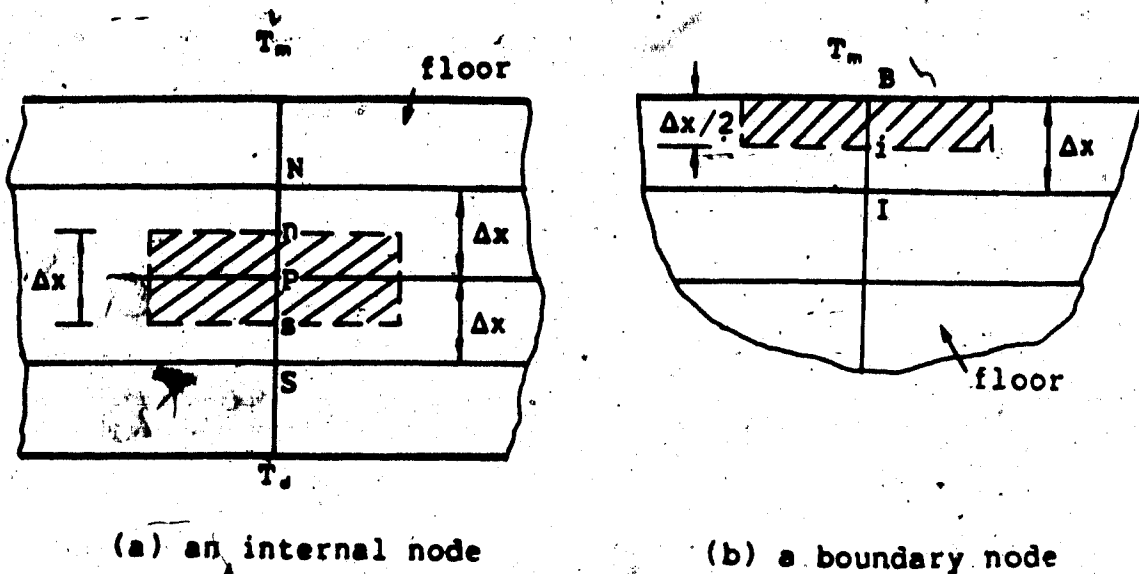


Figure 6.8 Interior and boundary nodes for the floor slab

$$X_B T_B = X_I T_I + X_m T_m + b \quad (6.54)$$

where $X_I = \frac{k}{\delta_i}$

$$X_m = U_{\text{floor}}$$

$$X_B^{\circ} = \frac{\rho C p_m \Delta x}{2 \Delta t}$$

$$b = X_B^{\circ} T_B$$

$$X_B = X_I + X_m + X_B^{\circ}$$

T_p = temperature at previous time ($^{\circ}\text{C}$), and

U_{floor} = heat transfer coefficient between room air and floor ($\text{Wm}^{-2}\text{C}^{-1}$).

The heat losses through the building envelope can be identified as:

$$Q_{\text{loss}} = Q_{n.\text{wall}} + Q_{s.\text{wall}} + Q_{e.\text{wall}} + Q_{\text{door}} + Q_{\text{ceiling}} + Q_{\text{floor}} + Q_{\text{found}}$$

$$= \Sigma S.U(T_m - T_o) + S_{\text{floor}}U_{\text{floor}}(T_m - T_o) \quad (6.55)$$

where $\Sigma S.U = S_{\text{n.wall}}U_{\text{n.wall}} + S_{\text{s.wall}}U_{\text{s.wall}} + S_{\text{e.wall}}U_{\text{e.wall}} + S_{\text{door}}U_{\text{door}} + S_{\text{ceiling}}U_{\text{ceiling}} + S_{\text{fund}}U_{\text{fund}}$.
Heat storage in the room air is approximated by,

$$Q_{\text{st}} = V_m \rho_m C_{p_m} (T_m - T_m) / \Delta t \quad (6.56)$$

Dividing both equations 6.55 and 6.56 by the floor area (S_{floor}) and combining them gives:

$$X_m X_m = X_I T_I + b \quad (6.57)$$

where $X_B = U_{\text{floor}}$

$$X_m^{\circ} = \frac{\rho_m C_{p_m} V_m}{\Delta t S_{\text{floor}}}$$

$$X_o = \Sigma S.U / S_{\text{floor}}$$

$$b = X_o T_o + X_m^{\circ} T_m + Q_{\text{gain}}$$

$$X_m = X_B + X_o + X_m^{\circ}$$

V_m = volume of room space (m^3), and

T_m = room temperature at previous time ($^{\circ}\text{C}$).

The resultant set of equations is in the form of triangular matrix, which can be solved easily with a subroutine in the simulation program.

6.3 Features of the Computer Model and Calculation Steps

The computer program (ACTVSYS), which is listed in Appendix B.2, consists of a main section and 16 subroutines coded in BASIC language. The program can be run on a microcomputer (IBM-PC, for example). Two separate input files are needed, one containing the construction information of the building and the collector, as well as the control parameters (i.e., the time increment, the output

time interval and the total length of the simulation time) for a simulation run, and the other containing environmental data. The format of file #1 is displayed in Appendix B.3. A sample of the output file is shown in Appendix B.4.

Since the radiant heat exchanges involved are temperature dependent, as are the natural convective transfers across enclosed spaces, iterations are required for each subregion in each time step for calculation of the collector performance.

The model is capable of simulating an active solar air heating system with up to three covers. The flow pattern can be selected either as two-path or one-path (back-path flow only). Two algorithms for solving matrices are included in the model, one (Gaussian elimination solver) for temperature calculations for the collector subregion and the other (triangular matrix solver) for the calculation of room air and floor temperatures.

The calculation procedure can be detailed as follows (the flowchart can be found in Appendix B.1):

1. Input (from input file #1) the physical dimensions of the building and of the collector, the assumed initial room air temperature, and the simulation control parameters.
2. Input (from the keyboard in response to prompts) the number of covers of glazing to be used, the number of collector panels to be used and the number of subregions for the collector model. In addition, the number of

- nodes to be used for the floor temperature computation also is input from the keyboard, as are the air flow velocities in the front and back-paths.
3. Calculate the effective absorptance of each cover in the collector cover array using the Edwards' algorithm (Edwards, 1977).
 4. Calculate the mean radiant temperature of the surroundings and estimate the temperatures for the covers, the absorbing plate and the insulation surface, based on an assumed inlet (room) temperature.
 5. Calculate all the temperature-dependent heat transfer coefficients using estimated temperatures.
 6. Determine the matrix coefficients and solve the matrix for temperatures in the subregion.
 7. Compare the old and the new absorbing plate temperatures. If not within specified accuracy, the newly-computed temperatures become the estimated temperature and the calculation is restarted from step 6. Otherwise the calculation goes to the next step.
 8. Heat balance is reached for one subregion and the calculation starts from step 4 for the next subregion.
 9. When the top of the collector is reached, the calculation is in the last subregion where the outlet air temperature is determined.
 10. Based on the calculated air outlet temperature and the air flow, the heat gain into the building is determined.
 11. Calculate the coefficients for the triangular matrix and

solve the matrix for the room air temperature and the floor temperature distribution.

12. The average of the newly-determined and the old room air temperatures is used as the estimated room air temperature for the repetition of the whole calculation procedure starting at step 4.
13. The second calculated room air temperature is then taken as the new room temperature.
14. Time is advanced and the results are printed at the printing time interval until the total run time is over.

The execution of the compiled program on an IBM-PC takes approximately 30 minutes for a two-day period of a simulation run with a sampling time interval (time step) of 15 minutes (10 subregions used).

7. COMPARISON OF THE ACTUAL AND THE SIMULATED SYSTEMS

7.1 Model Validation for the Active Solar Collector

In order to validate the active collector model, data were obtained from two flat-plate collectors built by Alberta Agriculture, and located on the University of Alberta's Parkland Research Station in Edmonton, Alberta. Specifications of the two flat-plate collectors are given in Appendix C.1.

The predicted transient performance of two flat-plate air collectors is plotted in Figures 7.1, 7.2, 7.3 and 7.4 together with the measured performance. One collector was single-glazed and the other double-glazed, and both were single-path (back-path). The construction parameters of these collectors were used in the simulation model. Reasonable values were assumed for the undetermined properties, such as the absorptivity of the collecting surface, the density of the metal collector sheet and the transmissivity of the glazing materials. Air was drawn into the collector from the outside.

Figures 7.1 and 7.2 show the comparison of the predicted and measured collector outlet temperatures of a single-glazed flat-plate collector for a cloudy day and a clear day, respectively. A good agreement of the two curves was seen throughout the day. The predicted temperatures,

The construction details of these collectors and the monitoring system can be obtained from the Engineering and Home Design Section of Alberta Agriculture, Edmonton, Alberta.

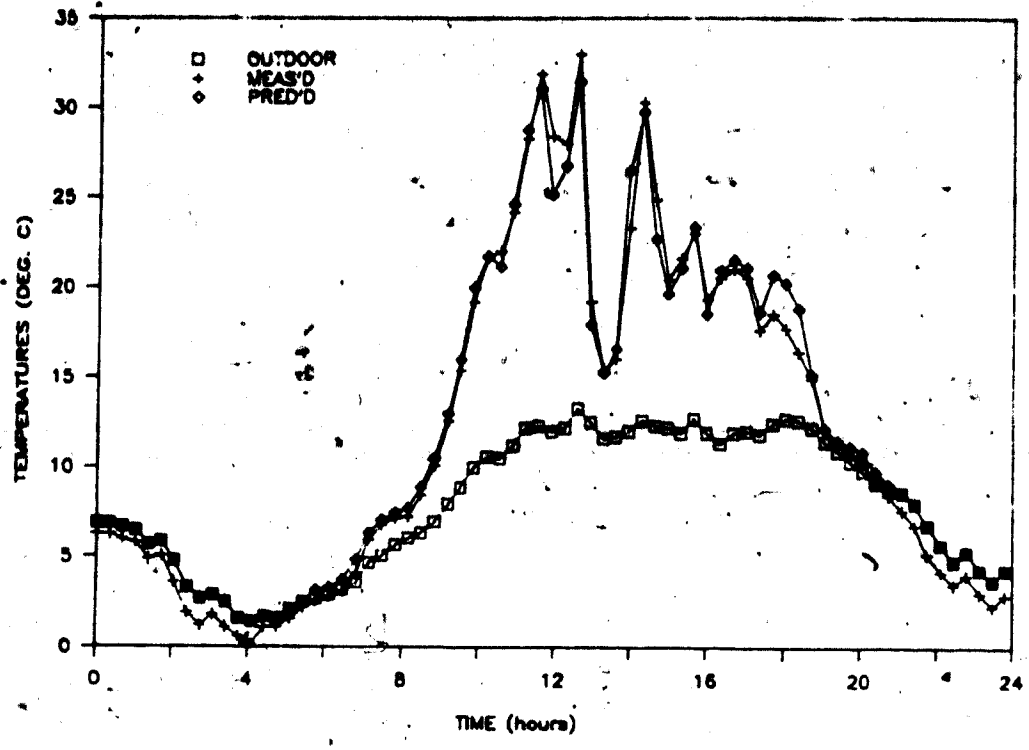


Figure 7.1 Measured and calculated outlet temperatures of a single-glazed one-path collector on a cloudy day

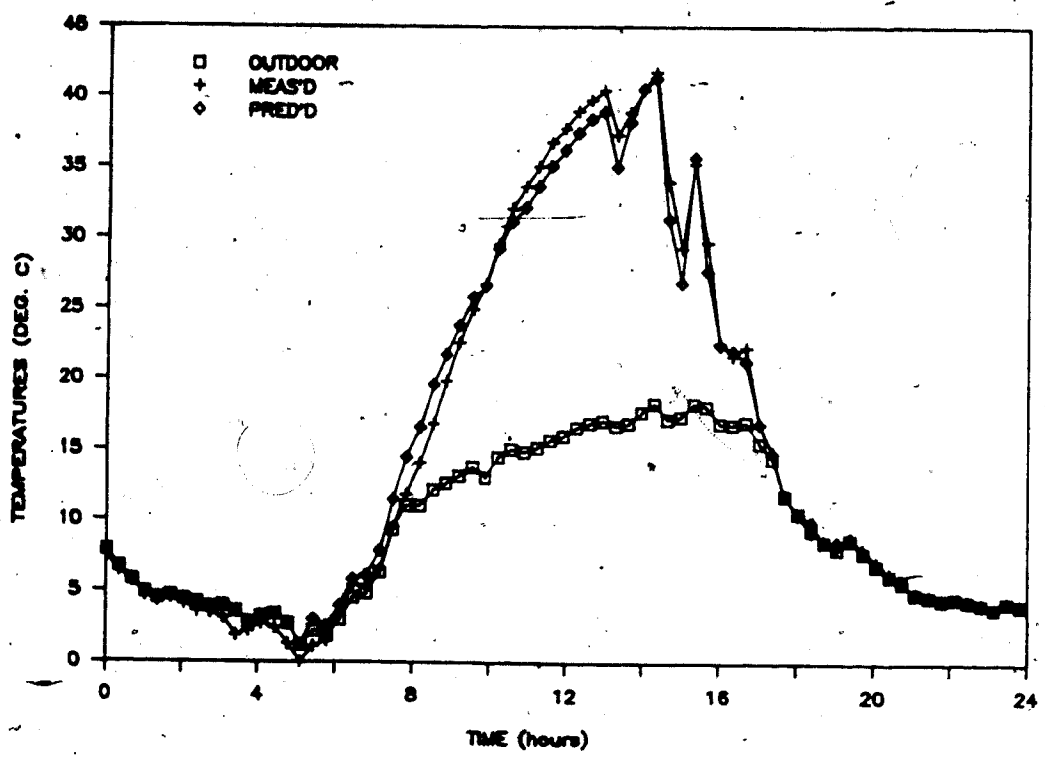


Figure 7.2 Measured and calculated outlet temperatures of a single-glazed one-path collector on a clear day

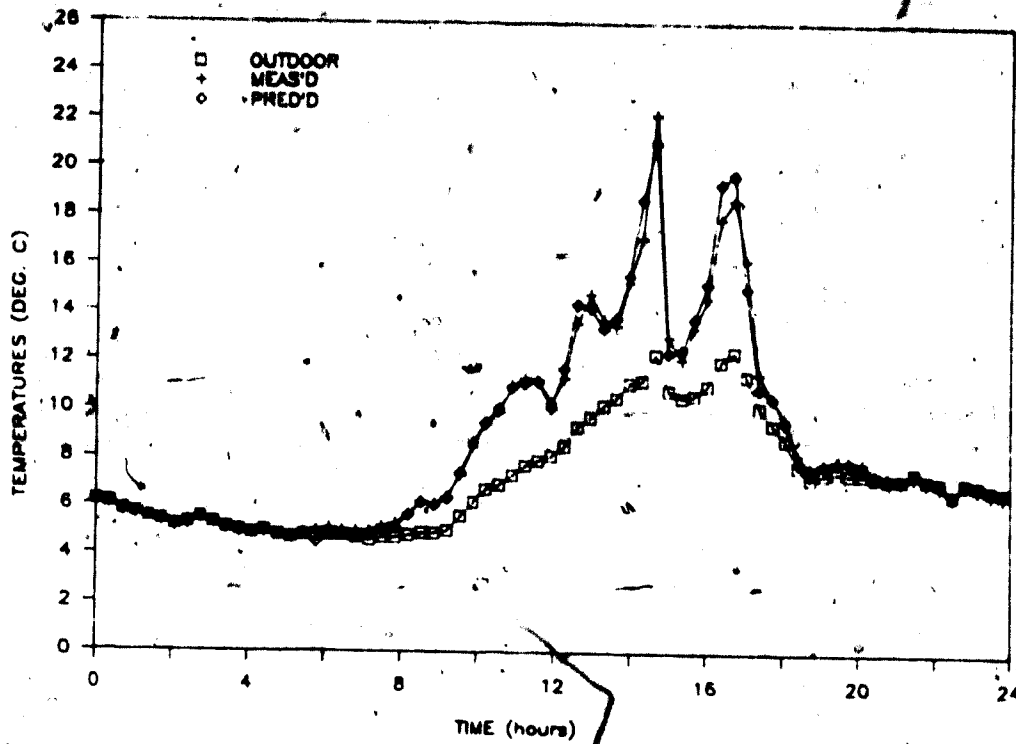


Figure 7.3 Measured and calculated outlet temperatures of a double-glazed one-path collector on a cloudy day

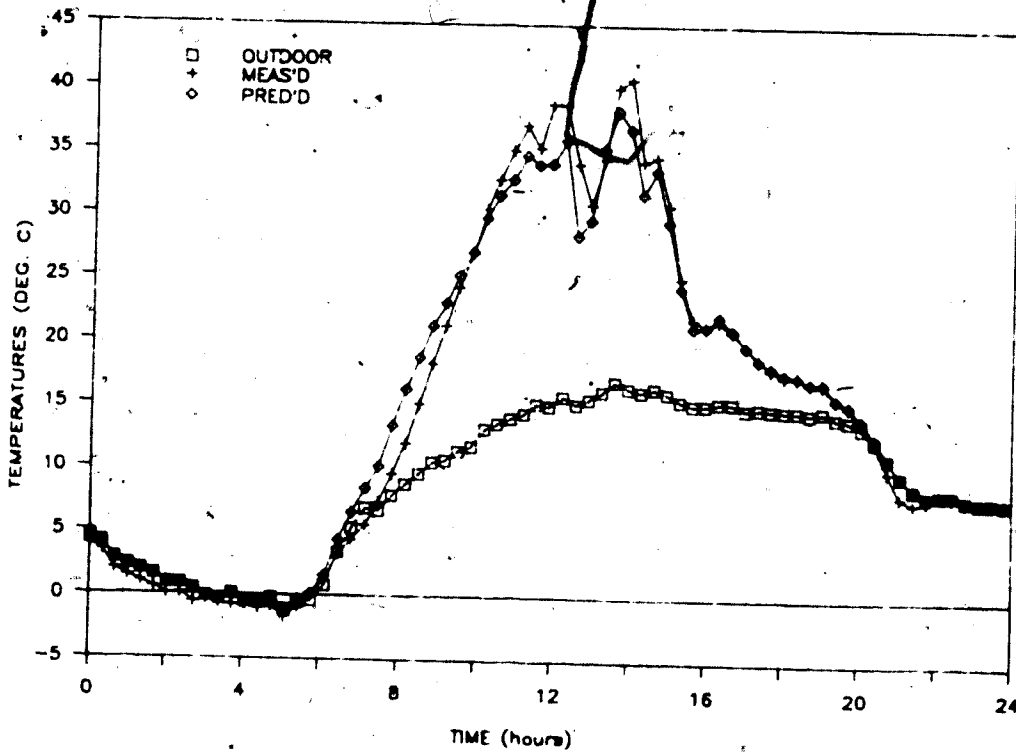


Figure 7.4 Measured and calculated outlet temperatures of a double-glazed one-path collector on a clear day

however, were observed to be, on average, 1.2°C higher than the monitored temperatures.

A typical comparison of the results for a double-glazed flat-plate collector is shown in Figure 7.3 for a cloudy day and in Figure 7.4 for a clear day. The average deviation of the predicted from the measured was seen to be within 2°C . A good agreement between the predicted and the measured collector's outlet temperatures was maintained for both days.

The predicted and measured amounts of energy collection are shown in Table 7.1 for the single-glazed collector and in Table 7.2 for the double-glazed collector. The simulation model predicted the performance of the single-glazed collector with differences ranging from 0.3% to 8% and that of the double-glazed collector with differences ranging from -3.7 to 2.6% (where the negative sign indicates an underestimation).

The deviations of the predicted performance from the measured performance may be due to the thermal mass effects of some materials that were neglected in the development of the simulation model. The effect of wind also may contribute to the deviations (the model is capable of taking the wind effect into account if the speed and the direction of wind are provided as input). In addition, the correlations used to estimate various heat transfer coefficients may be responsible for some errors.

Table 7.1. MEASURED & PREDICTED ENERGY COLLECTION FOR THE SINGLE-GLAZED COLLECTOR

mm/dd/yy	solar rad. KJ/m ²	energy collection measured	energy collection(KJ/m ²) predicted	difference %
05/10/86	4,620.36	1,843.35	1,992.10	+8.1
05/11/86	13,214.30	5,428.34	5,589.23	+3.0
05/12/86	17,498.12	6,775.44	7,152.52	+5.6
05/13/86	17,377.55	6,949.31	6,971.11	+0.3

Table 7.2. MEASURED & PREDICTED ENERGY COLLECTION FOR THE DOUBLE-GLAZED COLLECTOR

mm/dd/yy	solar rad. KJ/m ²	energy collection measured	energy collection(KJ/m ²) predicted	difference %
05/10/86	4,620.36	1,687.91	1,658.16	-1.8
05/11/86	13,214.30	4,728.91	4,849.54	+2.6
05/12/86	17,498.12	6,212.97	6,205.60	-0.1
05/13/86	17,377.55	6,281.39	6,048.56	-3.7

The model derived using the approach of thermal balance on surfaces within a collector has proven to be capable of predicting the performance of a flat-plate air solar collector with an acceptable accuracy, considering the simplicity of the method. The method of subdivision was used in setting up the analytical model. However, the previous results from a ten-subregion run did not show much difference from those from a one-subregion run. The maximum difference between the two was around 1.2°C. This is consistent with the similar finding of O'Brien-Bernini and McGowan (1984). The temperature profile along the collector might be of linear form so that one subregion is adequate for temperature calculations of the collector (This may be an interesting subject to study.). The time needed for the

completion of a one-subregion run was seen to be 80% less than that needed for the completion of a ten-subregion run.

The overall model prediction of the performance of flat-plate collectors was quite satisfactory. It closely followed the trend of the actual performance, and therefore, constitutes a validation of the computer model for simulating flat-plate active solar collectors.

7.2 Comparison of Different Systems

The comparisons of the measured and the simulated performance of systems for heating the farm shop under study are presented in Figures 7.5, 7.6, 7.7 and 7.8. Since the direct gain model has not been validated with actual measured data, the results predicted by the model can be interpreted only as indications of what might be expected in an actual direct gain system.

In terms of temperature rise inside the structure, the simulated direct gain system ranks first, followed by the active system and the thermosyphon system last. While the room temperature of the thermosyphon system reached a maximum of 14°C for Dec. 21, 1985, that of an active system would peak to 22°C and that of a direct gain system would reach 59°C. Similar heating patterns are seen for Dec. 22, 1985 and for Feb. 5, 1986. Both the active and the direct gain systems seem to start heating up earlier and faster than the thermosyphon system. The comparison of the three systems appears significant for Feb. 5 and 7, 1986, when the

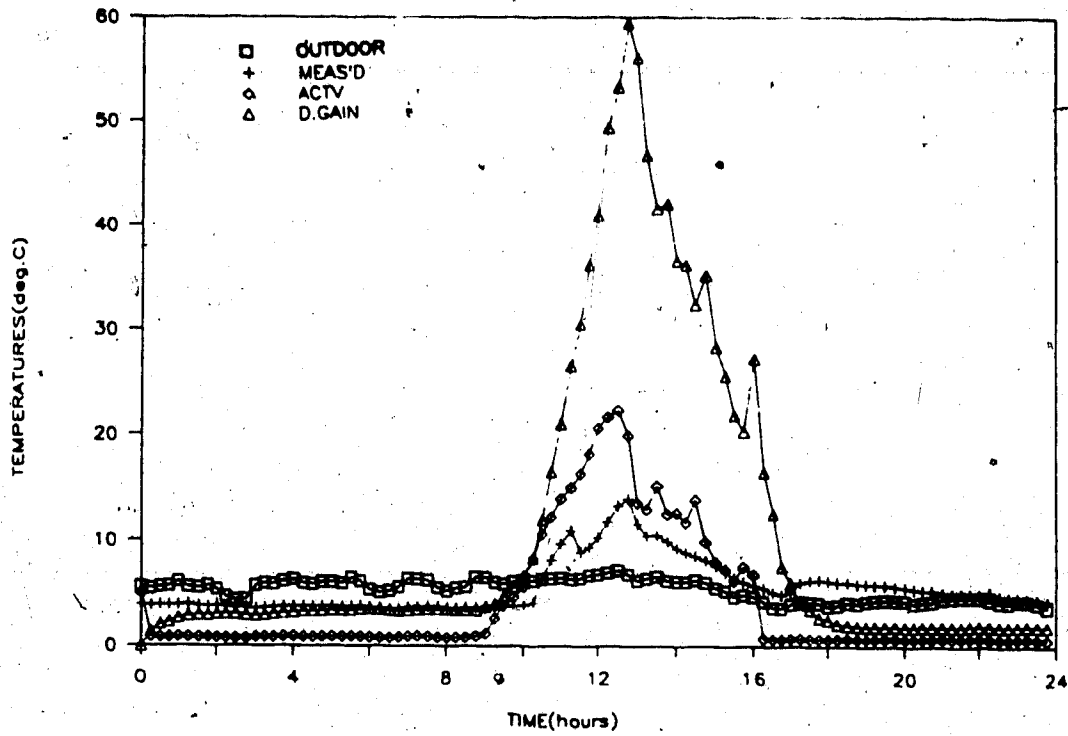


Figure 7.5 Performances of measured and simulated systems for Dec. 21, 1985

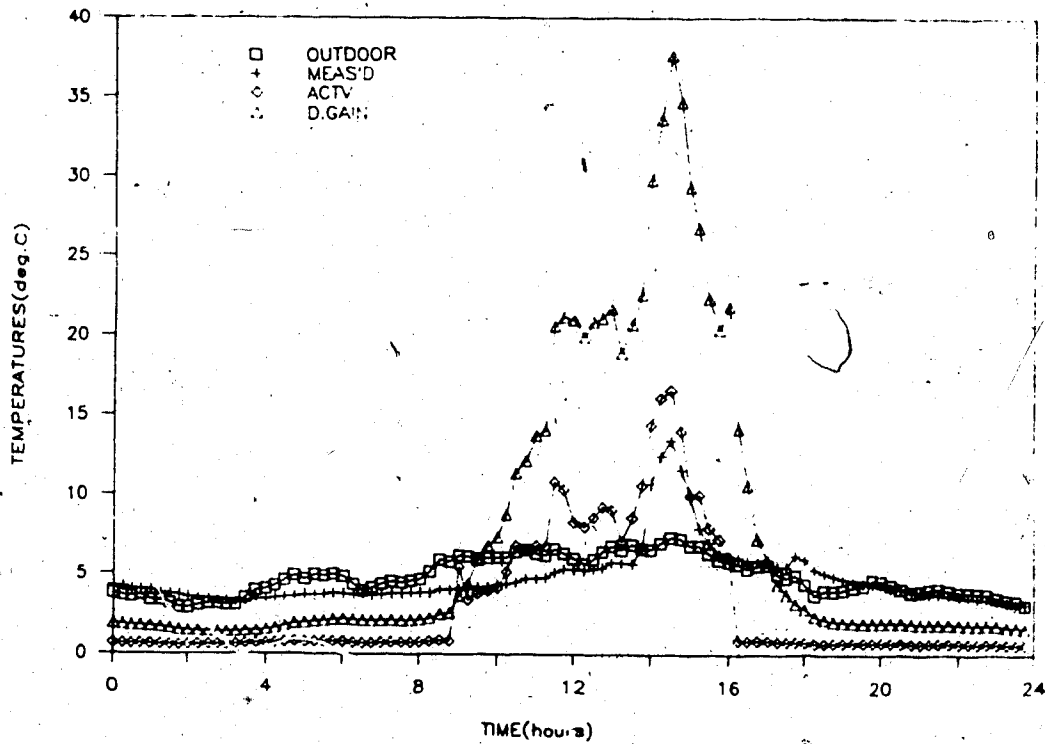


Figure 7.6 Performances of measured and simulated systems for Dec. 22, 1985

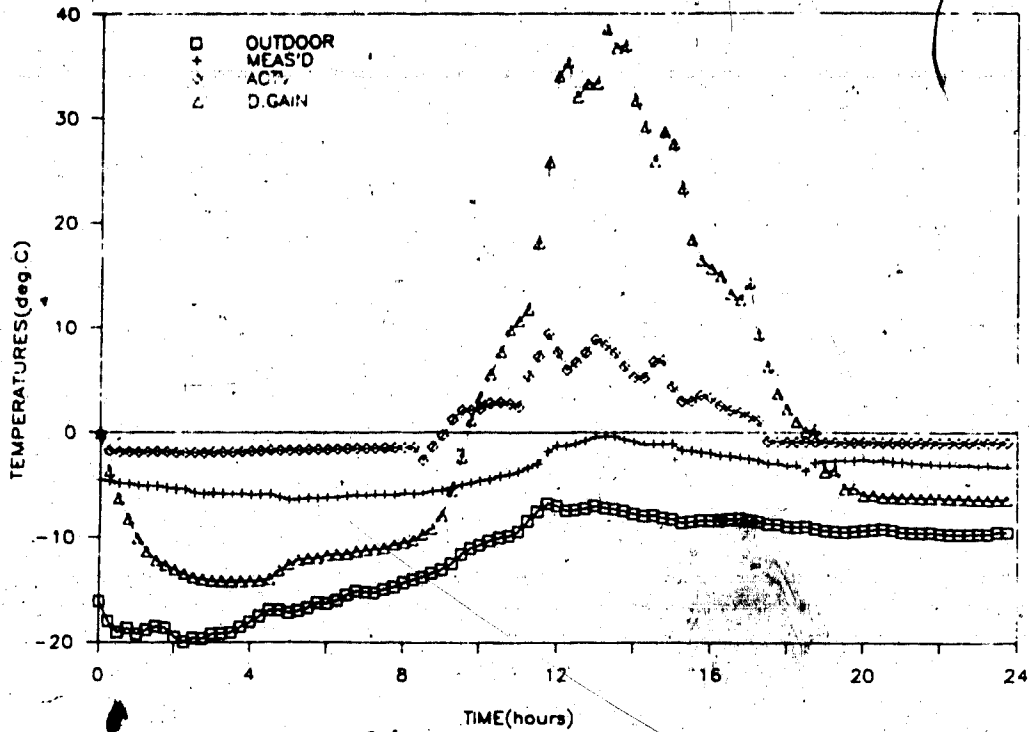


Figure 7.7 Performances of measured and simulated systems for Feb. 5, 1986

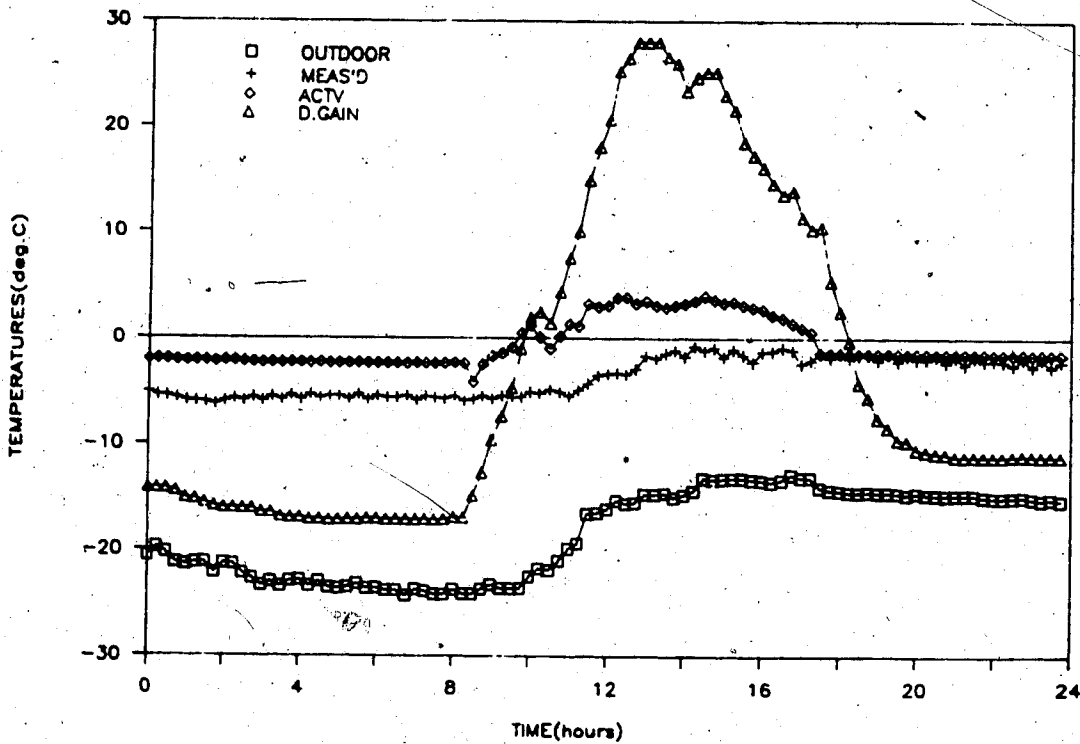


Figure 7.8 Performances of measured and simulated systems for Feb. 7, 1986

outdoor temperature stayed below -10°C . Of the three systems, only the direct gain system appeared to be able to heat the shop space to the desired daytime working condition of $+10^{\circ}\text{C}$. An active system would provide some heating but not enough to reach $+10^{\circ}\text{C}$, whereas the thermosyphon system was unable to climb over the zero-degree line.

Table 7.3 shows the daily energy collection and daily collector efficiencies for both active and thermosyphon systems. Efficiencies are not shown for the direct gain system since all solar radiation entering the building generally is considered to be absorbed inside the structure (Williams, 1983).

Apparently, more heat would be collected by blowing the air through the collector, resulting in higher daily collector efficiencies than with the thermosyphon system.

7.3 Discussions on Model Performance

The validated model of active flat-plate collectors was incorporated into the active system model to calculate the solar heat gain into the building. Using the fully-implicit finite difference method (with which convergence is guaranteed), the solar heat gain was used to calculate the room air temperature together with the floor temperature distribution. Therefore, the predicted performance of the active system was expected to be close to reality. This may be seen from the comparison of the solar heat gains (see Table 7.3) into the building, and from the comparison of

Table 7.3. COMPARISON OF ACTIVE AND THERMOSYPHON SYSTEMS

mm/dd/yy	I_o , KJ/m ²	ACTIVE		THERMOSYPHON	
		ΣQ , KJ/m ²	η , %	ΣQ , KJ/m ²	η , %
12/21/85	11,020.9	4,315.7	39.2	2,876.4	26.1
12/22/85	7,282.7	3,115.8	42.8	1,311.4	18.0
02/05/86	8,172.3	2,608.9	31.9	1,773.4	10.9
02/06/86	13,458.8	4,673.2	34.7	4,195.5	26.1
02/07/86	6,765.6	1,815.9	26.8	457.9	6.8

temperature rises in the building between the actual thermosyphon system and the simulated active system (see Figures 7.5 to 7.8). Table 7.3 shows, for example, that on Dec. 21, 1985 the energy collection of the existing shop was 2,876.4 KJ/m² and that of the active system would be 4,315.7 KJ/m² (1439.3 KJ/m² more than the existing system). In Figure 7.5, the room temperature of the active system is seen to be higher, but not too high, than that of thermosyphon system throughout the day.

The simulation model for the direct gain system, however, appears to be over-performing. Under cloudy day conditions such as those of Feb. 5 or 7, 1986, little direct solar radiation was available. Thus the indoor air temperature of a big shop with a large south window would be unlikely to heat up to 30°C while the outdoor temperature remained below -10°C. Overheating, however, in a direct gain building may occur on sunny days in winter time, as reported by other investigators (Mahajan and Liu, 1983; Scully, 1979; Sandia Laboratories, 1979). Therefore, the direct gain model was expected to follow the real system but with overestimation of the room air temperature to some degree.

This overestimation may be caused by neglecting the long-wave radiant heat losses through the glazing of the shop. The results from the model could serve as indications of what might happen approximately in a direct gain building.

7.4 Discussions on Performances of Different Systems

Several interesting points have been identified through the study of the project.

The existing thermosyphon system maintained a satisfactory environment when the outdoor temperature was above 0°C. In spite of high air temperature at the outlet, the thermosyphon system did not transport heat into the shop effectively when the sun was shining. This was mainly due to the low air flow rate induced by the buoyancy forces. When the outdoor temperature dropped below -10 °C, the system was unable to maintain a tolerable working temperature, although the mean room temperatures were approximately 20°C higher than the outdoor temperature. The daily collector efficiency of the building was seen to be lower for cloudy days than that for sunny days.

The comparison of the three systems (thermosyphon, active and direct-gain) indicates that a direct-gain system could perform just as well as the other two types of systems, if the south window were dimensioned properly, if provisions were made to avoid summer overheating and if low night-time temperatures could be tolerated. The large

temperature fluctuations in a diurnal cycle for the direct gain system is because, during daytime the glazed area is able to transmit up to 90% of the total solar radiation incident upon it, but at night the large window area, if uninsulated, is extremely effective in losing heat by both conduction and radiation. Overheating of the shop could occur, even in winter time, with a direct gain system if the window area were as big as the collecting area of the existing system. A properly dimensioned south-facing window with night insulation would certainly improve the thermal performance of the building.

From an economic point of view, the direct gain system appears to offer promise for heating of farm shops. The cost of the existing building was, according to the owner (Harrold, 1986), \$996.00 (materials) plus \$1,300.00 (labour). The extra cost due to the construction of the collector was around \$1,000.00. It is estimated that a direct gain system (without night insulation) with a south window area of 20 m² (less than half of the collector area) would save 50 - 70% of the extra cost, and would maintain a satisfactory daytime environment for a farm shop. Another obvious advantage of the direct gain system is its natural lighting during daytime.

Another viable option is the fan-forced flow, especially during cloudy days. The simulated results show that an air flow rate of 0.01 m³/s per m² collector area, would increase the daily efficiency of the collector by

about 20%. In addition, thermal stratification of room air could be—reduced. The fan could be controlled thermostatically or manually, being turned off when indoor temperature reached the desired point. Thermal storage seems unnecessary for this particular system, since heating is required only during daytime. Front-pair flow is not recommended for active systems since front flow increases the heat loss, dirties the glazing and deteriorates the absorbing surface.

The additional cost of installation of a fan plus necessary ducting seems to be not too high. The Koenders Model KV15 ventilation fan (1984 retail price: \$165.00, manufactured by Koender's Sales & Service, Englefeld, Sask.) with an air flow rate range of 345 to 706 L/sec, for example, would meet the flow requirement of 600 L/sec for the simulated active system. The running cost of such a fan (220 W) is estimated to be 10 ¢ a day on an eight-hour operation scheme (not including a service charge of \$7.15 per month).

Table 7.4 shows the cost, in terms of physical unit KWH, of using electric heaters instead of a fan to supply the same amount of heat into the shop as that collected and transported into the building by using a small fan. The capital investment was not taken into consideration for these systems. Electric heaters, for example, would have to provide an equivalent amount of heat of 7.60 KWH on Feb. 6 and 21.61 KWH on Feb. 7, 1986, whereas the running of a 220

Table 7.4. SAVINGS OF AN ACTIVE SYSTEM AGAINST ELECTRIC HEATERS

mm/dd/yy	energy collection			savings	
	thermosyphon KWH	fan KWH	diff. KWH	KWH	%
12/21/85	45.79	68.69	22.90	21.16	92.40
12/22/85	20.87	49.59	28.72	26.96	93.87
02/05/86	14.11	41.53	27.42	25.66	93.58
02/06/86	66.78	74.38	7.60	5.84	76.84
02/07/86	7.29	28.90	21.61	19.85	91.86

W fan in an active system on an eight-hour basis would be only 1.76 KWH. The savings of using a fan instead of electric heaters on these two days would be 76.84% and 91.86%, respectively. The above percentage savings would be the same if stated in terms of dollars.

The ceiling-mounted circulation fans for destratification of room air seems not as important in an active system as in a thermosyphon system, since room air has been stirred and circulated through the collector. In other words, these circulation fans would have little effect, when running, on the performance of an active system and, therefore, could be removed.

8. CONCLUSIONS AND RECOMMENDATIONS

The study of the project has shown:

1. No validated, accurate simulation model for a thermosyphon air system has been found to be available in the literature.
2. The validity of the active system collector model developed in this project has been proven and, therefore, can be used for simulation studies of flat-plate, (air) solar collectors.
3. Actual performance of the existing thermosyphon system is satisfactory for the owner's requirements (spring and fall daytime use).
4. On the basis of simulation, the efficiency of the existing system could be improved, on average, by 20% by using a small fan to provide a forced-flow active system.
5. For future similar installations consideration should be given to direct gain systems if low night-time temperatures could be tolerated.

For further study of this or similar projects, the following are recommended:

- Measurement on the performance of a direct gain system, if possible, should be performed to determine how such a system will actually behave in terms of the requirements of a farm shop, on one hand, and on the other hand, to check the direct gain model derived in this project.
- Systematic investigations on the effects of design

parameters of a thermosyphon air system on its performance might find the optimum design for the system. A computer simulation model is essential for such studies. A model of this type, however, would be complex and might require a great deal of effort to develop.

- The flat-plate solar collector model developed in this project may be used to study the effects of different flow patterns (front-path only, back-path only or both) on the collector performance.
- Since the simulation results of the flat-plate solar collector model shown a little difference between one-subregion runs and ten-subregion runs, the temperature profile along a collector may be an interesting subject to study. The results of such an investigation would help to understand better the nature of flat-plate solar collectors.

REFERENCES

- Akbari, H. and T.R. Borgers. 1979. Free convective laminar flow within the Trombe wall channel. Solar Energy. 22:165-174.
- ASHRAE. 1971. Procedure for Determining Heating and Cooling Loads for Computerized Energy Calculations - Algorithms for Building Heat Transfer Subroutines. Am. Soc. Heat. Refrig. Air-Cond. Engrs., Atlanta, GA.
- ASHRAE. 1976a. Thermophysical Properties of Refrigerants. pp. 171-175. Am. Soc. Heat. Refrig. Air-Cond. Engrs., Atlanta, GA.
- ASHRAE. 1976b. Subroutine Algorithms for Heating and Cooling Loads to Determine Building Energy Requirements. Am. Soc. Heat. Refrig. Air-Cond. Engrs., Atlanta, GA.
- ASHRAE. 1977. ASHRAE Handbook - 1977 FUNDAMENTALS. Am. Soc. Heat. Refrig. Air-Cond. Engrs., Atlanta, GA.
- ASHRAE. 1978. Test Standard 93-77: Method of Testing to Determine the Thermal Performance of Solar Collectors. Am. Soc. Heat. Refrig. Air-Cond. Engrs., Atlanta, GA.
- ASHRAE. 1981. ASHRAE FUNDAMENTALS 1981. Am. Soc. Heat. Refrig. Air-Cond. Engrs., Atlanta, GA.
- Borgers, T.R. and H. Akbari. 1984. Free convective turbulent flow within the Trombe wall channel. Solar Energy. 33(3/4):253-264.
- Brewer, R.N. 1981. Solar Applications in Agriculture. The Franklin Institute. Philadelphia, Penn.
- Calderwood, D.L. 1981. Rice drying techniques with solar

- heat. *Agricultural Energy*. 1:36-40. Am. Soc. Agric. Eng., St Joseph, MI.
- Carter, C. 1980. The Trombe solar wall in Canada. SOLWEST80: Proceedings of the Joint Solar Conference. pp.453-456. Sol. Ener. Soc. of Canada, Inc. and the Pacific Northwest Solar Energy Association.
- Chapman, A.J. 1984. Heat Transfer. McMillan Publishing Company. New York, NY.
- Chau, K.V. and C.D. Baird. 1981. Solar grain drying under hot and humid conditions. *Agricultural Energy*. 1:31-35. Am. Soc. Agric. Eng., St Joseph, MI.
- Chen, R and W.R. Jones. 1981. Test results - thermosyphon versus active solar domestic water heating systems. *Comptes Rendus/Proceedings 1981 La Societe D'Energie Solair du Canada Inc.*, pp. 215-217.
- Converse, H.H., F.S. Lai, D.F. Aldis and D.B. Sauer. 1981. Application of solar energy in grain drying. *Agricultural Energy*. 1:131-136. Am. Soc. Agric. Eng., St Joseph, MI.
- Cook, R.D. 1981. Concepts and Applications of Finite Element Analysis. John Wiley & Sons. New York, NY.
- Duffie, J.A. 1978. Simulation and design methods. *Tutorials of the 1978 Annual Meeting*. pp.33-38. Am. Sec. Int. Sol. Ener. Soc. (AS/ISES), Newark, DE.
- Duffie, J.A. and W.A Beckman. 1974. *Solar Energy Thermal Processes*. John Wiley & Sons. New York, NY.
- Eckert, E.R.G. and R.M. Drake (Jr). 1972. *Analysis of Heat*

- and Mass Transfer, McGraw-Hill, Inc., New York, NY.
- Edwards, D.K. 1977. Solar absorption by each element in an absorber - coverglass array. Solar Energy. 19:401-402.
- Ellis, L.V. and R.E. Phillips. 1982. Solar assisted sow-pig nursery unit. Proceedings of the 2nd International Livestock Environment Symposium - Livestock Environment II. pp. 115-118. Am. Soc. Agric. Eng., St Joseph, MI.
- Feddes, J.J.R., J.B. McQuitty and H.P. Harrison. 1980. Grain drying with solar-heated air. Canadian Agricultural Engineering. 22(1):81-84. Can. Agric. Eng.
- Fisk, M.J. and H.C.W. Anderson. 1982. Introduction to Solar Technology. Addison-Wesley Publishing Company, Inc., Menlo Park, CA.
- Gebhart, B. 1971. Heat Transfer. McGraw-Hill, Inc., New York, NY.
- Hagan, D.A., B. Wadsworth and L. Palmiter. 1980. Preliminary results of thermosiphon air panels retrofit. Proceedings of the 5th National Passive Solar Conference. pp. 1046-1050. Am. Sec. Int. Sol. Ener. Soc. (AS/ISES), Newark, DE.
- Halacy, D.S. 1973. The Coming Age of Solar Energy. Harper and Row, Publishers, Inc. New York, NY.
- Harrold, K. 1986. Personal communication. Harrold Farm, Lamont, Alberta.
- Hellickson, M.A. 1982. A multiple use solar system for heating livestock buildings. Proceedings of the 2nd International Livestock Environment Symposium -

- Livestock Environment II. pp. 138-145. Am. Soc. Agric. Eng., St Joseph, MI.
- Hollands, K.G.T., T.E. Unny, G.D. Raithby and L. Konicek. 1976. Free convective heat transfer across inclined air layers. J. Heat Transfer. 98(2):189-193.
- Jones, M.M. and W.S. Morris. 1980. Two innovative passive air thermosiphon houses in Santa Fe. Proceedings of the 5th National Passive Solar Conference. pp. 1051-1055. Am. Soc. Int. Sol. Ener. Soc. (AS/ISES), Newark, DE.
- Kohler, J. 1981. TAPFLOW. Solar Age. 6(3):48-50.
- Lasco Industries. 1982. Technical Bulletin. (Subject: Crystalite-T) Marketing Dept., Lasco Industries. Anaheim, CA.
- Lebens, R.M. 1979. A design tool to assess room air temperature of a passive heated space. Passive Systems '78. pp. 45-52. Am. Soc. Int. Sol. Ener. Soc. (AS/ISES), Newark, DE.
- Leon, S.J. 1980. Linear Algebra with Applications. Macmillan Pub. Co., Inc., New York, NY.
- Liu, B.Y.H. and R.C. Jordan. 1963. The long-term average performance of flat-plate solar energy collectors. Solar Energy. 7(2):53-74.
- Mahajan, B.M. and S.T. Liu. 1983. Initial results from the NBS passive solar test facility. Solar Engineering-1983. pp.109-115. Am. Soc. Mech. Engrs., New York, NY.
- Marshall, L.S., P.J. Burns and C.B. Winn. 1980. Analysis and performance evaluation of an air thermosiphon system.

Proceedings of the 5th National Passive Solar Conference. pp. 1056-1060. Am. Soc. Int. Sol. Ener. Soc. (AS/ISES), Newark, DE.

Marshall, L.S., P.J. Burns and C.B. Winn. 1981. The measured performance of an air thermosyphon system. Solar Engineering - 1981. pp. 122-129.

Mehta, D.P. and J.E. Woods. 1980. An experimental validation of a rational model for dynamic response of buildings. ASHRAE Trans. 86(2):497-518.

Mercer, W.E., W.M. Pearce and J.E. Hitchcock. 1967. Laminar forced convection in the entrance region between parallel flat-plates. J. Heat Transfer, 89:251-257.

Mitalas, G.P. and J.G. Arseneault. 1972. FORTRAN IV Program to Calculate Z-transfer Functions for the Calculation of Transient Heat Transfer Through Walls and Roofs. DBR Computer Program No.33. National Research Council of Canada. Ottawa, On.

Nogotov, E.F. 1978. Applications of Numerical Heat Transfer. United Nations Educational, Scientific, and Cultural Organization (Unesco). Paris, France.

O'Brien-Bernini, F.C. and J.G. McGowan. 1984. Performance modelling of non metallic flat-plate solar collectors. Solar Energy. 33(3/4):305-319.

Patankar, S.V. 1980. Numerical Heat Transfer. Hemisphere Pub. Corp., New York, NY.

Ramsey, J.W. and M. Charmchi. 1980. Variance in solar collector performance predictions due to different

- methods of evaluating wind heat transfer coefficients.
J. Heat Transfer, 102:766-768.
- Rapp, D. 1981. Solar Energy. Prentice-Hall, Inc. Englewood Cliffs. New Jersey, NY.
- Reif, D.K. 1980, Site built thermosiphoning air panels (TAPS). Proceedings of the 5th National Passive Solar Conference. pp. 318-320. Am. Sec. Int. Sol. Ener. Soc. (AS/ISES), Newark, DE.
- Reno, V. 1981. Thermosiphoning air panels: Going with the flow?. Proceedings of the 6th National Passive Solar Conference. pp. 149-153. Am. Sec. Int. Sol. Ener. Soc. (AS/ISES), Newark, DE.
- Sandia Laboratories. 1979. Passive Solar Building. pp.183-193. National Technical Information Service. Springfield, VA.
- Scully, D. 1979. Knowing and loving, and never knowing: two houses. Passive Systems'78. pp. 15-19. Am. Sec. Int. Sol. Ener. Soc. (AS/ISES), Newark, DE.
- Shewen, E.C. et al. 1980. Solar Energy Program. Solar Energy Project Report No.COLL-9. National Research Council of Canada. Ottawa, ON.
- Sparrow, E.M. and R.D. Cess. 1978. Radiation Heat Transfer. Hemisphere Pub. Corp., New York, NY.
- Sparrow, E.M., J.W. Ramsey and E.A. Mass. 1979. Effect of finite width on heat transfer and fluid flow about an inclined rectangular plate. J. Heat Transfer. 101:199-204.

- Stephenson, D.G. and G.P. Mitalas. 1967. Cooling load calculation by thermal response factor method. Trans. Am. Soc. Heat. Refrig. Air-Cond. Engrs., 73(I):III.1.1-1.7.
- Stetzel, W. 1983. Work place needs no backup heat. Solar Age. 8(8):17-20.
- Stout, B.A. 1978. Agricultural applications of solar energy. Solar Diversification: A Summary of the Basics in Solar Energy. pp. 96-107. Am. Soc. Int. Sol. Ener. Soc. (AS/ISES), Newark, DE.
- Stout, B.A. 1979. Energy for World Agriculture. Food and Agriculture Organization of the United Nations. New York, NY.
- Subbarao, K., J.V. Anderson and M. Connolly. 1983. A fourier transfer application to building simulations with thermostatic controls. Solar Engineering-1983. pp. 28-32. Am. Soc. Mech. Engrs., New York, NY.
- Sucec, J. 1975. Heat Transfer. Simon and Schuster, Inc., New York, NY.
- Thompson, T.L. and R.O. Pierce. 1981. Solar grain drying management. Agricultural Energy. 1:25-30. Am. Soc. Agric. Engrs., St Joseph, MI.
- Thorndike, E.H. 1976. Energy and Environment: a Primer for Scientists and Engineers. Addison-Wesley Publishing Comp., Inc., Menlo Park, CA.
- Waddell, E.L. (Jr), R.S. Pile and D.W. Burch. 1982. Solar energy: a farmstead application for broiler production.

- Proceedings of the 2nd International Livestock Environment Symposium - Livestock Environment II. pp. 133-137. Am. Soc. Agric. Eng., St Joseph, MI.
- Walls, I.G. 1973. The Complete Book of the Greenhouse. Ian G Walls & Ward Lock Ltd., London, Great Britain.
- Whiller, A. 1963. Plastic covers for solar collectors. Solar Energy. 7(3):148-151.
- Williams, J.R. 1983. Passive Solar Heating. Ann Arbor Science Publishers. Ann Arbor, MI.
- Winn, C.B. 1982. A simple tool for the design of passive solar buildings. J. of Solar Energy Engineering. 104(3):216-222.

APPENDIX A.1: FLOOR RESPONSE FACTORS USED IN THE DIRECT-GAIN MODEL

NUMERICAL DATA FOR THE CONCRETE FLOOR

(Floor is considered as one layer)
 LAYER THICKNESS CONDUCT. DENSITY SP HEAT RESISTANCE DESCRIPTION OF LAYERS

0.2030	1.0200	1280.0000	927.0000	0.0	Concrete floor
0.0	0.0	0.0	0.0	1.7800	Ground thermal resistance

THERMAL CONDUCTANCE, U= 0.505

SAMPLING TIME INTERVAL, DT= 900.00 seconds

RESPONSE FACTORS FOR CONCRETE FLOOR SLAB

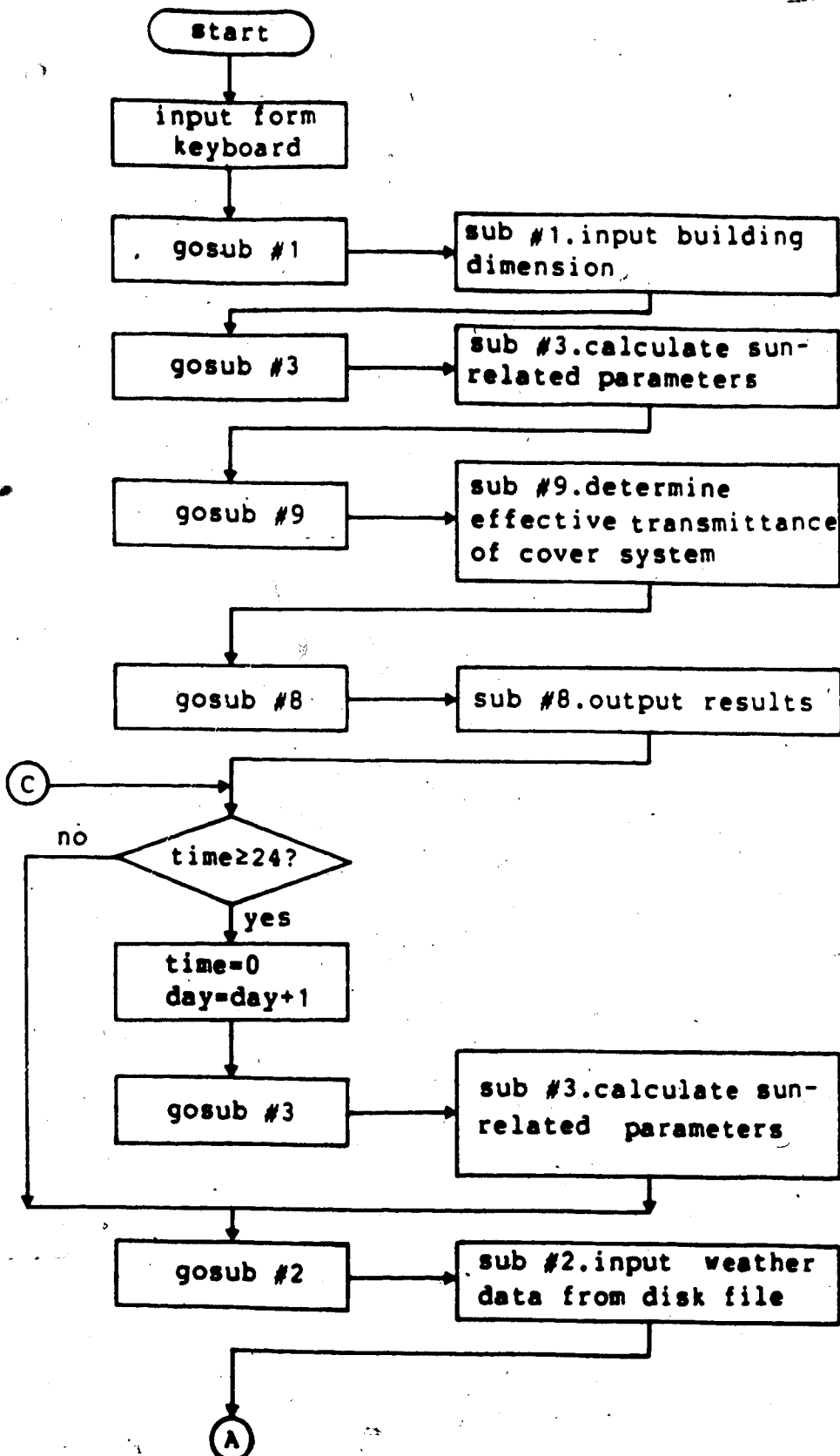
j	a(j)	b(j)	c(j)
0	0.000000	0.555389	1.000000
1	0.000066	-1.143933	-2.050275
2	0.001199	0.773756	1.379918
3	0.002610	-0.196120	-0.347679
4	0.001137	0.016366	0.028755
5	0.000107	-0.000338	-0.000582
6	0.000002	0.000001	0.000002
7	0.000000	-0.000000	-0.000000

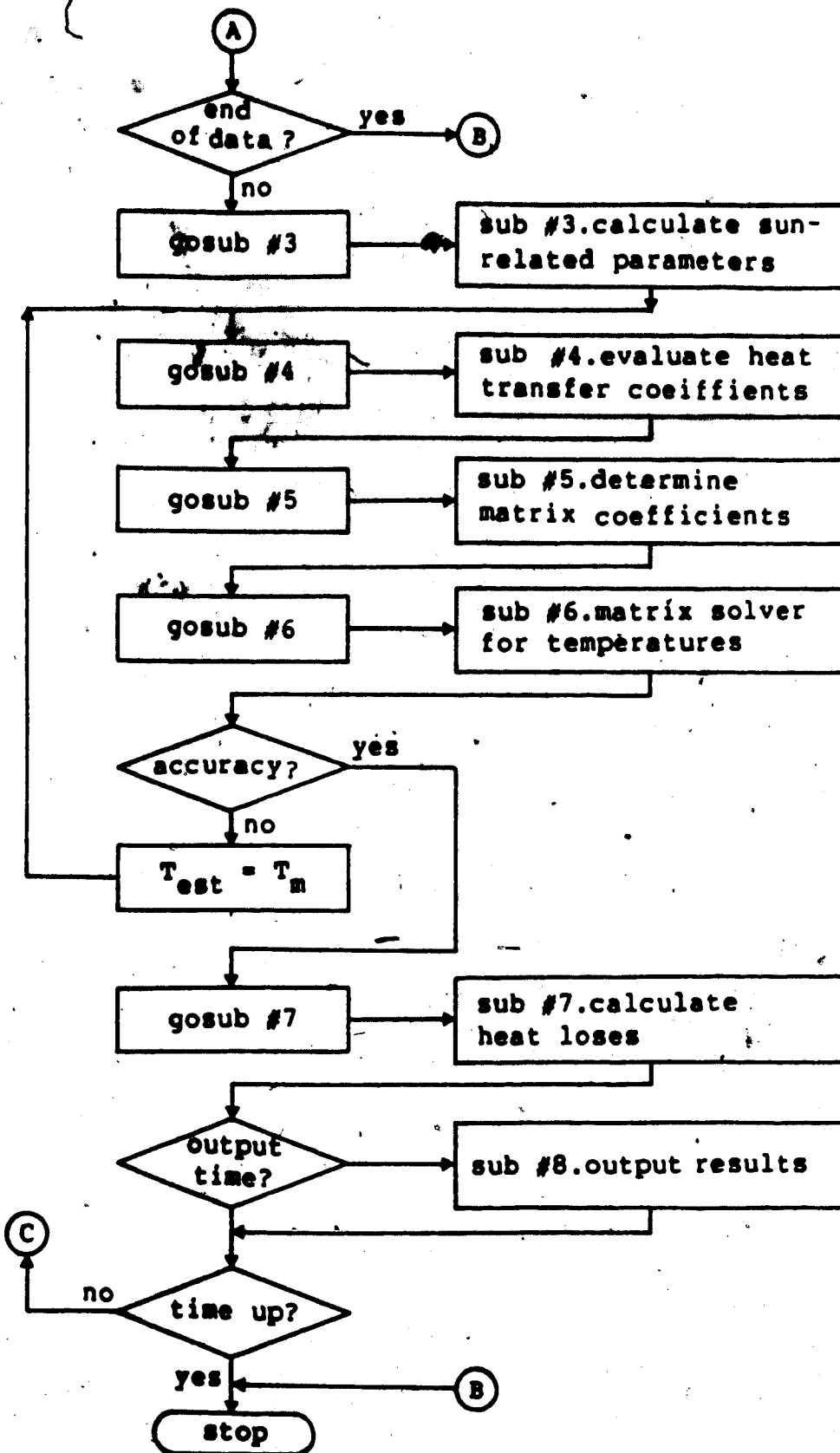
**APPENDIX A.2: ROOM SURFACE ANGLE FACTORS USED IN THE
DIRECT-GAIN MODEL**

F_{ij}

i \ j	1	2	3	4	5	6
1	.0	.3	.11	.18	.11	.3
2	.522	.0	.075	.216	.075	.138
3	.33	.195	.0	.21	.07	.195
4	.313	.204	.14	.0	.14	.204
5	.33	.195	.075	.21	.0	.195
6	.522	.138	.075	.216	.075	.0

APPENDIX A.3: FLOWCHART FOR THE DIRECT-GAIN MODEL





APPENDIX A.4: PROGRAM LISTING OF THE DIRECT-GAIN MODEL

```

10  $$$$$$$$$$$$$$$$$$$$$$$$$$$$$$$$$$$$$$$$$$$$$$$$$$$$$$$$$$$$$$$$$$$$$$$$
20  $$$$$$$$$$$$$$$$$$$$$$$$$$$$$$$$$$$$$$$$$$$$$$$$$$$$$$$$$$$$$$$$$$$$$$$$
30  $$$$$$$$$$$$$$$$$$$$$$$$$$$$$$$$$$$$$$$$$$$$$$$$$$$$$$$$$$$$$$$$$$$$$$$$
40  $$$$$$$$$$$$$$$$$$$$$$$$$$$$$$$$$$$$$$$$$$$$$$$$$$$$$$$$$$$$$$$$$$$$$$$$
50  $$$$$$$$$$$$$$$$$$$$$$$$$$$$$$$$$$$$$$$$$$$$$$$$$$$$$$$$$$$$$$$$$$$$$$$$
60  $$$$$$$$$$$$$$$$$$$$$$$$$$$$$$$$$$$$$$$$$$$$$$$$$$$$$$$$$$$$$$$$$$$$$$$$
70  $$$$$$$$$$$$$$$$$$$$$$$$$$$$$$$$$$$$$$$$$$$$$$$$$$$$$$$$$$$$$$$$$$$$$$$$
80  $$$$$$$$$$$$$$$$$$$$$$$$$$$$$$$$$$$$$$$$$$$$$$$$$$$$$$$$$$$$$$$$$$$$$$$$
90  $$$$$$$$$$$$$$$$$$$$$$$$$$$$$$$$$$$$$$$$$$$$$$$$$$$$$$$$$$$$$$$$$$$$$$$$
100 $$$$$$$$$$$$$$$$$$$$$$$$$$$$$$$$$$$$$$$$$$$$$$$$$$$$$$$$$$$$$$$$$$$$$$$$
110 $$$$$$$$$$$$$$$$$$$$$$$$$$$$$$$$$$$$$$$$$$$$$$$$$$$$$$$$$$$$$$$$$$$$$$$$
120 $$$$$$$$$$$$$$$$$$$$$$$$$$$$$$$$$$$$$$$$$$$$$$$$$$$$$$$$$$$$$$$$$$$$$$$$
130 $$$$$$$$$$$$$$$$$$$$$$$$$$$$$$$$$$$$$$$$$$$$$$$$$$$$$$$$$$$$$$$$$$$$$$$$
140 $$$$$$$$$$$$$$$$$$$$$$$$$$$$$$$$$$$$$$$$$$$$$$$$$$$$$$$$$$$$$$$$$$$$$$$$
150 $$$$$$$$$$$$$$$$$$$$$$$$$$$$$$$$$$$$$$$$$$$$$$$$$$$$$$$$$$$$$$$$$$$$$$$$
160 $$$$$$$$$$$$$$$$$$$$$$$$$$$$$$$$$$$$$$$$$$$$$$$$$$$$$$$$$$$$$$$$$$$$$$$$
170 $$$$$$$$$$$$$$$$$$$$$$$$$$$$$$$$$$$$$$$$$$$$$$$$$$$$$$$$$$$$$$$$$$$$$$$$
180 $$$$$$$$$$$$$$$$$$$$$$$$$$$$$$$$$$$$$$$$$$$$$$$$$$$$$$$$$$$$$$$$$$$$$$$$
190 $$$$$$$$$$$$$$$$$$$$$$$$$$$$$$$$$$$$$$$$$$$$$$$$$$$$$$$$$$$$$$$$$$$$$$$$
200 $$$$$$$$$$$$$$$$$$$$$$$$$$$$$$$$$$$$$$$$$$$$$$$$$$$$$$$$$$$$$$$$$$$$$$$$
210 $$$$$$$$$$$$$$$$$$$$$$$$$$$$$$$$$$$$$$$$$$$$$$$$$$$$$$$$$$$$$$$$$$$$$$$$
220 $$$$$$$$$$$$$$$$$$$$$$$$$$$$$$$$$$$$$$$$$$$$$$$$$$$$$$$$$$$$$$$$$$$$$$$$
230 $$$$$$$$$$$$$$$$$$$$$$$$$$$$$$$$$$$$$$$$$$$$$$$$$$$$$$$$$$$$$$$$$$$$$$$$
240 $$$$$$$$$$$$$$$$$$$$$$$$$$$$$$$$$$$$$$$$$$$$$$$$$$$$$$$$$$$$$$$$$$$$$$$$
250 $$$$$$$$$$$$$$$$$$$$$$$$$$$$$$$$$$$$$$$$$$$$$$$$$$$$$$$$$$$$$$$$$$$$$$$$
260 $$$$$$$$$$$$$$$$$$$$$$$$$$$$$$$$$$$$$$$$$$$$$$$$$$$$$$$$$$$$$$$$$$$$$$$$
270 $$$$$$$$$$$$$$$$$$$$$$$$$$$$$$$$$$$$$$$$$$$$$$$$$$$$$$$$$$$$$$$$$$$$$$$$
280 $$$$$$$$$$$$$$$$$$$$$$$$$$$$$$$$$$$$$$$$$$$$$$$$$$$$$$$$$$$$$$$$$$$$$$$$
290 $$$$$$$$$$$$$$$$$$$$$$$$$$$$$$$$$$$$$$$$$$$$$$$$$$$$$$$$$$$$$$$$$$$$$$$$
300 $$$$$$$$$$$$$$$$$$$$$$$$$$$$$$$$$$$$$$$$$$$$$$$$$$$$$$$$$$$$$$$$$$$$$$$$
310 $$$$$$$$$$$$$$$$$$$$$$$$$$$$$$$$$$$$$$$$$$$$$$$$$$$$$$$$$$$$$$$$$$$$$$$$
320 $$$$$$$$$$$$$$$$$$$$$$$$$$$$$$$$$$$$$$$$$$$$$$$$$$$$$$$$$$$$$$$$$$$$$$$$
330 $$$$$$$$$$$$$$$$$$$$$$$$$$$$$$$$$$$$$$$$$$$$$$$$$$$$$$$$$$$$$$$$$$$$$$$$
340 $$$$$$$$$$$$$$$$$$$$$$$$$$$$$$$$$$$$$$$$$$$$$$$$$$$$$$$$$$$$$$$$$$$$$$$$

PROGRAM DIRGAIN
=====
FOR THIS PROJECT
BY
   QIQIU ZHAO
DEPARTMENT OF AGRICULTURAL ENGINEERING
UNIVERSITY OF ALBERTA
DATE OF START: MARCH 15, 1986
SUPERVIZED BY: PROF. J.J. LEONARD
=====
THIS IS A COMPUTER MODEL WHICH SIMULATES THE THERMAL BEHAVIOR OF
PASSIVE DIRECT-GAIN STRUCTURES. ROOM AIR TEMPERATURE AT ANY INSTANT
IS CALCULATED WITH THE THERMAL BALANCE APPROACH. A SET OF MATRIX
COEFFICIENTS IS DETERMINED FROM THE CONDITIONS AT A GIVEN TIME, WHICH
INCLUDES THE EVALUATION OF HEAT TRANSFER COEFFICIENTS ON THE SURFACES
OF THE BUILDING WALL COMPONENTS. THERMAL MASS EFFECT IS ACCOUNTED FOR
BY USING RESPONSE METHOD FOR COMPUTATION OF HEAT CONDUCTION THROUGH
THE FLOOR CONCRETE. THE PROGRAM READS IN THE SOLAR DATA FOR THE DAY
CONSIDERED, WHICH INCLUDE SOLAR RADIATION, OUTDOOR TEMPERATURE AND THE
WIND VELOCITY.
THIS PROGRAM HAVE A MAIN SECTION AND 9 SUBROUTINES.
SUB #1: INPUT OF PHYSICAL AND THERMAL PARAMETERS OF THE BUILDING
SUB #2: READ-IN THE SOLAR DATA
SUB #3: CALCULATION OF SOLAR ANGLES & RADIATION RECEIVED BY EACH WALL
SUB #4: DETERMINATION OF HEAT TRANSFER COEFFICIENTS
SUB #5: CALCULATION OF MATRIX COEFFICIENTS
SUB #6: MATRIX SOLVER
SUB #7: CALCULATION OF HEAT LOSSES
SUB #8: OUTPUT ROUTINE
SUB #9: CALCULATION OF TRANSMITTANCE AND ABSORPTANCE OF COVER SYSTEM
DI --- GLOBAL SOLAR RADIATION, W/m^2
FNRO.A(X) --- AIR DENSITY AT TEMP X(K), kg/m^3

```

```

350 FNCP.A(X) --- AIR SPECIFIC HEAT AT TEMP X(K), J/kg-K
360 FNK.A(X) ---- AIR THERMAL CONDUCTIVITY AT TEMP X(K), W/m-K
370 FNMU.A(X) --- AIR DYNAMIC VISCOSITY AT TEMP X(K), N-sec/m^2
380 T ---- TEMPERATURES OF INTERIOR SURFACES(C)
390 TA --- AMBIENT TEMPERATURE(C)
400 TRR -- ROOM AIR TEMP FOR THE REAL SITUATION FOR COMPARISON(C)
410 VWD -- AMBIENT WIND SPEED(M/sec),
420
430 'MAIN SECTION OF THE PROGRAM
440 DIM AB(6), BETA(6), E(6), E1(6), F(6,6), H(6), S(6), U(6), U1(6)
450 DIM SAZM(2,6), SR(2,6), SS(6), F.SKY(6), F.GRD(6)
460 DIM ALFA(20), ROU(20), TAU1(20)
470 DIM A1(20), AE(20), Q(20), R(20), TRANS(20)
480 DIM A(7,7), B(7), G(6,6)
490 DIM C1(20), C2(20), C3(20), Q1(20), T(7), T1(20), TE(7)
500 DIM I01(100), DI1(100), TA1(100), TRR1(100), VWD1(100)
510 DEF FNARCSIN(X) = ATN(X)/SQR(1 - X*X)
520 DEF FNARCCOS(X) = 1.570796 - ATN(X)/SQR(1 - X*X)
530 DEF FNRO.A(X) = 3531/X
540 DEF FNCP1.A(X) = 10001*(1.032 - .001225 * X)
550 DEF FNCP2.A(X) = 10001*(1.02252 - .000176*X+4.02E-07*X*X-4.87E-11*X^3)
560 DEF FNK1.A(X) = SQR(X)/(385.859 + 911441/X - 26866701/X^2 + 5.52604E+07/X^3)
570 DEF FNK2.A(X) = SQR(X)/(328.052 + 1673231/X - 3.02953E+07/X^2 + 3.05862E+09/X^3)
580 DEF FNDEN(X) = .6717 + 85.23001/X - 2111.475/X^2 + 1064171/X^3
590 DEF FNMU.A(X) = SQR(X)/(FNDEN(X) * 1000000!)
600
610 OPEN "B:OKOUT" FOR OUTPUT AS #2
620 INPUT "Sub-increment for time step(sec.) is ";DT1 :PRINT
630 INPUT "Number of iterations on the 1st day's data is ";NORX :PRINT
640 INPUT "Reference Temperature(C) is ";T.REF :PRINT
650 INPUT "Number of Covers(<20) is ";NCX :PRINT
660 INPUT "Infiltration rate(Charges/hr) is ";R.ALK :PRINT
670 INPUT "Snow cover on ground(0.7 for yes; 0.2 for none)";SNOW :PRINT
680 COLOR 31
690 PRINT:PRINT"!!!!!!!!!! ATTENTION !!!!!!!!!!!" :PRINT :PRINT
700 COLOR 7

```

```

710 PRINT "I AM WORKING RIGHT NOW. DON'T SWITCH ME OFF, PLEASE."
720 PRINT: PRINT "THANKS."
730 GOSUB 1320
740 BW = (BW1 + BW2)/2!
750 PHY1 = ATN(BL/BW)
760 OPEN "B:DFILE2" FOR INPUT AS #1
770 FOR IX= 0 TO 95
780 INPUT #1, TIMM,I01(IX),DI1(IX),TA1(IX),V.A,T.TOP,TRR1(IX),ETA.1,VWD1(IX),WDIR1
790 PRINT, TIMM, DI1(IX), TA1(IX), VWD1(IX), TRR1(IX)
800 NEXT IX
810 TIM = 0! :TIM1 = 0! :PRTIM1 = 0! :DDTX = 0
820 FLAG1% = 0 :FLAG2% = 0 :FLAG3% = 0
830 NX = NSX :RPT% = 0
840 GOSUB 2690 'FOR INITIAL SOLAR DATA INPUT
850 GOSUB 2960 'CALCULATION OF SUNRISE & SUNSET TIME
860 GOSUB 5650 'FOR INITIAL PRINTOUT
870
880 WHILE TIM1 < FINTIM
890 WHILE PRTIM1 < PRTIM
900 TIM = TIM + DT :TIM1 = TIM1 + DT :PRTIM1 = PRTIM1 + DT
910 IF TIM < 24! GOTO 970
920 IF FLAG3%=0 THEN RPT%=RPT%+1 :DDTX=0 :TIM=0! :TIM1=0! :GOTO 970
930
940 IF IDX = 30 THEN MON% = MON% + 1 :IDX = 0
950 IF IDX < 30 THEN IDX = IDX + 1
960 FLAG1% = 0 :TIM = 0!
970
980 IF FLAG2% = 1 THEN 1000
990 IF RPT% = NOR% THEN FLAG2% = 1 :FLAG3% = 1 :TIM1 = 24! :GOTO 930
1000
1010 GOSUB 2690 'INPUT THE SOLAR DATA
1020 IF FLAG2% = 0 THEN DDTX = DDTX + 1
1030 GOSUB 2960 'DETERMINING SOLAR RADIATION ON EACH SURFACE
1040 DTT = 0!
1050 WHILE DTT < DT*3600!
1060

```

```

1070
1080
1090
1100
1110
1120
1130
1140
1150
1160
1170
1180
1190
1200
1210
1220
1230
1240
1250
1260
1270
1280
1290
1300
1310
1320
1330
1340
1350
1360
1370
1380
1390
1400
1410
1420
GOSUB 4380 ' DETERMINING HEAT TRANSFER COEFFICIENTS
GOSUB 4610 ' CALCULATING MATRIX COEFFICIENTS
GOSUB 4970 ' MATRIX SUBROUTINE TO SOLVE THE MATRIX FOR TEMP
IF ABS(T(7) - TR) > .05 THEN TR = T(7) :GOTO 1060
FOR I% = 1 TO NRES%
  IIX = NRES% + 1 - I%
  T1(IIX) = T1(IIX-1)
  Q1(IIX) = Q1(IIX-1)
NEXT I%
T1(0) = T(1) :TR1 = T(7) :TR = T(7)
GOSUB 5430 ' COMPUTATION OF THE HEAT GAIN INTO THE BUILDING
DTT = DTT + DT1
IF EOF(1) THEN 1270
WEND
WEND
IF RPT% < NOR% - 1 THEN 1240
GOSUB 5650 ' OUTPUT AND SAVE THE RESULTS
PRTIM1 = 0!
WEND
PRINT #2, :PRINT #2,
PRINT #2, " ===== TERMINATION OF THIS RUN ====="
CLOSE
END
*****
SUB #1 READ IN THE THERMAL PROPERTY VALUES FOR WALLS AND CEILING
*****
THIS SUBROUTINE READS IN THE INFORMATION ON BUILDING STRUCTURE AND
THERMAL PROPERTIES OF WALL COMPONENTS. MEANWHILE, IT PRINTS OUT THE
VALUES. ALL THE INFORMATION NEEDED FOR THE RUN OF IS INPUT HERE. IT
IS EXECUTED ONLY AT THE BEGINNING.
NOMENCLATURE
'AB ---- ABSORPTANCE OF SURFACES
'BETA -- TILT ANGLE OF SURFACE(DEG)
'BL,BW,BH, -- LENGTH, WIDTH AND HEIGHT OF THE BUILDING(m)

```

1430 'C1,C2,C3 --- RESPONSE FACTORS OF FLOOR
 1440 'CF ---- CLOUDINESS FACTOR
 1450 'CP,A -- SPECIFIC HEAT(J/kg) OF AIR AT NORMAL CONDITION
 1460 'DT ---- TIME INCREMENT(sec.)
 1470 'E,E1 -- EMITTANCE OF SURFACES
 1480 'F ---- VIEW FACTOS OF INTERIOR SUR.
 1490 'FGRD -- GROUND VIEW FACTOR OF THE GLAZING(DEG)
 1500 'FINTIM- TOTAL TIME FOR THE RUN(hrs)
 1510 'FSKY -- SKY VIEW FACTOR OF THE GLAZING(DEG)
 1520 'H ---- HEAT TRANSFER COEFFICIENTS OF INTERIOR WALL SURFACES(W/m^2.C)
 1530 'ID% --- DAY OF THE MONTH
 1540 'LG ---- LONGITUDE OF THE LOCATION(DEG)
 1550 'LT ---- LATITUDE OF THE LOCATION(DEG)
 1560 'MON% -- MONTH OF THE YEAR
 1570 'NRES% - NUMBER OF RESPONSE FACTORS
 1580 'NS% --- NUMBER OF INTERIOR SURFACES
 1590 'PRTIM - TIME INTRVAL FOR OUTPUT(hrs)
 1600 'R.ALK - RATE OF AIR LEAKAGE(CHARGES/hr)
 1610 'RO.A -- DENSITY(kg/m^3) OF AIR AT NORMAL CONDITION
 1620 'S ---- AREA OF SURFACES(m^2)
 1630 'SAZM -- SURFACE AZIMUTH(DEG.)
 1640 'STM --- STANDARD TIME MERIDIAN OF THE LOCATION(DEG)
 1650 'TAU --- TRANSMITTANCE OF THE GLAZING
 1660 'T.FX -- DESIRED FIX TEMPERATURE OF THE ROOM AIR(C)
 1670 'TG ---- GROUND TEMPERATURE(C)
 1680 'TIM --- TIME IN HOURS
 1690 'T.INI - ASSUMED INITIAL TEMPERATURE FOR ROOM AIR AND SURFACES(C)
 1700 'U,U1 -- CONDUCTANCE OF WALLS(W/m^2.C)
 1710 'V ---- VOLUME OF THE ROOM(m^3)
 1720 'YR% --- YEAR
 1730
 1740 PI = 3.141593 :SIGMA = 5.67E-08 | :NS% = 6 :N% = NS%
 1750 PI180 = PI/180!
 1760 FOR I% = 1 TO NS%
 1770 H(I%) = 11.88
 1780 NEXT I%

```

1790 OPEN "B:DFILE1" FOR INPUT AS #1
1800 INPUT #1, BL, BH, BW1, BW2, V, TAU
1810 INPUT #1, LG, LT, STM, CF
1820 INPUT #1, U1(1), U1(2), U1(3), U1(4), U1(5), U1(6)
1830 INPUT #1, S(1), S(2), S(3), S(4), S(5), S(6)
1840 INPUT #1, E(1), E(2), E(3), E(4), E(5), E(6)
1850 INPUT #1, E1(1), E1(2), E1(3), E1(4), E1(5), E1(6)
1860 INPUT #1, AB(1), AB(2), AB(3), AB(4), AB(5), AB(6)
1870 INPUT #1, BETA(1), BETA(2), BETA(3), BETA(4), BETA(5), BETA(6)
1880 FOR I% = 1 TO 2
1890 INPUT #1, SAZM(I%,1), SAZM(I%,2), SAZM(I%,3), SAZM(I%,4), SAZM(I%,5), SAZM(I%,6)
1900 NEXT I%
1910 FOR I% = 1 TO NS%
1920 INPUT #1, F(I%,1), F(I%,2), F(I%,3), F(I%,4), F(I%,5), F(I%,6)
1930 NEXT I%
1940 INPUT #1, NRES%
1950 FOR I% = 0 TO NRES%
1960 INPUT #1, C1(I%), C2(I%), C3(I%)
1970 NEXT I%
1980 INPUT #1, ID%, MON%, YR%
1990 INPUT #1, TG, T.INI, T.FX
2000 INPUT #1, DT, FINTIM, PRTIM, TIM
2010 TEST = T.INI :TR = T.INI :T(7) = T.INI
2020 CLOSE 1
2030 FOR I% = 0 TO NRES%
2040 T1(I%) = T.INI
2050 Q1(I%) = 0!
2060 NEXT I%
2070 FOR I%=1 TO NS%
2080 BETA(I%) = BETA(I%) * PI180
2090 F.SKY(I%) = (1 + COS(BETA(I%)))/2! :F.GRD(I%) = 1 - F.SKY(I%)
2100 FOR J% = 1 TO 2
2110 SAZM(J%,I%) = SAZM(J%,I%) * PI180
2120 NEXT J%
2130 NEXT I%
2140 FSKY = (1! + COS(BETA(6)))/2! :FGRD = 1 - FSKY

```

```

2150 PRINT #2, " %%%%%%%%%%%%%% OUTPUT OF THE SIMULATION RUN %%%%%%%%%%%%%%"
2160 PRINT #2, :PRINT #2,
2170 PRINT #2, " BUILDING LENGTH ----- ";BL;"(m)"
2180 PRINT #2, " BUILDING HEIGHT ----- ";BH;"(m)"
2190 PRINT #2, " BUILDING BOTTOM WIDTH ----- ";BW1;"(m)"
2200 PRINT #2, " BUILDING TOP WIDTH ----- ";BW2;"(m)"
2210 PRINT #2, " TOTAL VOLUME OF THE BUILDING --- ";V;"(m^3)"
2220 PRINT #2, " TRANSMITTANCE OF COVER GLAZING - ";TAU
2230 PRINT #2, " CLOUDINESS FACTOR ----- ";CF :PRINT #2, :PRINT #2,
2240 PRINT #2, " INFORMATION OF WALL COMPONENTS"
2250 PRINT #2, "-----"
2260 PRINT #2, "U1(I%) S(I%) E(I%) E1(I%) AB(I%) BETA(I%)"
2270 PRINT #2, " W/(m^2.C) m^2 DEG."
2280 PRINT #2, "-----"
2290 FOR IX = 1 TO 6
2300 PRINT #2, U1(I%), S(I%), E(I%), E1(I%), AB(I%), BETA(I%)/PI180
2310 NEXT IX
2320 PRINT #2, "-----"
2330 PRINT #2, :PRINT #2, " ANGLE FACTORS OF INTERIOR WALL SURFACES"
2340 PRINT #2, "-----"
2350 PRINT #2, "F(I%,1) F(I%,2) F(I%,3) F(I%,4) F(I%,5) F(I%,6)"
2360 PRINT #2, "-----"
2370 FOR IX = 1 TO NS%
2380 PRINT #2, F(I%,1), F(I%,2), F(I%,3), F(I%,4), F(I%,5), F(I%,6)
2390 NEXT IX
2400 PRINT #2, "-----"
2410 PRINT #2, " SURFACE AZIMUTH"
2420 PRINT #2, "-----"
2430 PRINT #2, " I% SAZM(1,I%) SAZM(2,I%) "
2440 PRINT #2, " DEG. DEG."
2450 PRINT #2, "-----"
2460 FOR IX=1 TO 6
2470 PRINT #2, I%, SAZM(1,I%), SAZM(2,I%)/PI180
2480 NEXT IX
2490 PRINT #2, "-----"
2500 PRINT #2, :PRINT #2, " NUMBER OF RESPONSE FACTORS = ";NRES% :PRINT #2,

```

```

2510 PRINT #2, "          RESPONSE FACTORS FOR FLOOR SLAB"
2520 PRINT #2, "-----"
2530 PRINT #2, " I%          C1(I%)          C2(I%)          C3(I%)"
2540 PRINT #2, "-----"
2550 FOR I% = 0 TO NRES%
2560 PRINT #2, I%, C1(I%), C2(I%), C3(I%)
2570 NEXT I%
2580 PRINT #2, "-----"
2590 GOSUB 5730
2600 PRINT #2, " GROUND TEMPERATURE -----";TG;"(C)"
2610 PRINT #2, " INITIAL TEMPERATURE ASSUMED - ";T.INI;"(C)"
2620 PRINT #2, " AIR LEAKAGE RATE -----";R.ALK;"(charges/hr)"
2630 PRINT #2, " TIME INCREMENT -----";DT;"(hrs)"
2640 PRINT #2, " PRINTING INTERVAL -----";PRTIM;"(hrs)"
2650 PRINT #2, " TOTAL TIME FOR THE RUN -----";FINTIM;"(hrs)"
2660 PRINT #2, " STARTING TIME FOR THE RUN ---";TIM;"(hrs)"
2670 PRINT #2, " :PRINT #2, :PRINT #2,
2680 RETURN
2690 ' *****
2700 ' SUB #2 SOLAR DATA INPUT
2710 ' *****
2720 '
2730 ' DI --- GLOBAL SOLAR RADIATION(W/m^2)
2740 ' FO --- HEAT TRANSFER COEFFICIENT OF EXTERIOR SURFACES(W/m^2.C)
2750 ' Q1 --- HEAT TRANSFER HISTORY THROUGH FLOOR(W/m^2)
2760 ' T1 --- TEMPERATURE HISTORY OF FLOOR SURFACE(C)
2770 ' T --- TEMPERATURES OF INTERIOR SURFACES(C)
2780 ' TA --- AMBIENT TEMPERATURE(C)
2790 ' TRR --- ROOM AIR TEMP FOR THE REAL SITUATION FOR COMPARISON(C)
2800 ' VWD --- AMBIENT WIND SPEED(M/sec),
2810
2820 IF FLAG2% = 0 THEN 2870
2830 INPUT #1, TIMM, IO, DI, TA, V.A, T.TOP, TRR, ETA.1, VWD, WDIR
2840 IF ETA.1 > 10 THEN ETA.1 = 0!
2845 IF VWD < 0! THEN VWD = 0!
2850 'PRINT , TIMM,DI,TA,VWD,TRR

```

```

2860 GOTO 2900
2870
2880 DI = DI1(DDT%) :TA = TA1(DDT%) :VWD = VWD1(DDT%) :TRR = TRR1(DDT%)
2890 IO = IO1(DDT%)
2900
2910 IF (TR+273!) < 260 THEN CP.A=FNCP1.A(TR+273!) ELSE CP.A=FNCP2.A(TR+273!)
2920 RO.CP = CP.A * FNRO.A(TR+273!)
2930 ALK = R.ALK * (V/3600!) * RO.CP :W1 = RO.CP * V/DT1
2940 FO = 5.7 + 3.8 * VWD :FO = FO * (1 + .2)
2950 RETURN
2960 ' *****
2970 ' SUB #3 CALCULATION OF SOLAR ANGLES & RADIATION ON EACH SURFACE
2980 ' *****
2990 'AZM --- SOLAR AZIMUTH MEASURED FROM SOUTH(DEG)
3000 'COSV, COSE & COSS --- DIRECTION COSINE OF THE SUN'S POSITION
3010 'DELT -- SOLAR DECLINATION ANLGE(DEG)
3020 'DFE --- DIFFUSE SOLAR RADIATION(W/m^2)
3030 'ET ---- EQUATION OF TIME(min.)
3040 'NDX --- DAY OF THE YEAR
3050 'OA ---- HOUR ANGLE(DEG)
3060 'SALT -- SOLAR ALTITUDE(DEG)
3070 'SRT --- SUNRISE TIME(HOURS)
3080 'SR ---- RADIATION RECEIVED BY WALL(W/m^2)
3090 'SS ---- AREA OF A SURFACE RECEIVING SOLAR RADIATION(m^2)
3100 'SST --- SUNSET TIME(HOURS)
3110
3120 IF FLAG1% = 1 GOTO 3530
3130 FLAG1% = 1
3140 IF MON% = 1 THEN NDX = ID% + 31
3150 IF MON% = 2 THEN NDX = ID% + 59
3160 IF MON% = 3 THEN NDX = ID% + 90
3170 IF MON% = 4 THEN NDX = ID% + 120
3180 IF MON% = 5 THEN NDX = ID% + 151
3190 IF MON% = 6 THEN NDX = ID% + 181
3200 IF MON% = 7 THEN NDX = ID% + 212
3210 IF MON% = 8 THEN NDX = ID% + 212

```

```

3220 IF MON% = 9 THEN ND% = ID% + 243
3230 IF MON% = 10 THEN ND% = ID% + 273
3240 IF MON% = 11 THEN ND% = ID% + 304
3250 IF MON% = 12 THEN ND% = ID% + 334
3260
3270 P = .9856 * PI180 * ND%
3280 DELT = .36-22.96*COS(P) - .37*COS(2!*P) - .15*COS(3!*P) + 4!*SIN(P)
3290
3300 IF (ND%>=1) AND (ND%<=106) THEN ET = -14.2*SIN((ND%+7)*PI/111!)
3310 IF (ND%>=107) AND (ND%<=166) THEN ET = 4!*SIN((ND%-106)*PI/59!)
3320 IF (ND%>=167) AND (ND%<=246) THEN ET = -6.5*SIN((ND%-166)*PI/80!)
3330 IF (ND%>=247) AND (ND%<=365) THEN ET = 16.4*SIN((ND%-247)*PI/113!)
3340
3350 LT1 = LT * PI180 : DELT = DELT * PI180
3360 OA1 = FNARCCOS(-TAN(LT1)*TAN(DELT))
3370 Y = OA1 * 121/PI
3380 OA1 = OA1/PI180
3390 SRT = 12! - ET/60! - (STM - LG + OA1)/15! : SST = SRT + 2!* Y
3400 PRINT #2, : PRINT #2, " ===== START OF ONE NEW DAY ====="
3410 PRINT #2,
3420 PRINT #2, " LOCATION: "; LG; " DEG. LONGITUDE & "; LT; " LATITUDE DEG. N" : PRINT #2,
3430 PRINT #2, " STANDARD TIME MERIDIAN = "; STM; " DEG." : PRINT #2,
3440 PRINT #2, " DELT = "; DELT/PI180; " DEGREE & ET = "; ET; " MINUTES" : PRINT #2,
3450 PRINT #2, " @@@ DATE (MON/DAY/YR): "; MON%; "/" ; ID%; "/" ; YR% : PRINT #2,
3460 PRINT #2, " DAY OF THE YEAR: "; ND% : PRINT #2,
3470 PRINT #2, " SUNRISE TIME: "; SRT; " HOURS" : PRINT #2,
3480 PRINT #2, " SUNSET TIME: "; SST; " HOURS" : PRINT #2,
3490 PRINT #2, : PRINT #2,
3500 PRINT #2, " 1
3510 PRINT #2, " TIME DI TA TRR T.RM"
3520 PRINT #2, " (hrs) (w/m^2) (DEG.C) (DEG.C) (DEG.C)" : PRINT #2,
3530
3540 OA = 180! - 15!* TIM - ET/4! - STM + LG
3550 IF ABS(OA) > ABS(OA1) GOTO 4210
3560 OA = OA * PI180
3570 COSV = SIN(LT1) * SIN(DELT) + COS(LT1) * COS(DELT) * COS(OA)

```

```

3580 COSE = COS(DELTA) * SIN(OA)
3590 COSS = COS(DELTA) * COS(OA) * SIN(LT1)
3600 P1 = ABS(COSS)
3610 IF COS(OA) > TAN(DELTA)/TAN(LT1) THEN COSS = P1 ELSE COSS = - P1
3620 SALT = FNARCSIN(COSV) :AZM = FNARCSIN(COSE/COS(SALT))
3630 IF COSS<0! THEN AZM = PI - AZM
3640
3650 ' FOLLOWING ARE THE CALCULATION OF SOLAR RADIATION ON EACH SURFACE
3660
3670 DFF = CF * I0 :SR(1,1) = 0!
3680 SR(1,6) = DI
3690 COSQ.H = SIN(SALT)
3700 IF COSQ.H = 0! THEN 4210
3710 FOR J% = 2 TO NS%-1
3720 GAMA = AZM - SAZM(1,J%)
3730 IF ABS(GAMA) >= PI/2! THEN SR(1,J%) = 0! :GOTO 3810
3740 IF BETA(J%) = 0! THEN 3830
3750 IF BETA(J%) = PI/2! THEN COSQ = COS(SALT) * COS(GAMA) :GOTO 3770
3760 COSQ = COS(SALT)*COS(GAMA)*SIN(BETA(J%)) - COSV*COS(BETA(J%))
3770
3780 R.B = COSQ/COSQ.H
3790 RATIO = (1 - CF) * R.B + CF * F.SKY(J%) + SNOW * F.GRD(J%)
3800 SR(1,J%) = I0 * RATIO :GOTO 3850
3810
3820 SR(1,J%) = DFF :GOTO 3850
3830
3840 SR(1,J%) = I0
3850
3860 NEXT J%
3870 EA = FNARCCOS(COSE) :EA = ABS(EA) :ANGLE1 = ABS(AZM)
3880 ANGLE2 = FNARCSIN(COSV/SIN(EA))
3890 IF ANGLE1 = 0! THEN X1 = 0! :X3 = 0 :GOTO 3920
3900 IF ANGLE1 <= PHY1 THEN X1 = BW * TAN(ANGLE1) :X3 = BW :GOTO 3920
3910 IF ANGLE1 > PHY1 THEN X1 = BL :X3 = BL/TAN(ANGLE1)
ELSE PRINT "ANGLE1 IS OUT OF RANGE. CHECK IT PLEASE!" :STOP
3920

```

```

3930 ANGLE2 = ABS(ANGLE2)
3940 IF ANGLE2 = 0! THEN X2 = 0! :X4 = 0! :GOTO 3970
3950 IF ANGLE2 <= PHY2 THEN X2 = BW * TAN(ANGLE2) :X4 = BW
      ELSE X2 = BH :X4 = BH/TAN(ANGLE2)
3960 IF ANGLE2 > PI/2! THEN PRINT "ANGLE2 OUT OF RANGE!" :STOP
3970
3980 SS(1) = X4*BL - X4*X4*X1/(2!* BW) :SS(2) = X2*BL - X1 * X2
3990 SS(3) = 0! :SS(4) = 0! :SS(5) = 0!
4000 SS(6) = S(6) :W = X3 * (BH - X2)
4010 IF AZM > 0! THEN SS(3) = W ELSE SS(5) = W
4012 FOR I%= 1 TO 6
4014 PRINT" SS(",I%,")=",SS(I%)
4016 NEXT I%
4020 IID = I0 * TRANS(2) :INDF = DFF * TRANS(2)
4030 SR(2,6) = DI*TRANS(2)
4040 SR(2,1) = IID
4050 FOR I% = 2 TO 5
4060 GAMA = AZM - SAZM(2,I%)
4070 IF I% = 2 THEN BETA(I%) = PI - BETA(I%)
4080 IF ABS(GAMA) >= PI/2! THEN SR(2,I%) = 0! :GOTO 4160
4090 IF BETA(I%) = 0! THEN COSQ = SIN(SALT) :GOTO 4120
4100 IF BETA(I%) = PI/2! THEN COSQ = COS(SALT) * COS(GAMA) :GOTO 4120
4110 COSQ = COS(SALT)*COS(GAMA)*SIN(BETA(I%)) - COSV*COS(BETA(I%))
4120
4130 R.B = COSQ/COSQ.H
4140 RATIO = (1 - CF) * R.B
4150 SR(2,I%) = IID * RATIO * SS(I%)/S(I%) :GOTO 4180
4160
4170 SR(2,I%) = INDF
4180
4190 NEXT I%
4200 GOTO 4280
4210
4220 FOR I% = 1 TO 2
4230 FOR J% = 1 TO NS%
4240 SR(I%,J%) = 0!

```

```

4250 NEXT J%
4260 NEXT I%
4270 DI = 0!
4280
4290 'CALCULATION OF SURFACE SOL-AIR TEMPERATURES
4300
4310 FOR I% = 2 TO NS%-1
4320 IF I% <> 4 THEN DR = 36! ELSE DR = 0!
4330 TE(I%) = TA + E1(I%) * (SR(1,I%) - DR)/FO
4340 NEXT I%
4350 TE(NS%) = TA + (AB(NS%) * SR(1,NS%) - E1(NS%) * DR)/FO
4360
4370 RETURN
4380 '*****
4390 ' SUB #4 DETERMINATION OF HEAT TRANSFER COEFFICIENTS
4400 '*****
4410 'HR6 -- RADIATION HEAT TRANSFER COEFFICIENT OF GLAZING(W/m^2.C)
4420 'TAM -- MEAN RADIANT TEMPERATURE OF AMBIENT(C)
4430
4440
4450 FOR I% = 1 TO NS%
4460 FOR J% = 1 TO NS%
4470 G(I%,J%) = 4! * SIGMA * E(I%) * F(I%,J%) * (TA + 273!)^3
4480 NEXT J%
4490 NEXT I%
4500 FOR I% = 2 TO 6
4510 U(I%) = U1(I%)*FO/(U1(I%) + FO)
4520 NEXT I%
4530 U(1) = U1(1)
4590 ' PRINT" U's";U(1);U(2);U(3);U(4);U(5);U(6); "HR6=";HR6;"FO=";FO
4600 RETURN
4610 '*****
4620 ' SUB #5 CALCULATION OF MATRIX COEFFICIENTS
4630 '*****
4640 'Q1 --- HEAT TRANSFER HISTORY THROUGH FLOOR(W/m^2)
4650 'QT --- RADIANT HEAT GAIN OF SURFACES(W/m^2)

```

```

4660 'T1 --- TEMPERATURE HISTORY OF FLOOR SURFACE(C)
4670
4680 SUMM = 0!
4690 FOR IX = 1 TO NSX
4700   SUM = 0!
4710   FOR JX = 1 TO NSX
4720     IF JX = IX GOTO 4750
4730     A(IX,JX) = -G(IX,JX)
4740     SUM = SUM + G(IX,JX)
4750
4760   NEXT JX
4770   A(IX,IX) = H(IX) + U(IX) + SUM
4780   IF IX = 1 GOTO 4810
4790   B(IX) = QT + U(IX) * TE(IX) + H(IX) * TR
4800   GOTO 4910
4810
4820   SUM1 = 0!
4830   FOR JX = 1 TO NRESX
4840     SUM1 = SUM1 + C1(JX)
4850     SUM2 = SUM2 - C2(JX) * T1(JX)
4860     SUM3 = SUM3 - C3(JX) * Q1(JX)
4870     SUM3 = -.9898594 * QL1
4880   NEXT JX
4890   SUM1 = SUM1 + C1(0)
4900   B(IX) = QT + SUM1 * TG + SUM2 + SUM3 + H(IX) * TR
4910
4920 NEXT IX
4930 RETURN
4940 ' *****
4950 ' SUB #6 MATRIX SOLVER
4960 ' *****
4970 ' A, B --- MATRIX COEFF. AND RIGHT-SIDE TERMS
4980 ' T ----- INTERIOR SURFACE TEMPERATURES
4990 FOR IX = 1 TO NX
5000   T(IX) = 0!
5010 NEXT IX

```



```

5050 N1% = N% - 1
5060 FOR IX = 1 TO N1%
5070 XK = A(IX,IX)
5080 IF XK = 0! THEN PRINT"XK(";IX;";" IS ZERO." :STOP
5090 FOR J% = IX TO N%
5100 A(IX,J%) = A(IX,J%)/XK
5110 NEXT J%
5120 B(IX) = B(IX)/XK
5130 FOR I1% = IX + 1 TO N%
5140 FOR J% = IX + 1 TO N%
5150 A(I1%,J%) = A(I1%,J%) - A(I1%,IX) * A(IX,J%)
5160 NEXT J%
5170 B(I1%) = B(I1%) - A(I1%,IX) * B(IX)
5180 NEXT I1%
5190 NEXT IX
5200
5210 ' BACK SUBSTITUTION
5220
5230 IF A(N%,N%) = 0! THEN PRINT" A(";N%;";";N%;") = 0.0" :STOP
5240 T(N%) = B(N%)/A(N%,N%)
5250 FOR IX = 1 TO N1%
5260 I1% = N% - IX
5270 XK = 0!
5280 FOR J% = I1% + 1 TO N%
5290 XK = A(I1%,J%) * T(J%) + XK
5300 NEXT J%
5310 T(I1%) = B(I1%) - XK
5320 NEXT IX
5330 SUM1 = 0! :SUM2 = 0!
5340 FOR IX = 1 TO NS%
5350 SUM1 = SUM1 + H(IX)*T(IX)*S(IX)
5360 SUM2 = SUM2 + H(IX) * S(IX)
5370 NEXT IX
5380 WQ1 = SUM1 + (ALK+23.18*1.02) * TA + W1 * TR1
5390 WQ2 = SUM2 + ALK + W1 + 23.18*1.02 'FOUNDATION LOSS ADDED
5400 T(7) = WQ1/WQ2 :TRM = T(7) + T.REF

```

```

5410 PRINT 'T's ';T(1);T(2);T(3);T(4);T(5);T(6);T(7) :PRINT
5420 RETURN
5430 *****
5440 SUB #7 CALCULATION OF HEAT TRANSFERED INTO THE BUILDING *****
5450 *****
5460 *****
5470 SUM1 = 0! :SUM2 = 0! :SUM3 = 0!
5480 FOR IX = 0 TO NRESX
5490 SUM1 = SUM1 + C1(IX)
5500 SUM2 = SUM2 + C2(IX) * T1(IX)
5510 I1X = IX + 1
5520 IF I1X > NRESX GOTO 4980
5530 SUM3 = SUM3 + C3(I1X) * Q1(I1X)
5540 SUM3 = .9898594 * QL1
5550 *****
5560 NEXT IX
5570 Q1(0) = -SUM1 * TG + SUM2 - SUM3
5580 QL1 = -SUM1 * TG + SUM2 + SUM3
5590 Q.LSS = 0!
5600 FOR IX = 1 TO NSX
5610 Q.LSS = Q.LSS + H(IX) * S(IX) * (T(7) - T(IX))/1000!
5620 NEXT IX
5630 Q.LSS = Q.LSS + ALK * (T(7) + T.REF - TA)/1000!
5640 RETURN
5650 *****
5660 SUB #8. OUTPUT OF THE CALCULATED RESULTS *****
5670 *****
5680 *****
5690 WRITE #2, TIM, DI, TA, TRR, TRM
5700 PRINT TIM, DI, TA, TRR, TRM
5710 *****
5720 RETURN
5730 *****
5740 SUB #9 EFFAB *****
5750 *****
5760 THIS PROGRAM IS USED TO COMPUTE THE ABSORPTANCE, REFLECTANCE AND

```

5770 'TRANSMITTANCE OF GLASS LAYER IN A MULTILAYER COVER SYSTEM.THE METHOD
5780 'USED HERE IS FROM EDWARDS' ALGORITHM REPORTED IN "SOLAR ENERGY",
5790 'VOL.19, PP.401 - 402, 1977.
5800 'THE CALCULATION IS BASED ON THE ASSUMPTION THAT THE COVERS ARE
5810 'MADE OF THE SAME MATERIAL, I.E., THEY HAVE THE SAME THERMAL
5820 'PROPERTIES. FOR DIFFERENT NUMBER OF COVERS, THE THERMAL
5830 'CONDUCTANCE OF THE COVER SYSTEM IS ESTIMATED ACCORDING TO THE
5840 'VALUES GIVEN BY ASHRAE 1981-FUNDAMENTALS(P.23.28).
5850 'DATE: MARCH 30TH, 1986
5860 'BY: QIQIU ZHAO
5870
5880 'AB(6) -- ABSORPTANCE OF COVER PLATE
5890 'ALFA(1) - ABSORPTANCE OF ABSORBER, OR ROOM BEHIND THE C
5900 'NC% ---- NUMBER OF COVER LAYERS
5910 'RL.CV -- REFLECTANCE OF COVER PLATE
5920 'ROU11) - REFLECTANCE OF ABSORBER, OR ROOM BEHIND COVER SYSTEM
5930 'TAU ---- TRANSMITTANCE OF COVER PLATE
5940 'A1(IX) - TOP-OF-THE-STACK ABSORPTANCE
5950 'R(IX) -- OVERALL REFLECTANCE OF THE STACK
5960 'TRANS(IX) -- TOP-OF-THE-STACK TRANSMITTANCE
5970 'AE(IX) - WITHIN-STACK ABSORPTANCE
5980
5990 'DATA .05, .95, .0735, .879, .0475
6000 NC1% = NC% + 1 :IX = 1
6010 FOR IX = 2 TO NC1%
6020 ROU(IX) = 1-TAU-AB(6) :TAU1(IX) = TAU :ALFA(IX) = AB(6)
6030 NEXT IX
6040 NC1% = NC% + 1 :IX = 1
6050 R(1) = .05 :TRANS(1) = 0! :A1(1) = .95
6060 PRINT #2," TOP-OF-STACK THERMAL PROPERTIES"
6070 PRINT #2,"-----"
6080 PRINT #2," # COVERS REFL. TRANSM. ABSORPTANCE"
6090 PRINT #2," (n) (Rn) (Tn) (An)"
6100 PRINT #2,"-----"
6110 PRINT #2, IX-1, R(1), TRANS(1), A1(1)
6120 FOR IX = 2 TO NC1%

```

6130 DEN = 11 - ROU(I%) * R(I%-1)
6140 R(I%) = ROU(I%) + TAU1(I%)^2 * R(I%-1)/DEN
6150 TRANS(I%) = TAU1(I%)/DEN
6160 A1(I%) = ALFA(I%) * R(I%-1) * TAU1(I%)/DEN + ALFA(I%)
6170 PRINT #2, I%-1, R(I%), TRANS(I%), A1(I%)
6180 NEXT I%
6190 PRINT #2, "-----" : PRINT #2,
6200 Q(NC1%) = J1
6210 PRINT #2, " WITHIN-STACK ABSORPTANCE"
6220 PRINT #2, "-----"
6230 PRINT #2, " # COVERS      ABSORPTANCE"
6240 PRINT #2, "-----"
6250 AE(NC1%) = Q(NC1%) * A1(NC1%)
6260 FOR I% = 2 TO NC1%
6270   J% = NC1% - I% + 1
6280   Q(J%) = TRANS(J%+1) * Q(J%+1)
6290   AE(J%) = A1(J%) * Q(J%)
6300 NEXT I%
6310 FOR I% = 1 TO NC%
6320   PRINT #2, I%-1, AE(I%)
6330 NEXT I%
6340 PRINT #2, "-----" : PRINT #2,
6350 U1(6) = U1(6)/NC%      : AB(6) = AE(2)
6360 RETURN

```

APPENDIX A.5: FORMAT OF INPUT FILE #1 FOR THE DIRECT-GAIN MODEL

BL (m)	BH (m)	BW1 (m)	BW2 (m)	V (m ³)	TAU
14.64	4.88	9.76	5.62	549.3	0.85
LG (deg.)	LT (deg.)	STM (deg.)	CF		
113.5	53.4	105	0.1		
U(1)	U(2)	U(3)	U(4)	U(5)	U(6)
0.0	0.280	0.133	0.255	0.278	8.5
S(1)	S(2)	S(3)	S(4)	S(5)	S(6)
142.89	70.34	21.48	83.00	73.78	70.34
E(1)	E(2)	E(3)	E(4)	E(5)	E(6)
0.85	0.85	0.85	0.85	0.85	0.85
E1(1)	E1(2)	E1(3)	E1(4)	E1(5)	E1(6)
0.80	0.80	0.80	0.80	0.80	0.80
AB(1)	AB(2)	AB(3)	AB(4)	AB(5)	AB(6)
0.85	0.85	0.85	0.85	0.85	0.10
BETA(1)	BETA(2)	BETA(3)	BETA(4)	BETA(5)	BETA(6)
0.0	67.0	90.0	0.0	90.0	67.0
SAZM(1,1)	SAZM(1,2)	SAZM(1,3)	SAZM(1,4)	SAZM(1,5)	SAZM(1,6)
0.0	180.0	-90.0	0.0	90.0	0.0
SAZM(2,1)	SAZM(2,2)	SAZM(2,3)	SAZM(2,4)	SAZM(2,5)	SAZM(2,6)
0.0	0.0	90.0	0.0	-90.0	180.0
F(1,1)	F(1,2)	F(1,3)	F(1,4)	F(1,5)	F(1,6)
0.0	0.3	0.11	0.18	0.11	0.3

F(2,1) 0.522	F(2,2) 0.0	F(2,3) 0.075	F(2,4) 0.216	F(2,5) 0.075	F(2,6) 0.138
F(3,1) 0.33	F(3,2) 0.195	F(3,3) 0.0	F(3,4) 0.21	F(3,5) 0.07	F(3,6) 0.195
F(4,1) 0.313	F(4,2) 0.204	F(4,3) 0.14	F(4,4) 0.0	F(4,5) 0.14	F(4,6) 0.204
F(5,1) 0.33	F(5,2) 0.195	F(5,3) 0.075	F(5,4) 0.21	F(5,5) 0.0	F(5,6) 0.195
F(6,1) 0.522	F(6,2) 0.138	F(6,3) 0.075	F(6,4) 0.216	F(6,5) 0.075	F(6,6) 0.0
NR					
7					
C1(0) 0.000000	C2(0) 0.555389	C3(0) 1.000000			
C1(1) 0.000066	C2(1) -1.143933	C3(1) -2.050275			
C1(2) 0.001199	C2(2) 0.773756	C3(2) 1.379913			
C1(3) 0.002619	C2(3) -0.196120	C3(3) -0.347679			
C1(4) 0.001137	C2(4) 0.016366	C3(4) 0.028755			
C1(5) 0.000107	C2(5) -0.000338	C3(5) -0.000582			

C1(6) 0.000002 C2(6) 0.000001 C3(6) 0.000002

C1(7) 0.000000 C2(7) -0.000000 C3(7) -0.000000

DD 21 MM 12 YY 1985

TG 5.0 T.INI 0.0 T.FX 10.0

DT 0.25 FINTIM 48.0 PRTIM 0.25 TIM 0.0

APPENDIX A.6: A SAMPLE OUTPUT FILE FROM THE DIRECT-GAIN MODEL

XXXXXXXXXXXXXXXXX OUTPUT OF THE SIMULATION RUN XXXXXXXXXXXXXXXXXXXXXXXX

BUILDING LENGTH ----- 14.64 (m)
 BUILDING HEIGHT ----- 4.88 (m)
 BUILDING BOTTOM WIDTH ----- 9.76 (m)
 BUILDING TOP WIDTH ----- 5.62 (m)
 TOTAL VOLUME OF THE BUILDING ----- 549.3 (m³)
 TRANSMITTANCE OF COVER GLAZING - .85
 CLOUDINESS FACTOR ----- .1

INFORMATION OF WALL COMPONENTS

U1(I%)	S(I%)	E(I%)	E1(I%)	AB(I%)	BETA(I%)
W/(m ² .C)	m ²				DEG.
0	142.89	.85	.85	.85	0
.28	70.34	.85	.8	.85	113
.133	21.48	.85	.8	.85	90
.255	83	.85	.8	.85	0
.278	73.78	.85	.8	.85	90
8.5	70.34	.85	.8	.1	67

ANGLE FACTORS OF INTERIOR WALL SURFACES

F(I%,1)	F(I%,2)	F(I%,3)	F(I%,4)	F(I%,5)	F(I%,6)
0	.3	.11	.18	.11	.3
.522	0	.075	.216	.075	.138

.33	.195	0	.21	.07	.195
.313	.204	.14	0	.14	.204
.33	.195	.075	.21	0	.195
.522	.138	.075	.216	.075	0

SURFACE AZIMUTH

I%	SAZM(1,I%) DEG.	SAZM(2,I%) DEG.
1	0	0
2	180	0
3	-90	90
4	0	0
5	90	-90
6	0	0

NUMBER OF RESPONSE FACTORS = 7

RESPONSE FACTORS FOR FLOOR SLAB

I%	C1(I%)	C2(I%) ²	C3(I%)
0	0	.555389	1
1	.000066	-1.143933	-2.050275
2	.001199	.773756	1.379913
3	.00261	-.19612	-.347679
4	.001137	.016366	.028755
5	.000107	-.000338	-.000582
6	.000002	.000001	.000002

7 0 0 0 0

TOP-OF-STACK THERMAL PROPERTIES

# COVERS (n)	REFL. (Rn)	TRANSM. (Tn)	ABSORPTANCE (An)
0	.05	0	.95
1	.0862155	.8521304	.1042607

WITHIN-STACK ABSORPTANCE

# COVERS	ABSORPTANCE
0	.8095238
1	.1042607

GROUND TEMPERATURE ----- 5 (C)
 INITIAL TEMPERATURE ASSUMED - 5 (C)
 AIR LEAKAGE RATE ----- .5 (charges/hr)
 TIME INCREMENT ----- .25 (hrs)
 PRINTING INTERVAL ----- .25 (hrs)
 TOTAL TIME FOR THE RUN ----- 96 (hrs)
 STARTING TIME FOR THE RUN --- 0 (hrs)

===== START OF ONE NEW DAY =====

LOCATION: 113.5 DEG. LONGITUDE & 53.4 LATITUDE DEG. N

STANDARD TIME MERIDIAN = 105 DEG.

DELT = -23.42229 DEGREE & ET = 2.272403 MINUTES

DATE (MON/DAY/YR): 12 / 21 / 1985

DAY OF THE YEAR: 355

SUNRISE TIME: 8.907685 HOURS

SUNSET TIME : 16.1499 HOURS

1	2	3	4	5
TIME (hrs)	DI (W/m ²)	TA (DEG.C)	TRR (DEG.C)	T.RM (DEG.C)

0,0,5.596,3.9595,0				
.25,0,5.596,3.9595,2.598329				
.5,0,5.477,3.925,3.86088				
.75,0,5.626,3.9865,4.23604				
1,0,5.709,3.948,4.904297				
1.25,0,6.109,3.9545,5.277973				
1.5,0,5.583,4.031,5.441652				
1.75,0,5.491,3.888,5.475933				
2,0,5.76,3.8465,5.636355				
2.25,0,5.36,3.9255,5.646721				
2.5,0,4.658,3.784,5.554351				
2.75,0,4.313,3.6635,5.370364				
3,0,4.429,3.67,5.321131				
3.25,0,5.718,3.6285,5.486805				
3.5,0,5.955,3.7105,5.670389				
3.75,0,5.859,3.792,5.765477				
4,0,6.129,3.778,5.935359				
4.25,0,6.295,3.835,6.109856				
4.5,0,5.968,3.878,6.141393				

4.75,0,5.846,3.795,6.160913
5,0,6.051,3.847,6.197595

. . . .
. . . .
. . . .

23.0,4.102,4.8235,3.576295
23.25,0,4.266,4.7305,3.575394
23.5,0,4.245,4.6085,3.573358
23.75,0,4.039,4.569,3.551752

===== START OF ONE NEW DAY =====

LOCATION: 113.5 DEG. LONGITUDE & 53.4 LATITUDE DEG. N

STANDARD TIME MERIDIAN = 105 DEG.

DELTA = -23.42838 DEGREE & ET = 1.820036 MINUTES

DATE (MON/DAY/YR): 12 / 22 / 1985

DAY OF THE YEAR: 356

SUNRISE TIME: 8.916024 HOURS

SUNSET TIME : 16.15664 HOURS

1	2	3	4	5
TIME	DI	TA	TRR	T.RM
(hrs)	(W/m ²)	(DEG.C)	(DEG.C)	(DEG.C)

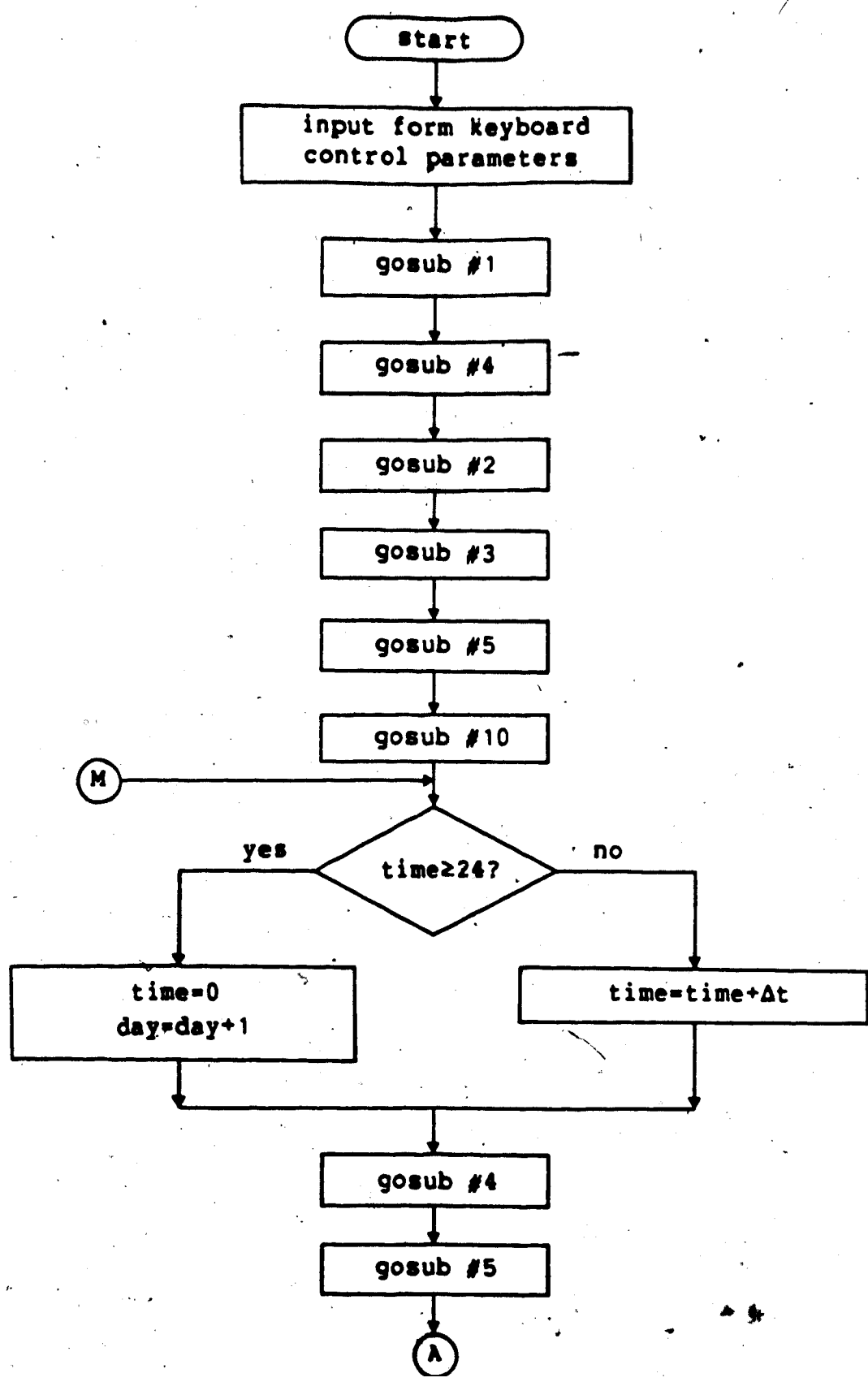
0,0,3.782,4.289,3.509759				
.25,0,3.655,4.2745,3.460971				
.5,0,3.567,4.1235,3.367233				
.75,0,3.683,4.047,3.336198				
1,0,3.347,4.032,3.22759				

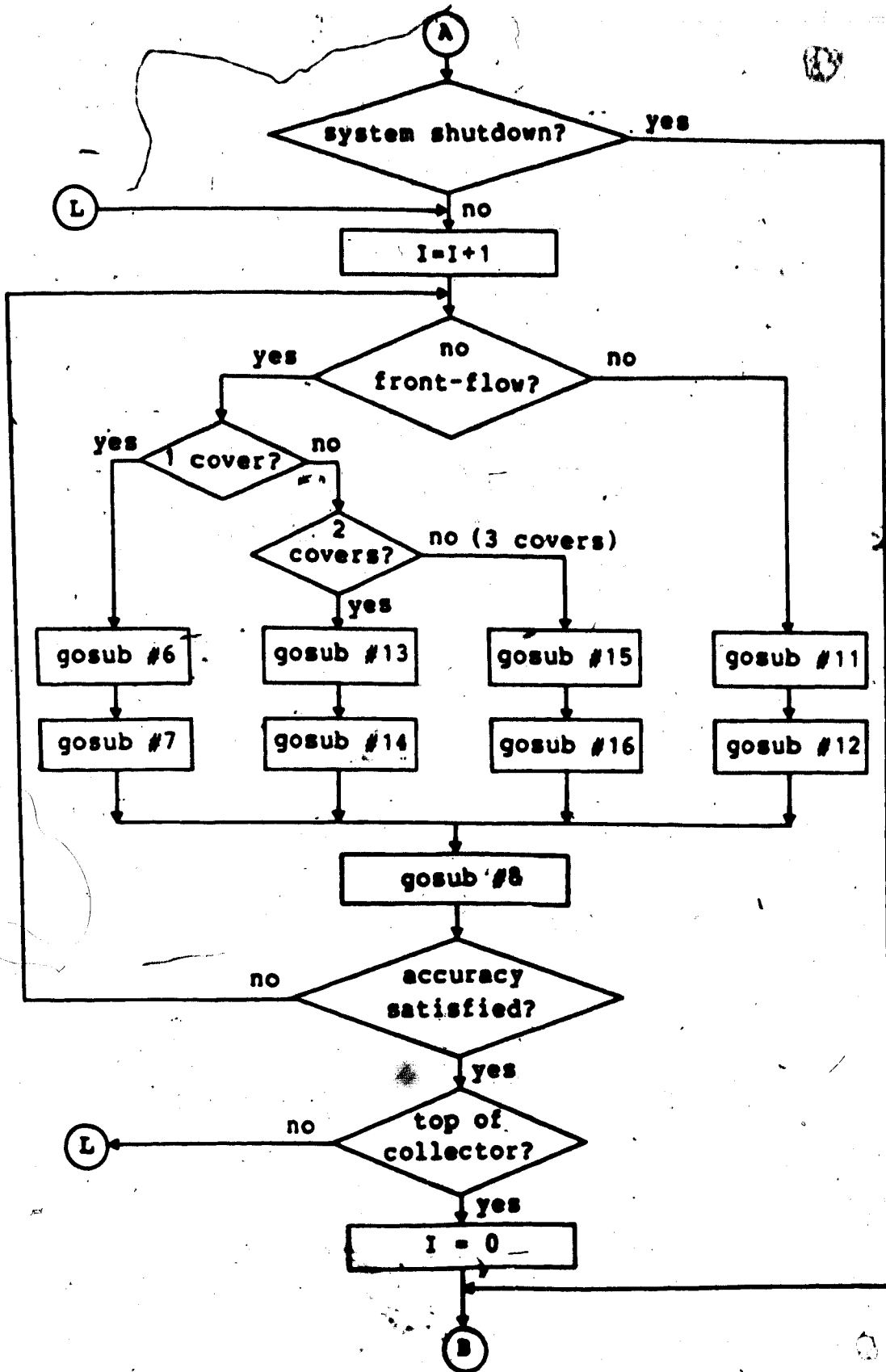
1.25,0,3.376,3.86,3.182223
1.5,0,3.182,3.8205,3.070243
1.75,0,2.942,3.7725,2.901596
2,0,2.91,3.609,2.800353
2.25,0,3.07,3.611,2.762582
2.5,0,3.198,3.5305,2.740466

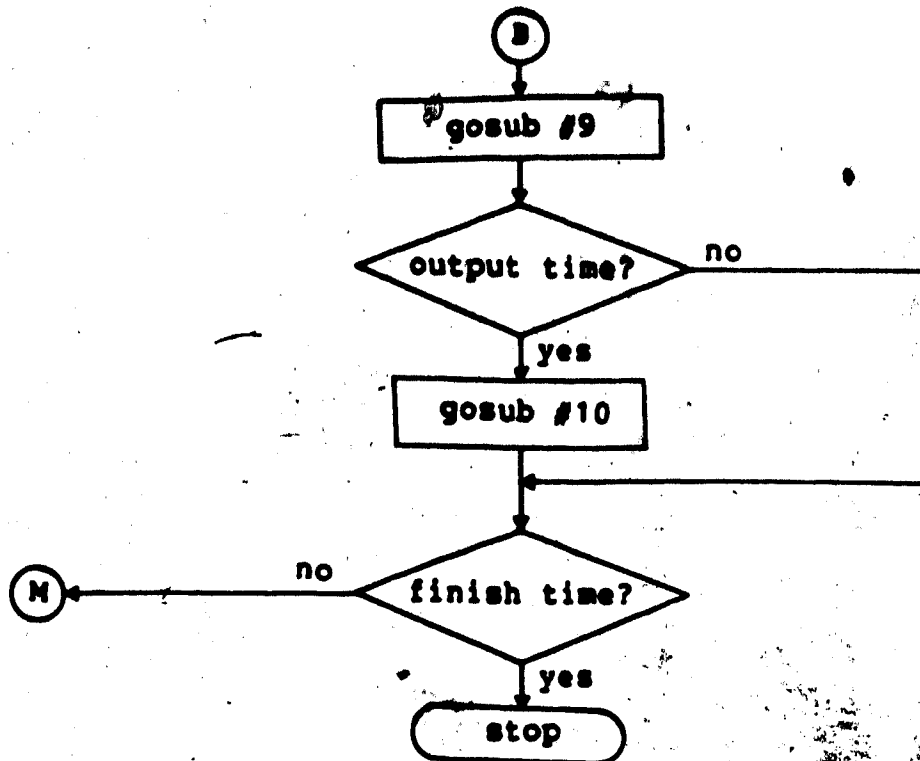
. . . .
. . . .
. . . .

===== TERMINATION OF THIS RUN =====

APPENDIX B.1: FLOWCHART OF THE ACTIVE SYSTEM MODEL







- sub #1. input physical & thermal parameters of the building
- sub #2. calculate effective absorptance and transmittance of cover system
- sub #3. compute heat transfer coefficients for the forced convection inside the collector channels
- sub #4. read in solar data
- sub #5. determine solar angles & solar radiation on the collector surface
- sub #6. determine varying heat transfer coefficients for a one-cover two-pass system
- sub #7. calculate matrix coefficients for a one-cover two-pass system
- sub #8. matrix solver
- sub #9. calculate heat gains into the building
- sub #10. output routine
- sub #11. determine varying heat transfer coefficients for a one-cover one-pass (back-pass) system
- sub #12. calculate matrix coefficients for a one-cover two-pass (back-pass) system
- sub #13. determine varying heat transfer coefficients for a two-cover two-pass system
- sub #14. calculate matrix coefficients for a two-cover two-pass system
- sub #15. determine varying heat transfer coefficients for a three-cover two-pass system
- (u) sub #16. calculate matrix coefficients for a three-cover two-pass system

APPENDIX B.2: PROGRAM LISTING OF THE ACTIVE SYSTEM MODEL

```

10  $$$$$$$$$$$$$$$$$$$$$$$$$$$$$$$$$$$$$$$$$$$$$$$$$$$$$$$$$$$$$$$$$$$$
20  $$$$$$$$$$$$$$$$$$$$$$$$$$$$$$$$$$$$$$$$$$$$$$$$$$$$$$$$$$$$$$$$$$$$
30  $$$$$$$$$$$$$$$$$$$$$$$$$$$$$$$$$$$$$$$$$$$$$$$$$$$$$$$$$$$$$$$$$$$$
40  $$$$$$$$$$$$$$$$$$$$$$$$$$$$$$$$$$$$$$$$$$$$$$$$$$$$$$$$$$$$$$$$$$$$
50  $$$$$$$$$$$$$$$$$$$$$$$$$$$$$$$$$$$$$$$$$$$$$$$$$$$$$$$$$$$$$$$$$$$$
60  $$$$$$$$$$$$$$$$$$$$$$$$$$$$$$$$$$$$$$$$$$$$$$$$$$$$$$$$$$$$$$$$$$$$
70  $$$$$$$$$$$$$$$$$$$$$$$$$$$$$$$$$$$$$$$$$$$$$$$$$$$$$$$$$$$$$$$$$$$$
80  $$$$$$$$$$$$$$$$$$$$$$$$$$$$$$$$$$$$$$$$$$$$$$$$$$$$$$$$$$$$$$$$$$$$
90  $$$$$$$$$$$$$$$$$$$$$$$$$$$$$$$$$$$$$$$$$$$$$$$$$$$$$$$$$$$$$$$$$$$$
100 $$$$$$$$$$$$$$$$$$$$$$$$$$$$$$$$$$$$$$$$$$$$$$$$$$$$$$$$$$$$$$$$$$$$
    PROGRAM ACTVSYS
    =====
110 $$$$$$$$$$$$$$$$$$$$$$$$$$$$$$$$$$$$$$$$$$$$$$$$$$$$$$$$$$$$$$$$$$$$
    FOR THESIS PROJECT
    BY
120 $$$$$$$$$$$$$$$$$$$$$$$$$$$$$$$$$$$$$$$$$$$$$$$$$$$$$$$$$$$$$$$$$$$$
    QIQIU ZHAO
130 $$$$$$$$$$$$$$$$$$$$$$$$$$$$$$$$$$$$$$$$$$$$$$$$$$$$$$$$$$$$$$$$$$$$
    DEPARTMENT OF AGRICULTURAL ENGINEERING
    UNIVERSITY OF ALBERTA
140 $$$$$$$$$$$$$$$$$$$$$$$$$$$$$$$$$$$$$$$$$$$$$$$$$$$$$$$$$$$$$$$$$$$$
150 $$$$$$$$$$$$$$$$$$$$$$$$$$$$$$$$$$$$$$$$$$$$$$$$$$$$$$$$$$$$$$$$$$$$
160 $$$$$$$$$$$$$$$$$$$$$$$$$$$$$$$$$$$$$$$$$$$$$$$$$$$$$$$$$$$$$$$$$$$$
170 $$$$$$$$$$$$$$$$$$$$$$$$$$$$$$$$$$$$$$$$$$$$$$$$$$$$$$$$$$$$$$$$$$$$
180 $$$$$$$$$$$$$$$$$$$$$$$$$$$$$$$$$$$$$$$$$$$$$$$$$$$$$$$$$$$$$$$$$$$$
190 $$$$$$$$$$$$$$$$$$$$$$$$$$$$$$$$$$$$$$$$$$$$$$$$$$$$$$$$$$$$$$$$$$$$
200 $$$$$$$$$$$$$$$$$$$$$$$$$$$$$$$$$$$$$$$$$$$$$$$$$$$$$$$$$$$$$$$$$$$$
210 $$$$$$$$$$$$$$$$$$$$$$$$$$$$$$$$$$$$$$$$$$$$$$$$$$$$$$$$$$$$$$$$$$$$
220 $$$$$$$$$$$$$$$$$$$$$$$$$$$$$$$$$$$$$$$$$$$$$$$$$$$$$$$$$$$$$$$$$$$$
230 $$$$$$$$$$$$$$$$$$$$$$$$$$$$$$$$$$$$$$$$$$$$$$$$$$$$$$$$$$$$$$$$$$$$
240 $$$$$$$$$$$$$$$$$$$$$$$$$$$$$$$$$$$$$$$$$$$$$$$$$$$$$$$$$$$$$$$$$$$$
250 $$$$$$$$$$$$$$$$$$$$$$$$$$$$$$$$$$$$$$$$$$$$$$$$$$$$$$$$$$$$$$$$$$$$
260 $$$$$$$$$$$$$$$$$$$$$$$$$$$$$$$$$$$$$$$$$$$$$$$$$$$$$$$$$$$$$$$$$$$$
270 $$$$$$$$$$$$$$$$$$$$$$$$$$$$$$$$$$$$$$$$$$$$$$$$$$$$$$$$$$$$$$$$$$$$
280 $$$$$$$$$$$$$$$$$$$$$$$$$$$$$$$$$$$$$$$$$$$$$$$$$$$$$$$$$$$$$$$$$$$$
290 $$$$$$$$$$$$$$$$$$$$$$$$$$$$$$$$$$$$$$$$$$$$$$$$$$$$$$$$$$$$$$$$$$$$
300 $$$$$$$$$$$$$$$$$$$$$$$$$$$$$$$$$$$$$$$$$$$$$$$$$$$$$$$$$$$$$$$$$$$$
310 $$$$$$$$$$$$$$$$$$$$$$$$$$$$$$$$$$$$$$$$$$$$$$$$$$$$$$$$$$$$$$$$$$$$
320 $$$$$$$$$$$$$$$$$$$$$$$$$$$$$$$$$$$$$$$$$$$$$$$$$$$$$$$$$$$$$$$$$$$$
330 $$$$$$$$$$$$$$$$$$$$$$$$$$$$$$$$$$$$$$$$$$$$$$$$$$$$$$$$$$$$$$$$$$$$
340 $$$$$$$$$$$$$$$$$$$$$$$$$$$$$$$$$$$$$$$$$$$$$$$$$$$$$$$$$$$$$$$$$$$$

```

```

10
20
30
40
50
60
70
80
90
100
110
120
130
140
150
160
170
180
190
200
210
220
230
240
250
260
270
280
290
300
310
320
330
340

```

```

SUB #1: INPUT OF PHYSICAL AND THERMAL PARAMETERS OF THE BUILDING
SUB #2: CALCULATION OF EFFECTIVE ABSORPTANCE & TRANSMITTANCE OF COVER
SYSTEM
SUB #3: COMPUTATION OF HEAT TRANSFER COEFFICIENTS FOR THE FORECD

```

```

350 CONVECTION INSIDE THE COLLECTOR CHANNELS.
360 SUB #4: READ-IN THE SOLAR DATA
370 SUB #5: CALCULATION OF SOLAR ANGLES & RADIATION RECEIVED BY EACH WALL
380 SUB #6: DETERMINATION OF VARYING HEAT TRANSFER COEFFICIENTS FOR
390 ONE-COVER SYSTEM
400 SUB #7: CALCULATION OF MATRIX COEFFICIENTS FOR ONE-COVER SYSTEM
410 SUB #8: MATRIX SOLVER
420 SUB #9: CALCULATION OF HEAT GAIN INTO THE BUILDING
430 SUB #10: OUTPUT ROUTINE
440 SUB #11: DETERMINATION OF VARYING HEAT TRANSFER COEFFICIENTS FOR
450 ONE-PASS & ONE-COVER SYSTEM (OR CONVENTIONAL DESIGN)
460 SUB #12: CALCULATION OF MATRIX COEFFICIENTS FOR ONE-PASS & ONE-COVER
470 SYSTEM (CONVENTIONAL DESIGN)
480 SUB #13: DETERMINATION OF VARYING HEAT TRANSFER COEFFICIENTS FOR
490 TWO-COVER SYSTEM
500 SUB #14: CALCULATION OF MATRIX COEFFICIENTS FOR TWO-COVER SYSTEM
510 SUB #15: DETERMINATION OF VARYING HEAT TRANSFER COEFFICIENTS FOR
520 THREE-COVER SYSTEM
530 SUB #16: CALCULATION OF MATRIX COEFFICIENTS FOR THREE-COVER SYSTEM
540
550 DI --- GLOBAL SOLAR RADIATION (W/m^2)
560 FNRO.A(X) --- AIR DENSITY AT TEMP X(K), kg/m^3
570 FNCP.A(X) --- AIR SPECIFIC HEAT AT TEMP X(K), J/kg-K
580 FNK.A(X) --- AIR THERMAL CONDUCTIVITY AT TEMP X(K), W/m-K
590 FNMU.A(X) --- AIR DYNAMIC VISCOSITY AT TEMP X(K), N-sec/m^2 (or kg-m/s)
600 T --- TEMPERATURES OF INTERIOR SURFACES (C)
610 TA --- AMBIENT TEMPERATURE (C)
620 TRR --- ROOM AIR TEMP FOR THE REAL SITUATION FOR COMPARISON (C)
630 VWD --- AMBIENT WIND SPEED (M/sec)
640
650 MAIN SECTION OF THE PROGRAM
660 DIM AB(6), BETA(6), E(6), E1(6), F(6,6), H(6), S(6), U(6), U1(6)
670 DIM SAZM(2,6), SR(2,6), SS(6)
680 DIM ALFA(5), ROU(5), TAU1(5)
690 DIM A1(5), AE(5), Q(5), R(5), TRANS(5)
700 DIM A#(10,10), B#(10), T(10), T2(80), T4(80), T3OLD(80)

```

```

710 DIM C1(20), C2(20), C3(20), Q1(20), TE(7), TR1(20)
720 DIM FAA#(20), FBB#(20), FCC#(20), FDD#(20), EBETA#(20), FGMA#(20)
730 DIM TFP#(20), TFPO#(20)
740 DEF FNARCSIN(X) = ATN(X/SQR(1 - X*X))
750 DEF FNARCCOS(X) = 1.570796 - ATN(X/SQR(1 - X*X))
760 DEF FNRO.A(X) = 3531/X
770 DEF FNCP1.A(X) = 1000!*(1.032 - .001225*X)
780 DEF FNCP2.A(X) = 1000!*(1.02252 - .000176*X + 4.02E-07*X*X - 4.87E-11*X^3)
790 DEF FNK1.A(X) = SQR(X)/(385.859 + 91144!/X - 2686670!/X^2 + 5.52604E+07/X^3)
800 DEF FNK2.A(X) = SQR(X)/(328.052 + 167323!/X - 3.02953E+07/X^2 + 3.05862E+09/X^3)
810 DEF FNDEN(X) = .6717 + 85.23001/X - 2111.475/X^2 + 106417!/X^3
820 DEF FNMU.A(X) = SQR(X)/(FNDEN(X) * 1000000#)
830
840 OPEN "B:ACTOUT" FOR OUTPUT AS #2
850 INPUT "Number of subregions to be used(<80) is ";NSUBX :PRINT
860 INPUT "Number of nodes to be used for floor concrete(<20) is ";NFLRX :PRINT
870 INPUT "Number of panels to be used(<22) ";PNLX :PRINT
880 INPUT "Number of covers(maximum 3) is ";NCX :PRINT
890 INPUT "Air velocity in back-pass(max 1 m/sec) is ";V.AIR :PRINT
900 INPUT "Ratio of air velocity in front to that in back is ";FB :PRINT
910 INPUT "Infiltration rate(Charges/hr) is ";R.ALK :PRINT
920 COLOR 31
930 PRINT:PRINT "!!!!!!!!!!!!!! ATTENTION !!!!!!!!!!!!!!!" :PRINT :PRINT
940 COLOR 7
950 PRINT " I AM WORKING RIGHT NOW. DON'T SWITCH ME OFF, PLEASE." :PRINT
960 PRINT " THANKS."
970 GOSUB 1920 'FOR INPUT DATA
980 BW = (BW1 + BW2)/2!
990 OPEN "B:DFILE2.ACT" FOR INPUT AS #1
1000
1010 TIM = 0! :PRTIM1 = 0! :QTT = 0!
1020 FLAG1% = 0 :FLAG2% = 0 :FLAG3% = 0 :DDT% = 0
1030 GOSUB 4740 'FOR INITIAL SOLAR DATA INPUT
1040 GOSUB 3630 'FOR TRANSMITTANCE OF COVER SYSTEM
1050 GOSUB 4260 'DETERMINATION OF HEAT TRANSFER COEFFICIENTS
1060 GOSUB 4940 'CALCULATION OF SUNRISE & SUNSET TIME

```

```

1070 GOSUB 7830
1080 TP = TF.M + 10!
1090 TC1 = (TC + TF.M)/2! :TC2 = TC
1100
1110 WHILE TIM1 < FINTIM
1120   WHILE PRTIM1 < PRTIM
1130     TIM = TIM + DT :TIM1 = TIM1 + DT :PRTIM1 = PRTIM1 + DT
1140     IF TIM < 24! THEN 1200
1150
1160     IF IDX = 30 THEN MON% = MON% + 1 :IDX = 0
1170     IF IDX < 30 THEN IDX = IDX + 1
1180     PRINT #2, "***** TOTAL HEAT COLLECTED THIS DAY IS";QTT;" KJ" :PRINT #2,
1190     FLAG1% = 0 :TIM = 0! :QTT = 0!
1200
1210 GOSUB 4740
1220 GOSUB 4940
1230 IF SHUTDOWN% = 1 THEN Q.GAIN = 0! :GOTO 1720
1240 T3OLD(0) = 0! :T3OLD(NSUB%+1) = 0! :Q2 = 0!
1250
1260 T2(0) = TR :T4(0) =
1270 FOR IIX = 1 TO NSUB%
1280   IF IIX=1 THEN VT = 1! :GOTO 1310
1290   IF IIX=NSUB% THEN V1 = 1! :GOTO 1310
1300   V1 = 2!
1310
1320   IF (NC%=1) AND (FB<=0!) THEN NX = 5 :GOTO 1360
1330   IF (NC%=1) AND (FB=0!) THEN NX = 4 :GOTO 1440
1340   IF (NC%=2) AND (FB<>0!) THEN NX = 6 :GOTO 1510
1350   IF (NC%=3) AND (FB<>0!) THEN NX = 7 :GOTO 1580
1360
1370 GOSUB 5890
1380 GOSUB 6170
1390 GOSUB 6580
1400 IF ABS(T(3)-TP) > .001 THEN TP=T(3) :TC=T(5) :TI =T(1) :GOTO 1360
1410 T2(IIX) = T(2) :T4(IIX) = T(4) :T3OLD(IIX) = T(3)
1420 TP = T(3) :TC = T(5) :TI = T(1)

```

```

1430      GOTO 1640
1440
1450      'DETERMINE VARYING HEAT TRANSFER COEFFICIENTS
1460      'CALCULATION OF MATRIX COEFFICIENTS
1470      'MATRIX SUBROUTINE TO SOLVE THE MATRIX FOR TEMP
1480      IF ABS(T(3)-TP)>.001 THEN TP=T(3) :TC=T(4) :TI=T(1) :GOTO 1440
1490      T2(II%) = T(2) :T3OLD(II%) = T(3) :TP = T(3) :TC = T(4) :TI=T(1)
1500      GOTO 1640
1510
1520      'DETERMINE VARYING HEAT TRANSFER COEFFICIENTS
1530      'CALCULATION OF MATRIX COEFFICIENTS
1540      'MATRIX SUBROUTINE TO SOLVE THE MATRIX FOR TEMP
1550      IF ABS(T(3)-TP)>.001 THEN TP=T(3) :TC1=T(5) :TC2=T(6) :TI=T(1) :GOTO 1510
1560      T2(II%)=T(2) :T4(II%)=T(4) :T3OLD(II%)=T(3) :TP=T(3) :TC1=T(5)
1565      TC2=T(6) :TI=T(1)
1570      GOTO 1640
1580
1590      'DETERMINE VARYING HEAT TRANSFER COEFFICIENTS
1600      'CALCULATION OF MATRIX COEFFICIENTS
1610      'MATRIX SUBROUTINE TO SOLVE THE MATRIX FOR TEMP
1620      IF ABS(T(3)-TP)>.001
1630          THEN TP=T(3) :TC1=T(5) :TC2=T(6) :TC3=T(7) :TI=T(1) :GOTO 1580
1635      T2(II%)=T(2) :T4(II%)=T(4) :T3OLD(II%)=T(3) :TP=T(3) :TC1=T(5)
1640      TC2=T(6) :TC3=T(7) :TI=T(1)
1650      BEEP
1660      Q2 = Q2 + DA * U(6) * (TI - TR)
1670      NEXT II%
1680      PRINT : PRINT " TIME NOW IS";TIM
1690      FOR II% = 1 TO NSUB%
1700          PRINT"**** T2( ";II%; ") = ";T2(II%); "T4( ";II%; ") = ";T4(II%); "*****"
1710      NEXT II%
1720
1730      'COMPUTATION OF THE HEAT GAIN INTO THE BUILDING
1740      IF COUNT% = 1 THEN COUNT% = 0 :GOTO 1770
1750      TR = (TR0 + TR)/2 :COUNT% = COUNT% + 1

```

```

1760 IF SHUTDOWN% <> 1 THEN 1250
1770
1780 QTT = QTT + Q1 * DT * 3.6
1790 TR0 = TR :QL1 = QGRD
1800 PRINT " BALANCE REACHED!! ROOM AIR TEMP IS";TR :PRINT
1810 IF EOF(1) THEN 1870
1820 WEND
1830 GOSUB 7830 'OUTPUT AND SAVE THE RESULTS
1840
1850 PRTIM1 = 01
1860 WEND
1870
1880 PRINT #2, :PRINT #2,
1890 PRINT #2, "====TERMINATION OF THIS RUN ====="
1900 CLOSE
1910 END
1920 *****
1930 ' SUB #1 READ IN THE THERMAL PROPERTY VALUES FOR WALLS AND CEILING
1940 *****
1950 'THIS SUBROUTINE READS IN THE INFORMATION ON BUILDING STRUCTURE,
1960 'COLLECTOR AND THERMAL PROPERTIES OF WALL COMPONENTS. MEANWHILE, IT
1970 'PRINTS OUT THE VALUES OF THE INPUT INFORMATION. ALL THE INFORMATION
1980 'NEEDED FOR THE RUN OF IS INPUT HERE. IT IS EXECUTED ONLY AT THE
1990 'BEGINNING OF EACH SIMULATION RUN.
2000 'NOMENCLATURE
2010 'AB ---- ABSORPTANCE OF SURFACES
2020 'BETA -- TILT ANGLE OF SURFACE(DEG)
2030 'BL,BW,BH, -- LENGTH, WIDTH AND HEIGHT OF THE BUILDING(m)
2040 'C1,C2,C3 --- RESPONSE FACTORS OF FLOOR
2050 'CF ---- CLOUDINESS FACTOR
2060 'CL,CH - LENGTH AND WIDTH OF THE COLLECTOR(m)
2070 'CP.A -- SPECIFIC HEAT(J/kg) OF AIR AT NORMAL CONDITION
2080 'CP.P -- SPECIFIC HEAT(J/kg) OF ABSORBING PLATE
2090 'DT ---- TIME INCREMENT(sec.)
2100 'E, E1 -- EMITTANCE OF SURFACES
2110 'F ---- VIEW FACTOS OF INTERIOR SUR.

```

2120 'FGRD -- GROUND VIEW FACTOR OF THE GLAZING(DEG)
 2130 'FINTIM-- TOTAL TIME FOR THE RUN(hrs)
 2140 'FSKY -- SKY VIEW FACTOR OF THE GLAZING(DEG)
 2150 'H ----- HEAT TRANSFER COEFFICIENTS OF INTERIOR WALL SURFACES(W/m^2.C)
 2160 'ID% ---- DAY OF THE MONTH
 2170 'K.P ---- THERMAL CONDUCTIVITY OF ABSORBING PLATE(W/m.C)
 2180 'LG ---- LONGITUDE OF THE LOCATION(DEG)
 2190 'LT ---- LATITUDE OF THE LOCATION(DEG)
 2200 'MON% --- MONTH OF THE YEAR
 2210 'NRES% -- NUMBER OF RESPONSE FACTORS
 2220 'NS% --- NUMBER OF INTERIOR SURFACES
 2230 'PNL% --- NUMBER OF PANNELS
 2240 'PRTIM -- TIME INTRVAL FOR OUTPUT(hrs)
 2250 'R.ALK -- RATE OF AIR LEAKAGE(CHARGES/hr)
 2260 'RO.A -- DENSITY(kg/m^3) OF AIR AT NORMAL CONDITION
 2270 'RO.P -- DENSITY(kg/m^3) OF ABSORBING PLATE
 2280 'S ---- AREA OF SURFACES(m^2)
 2290 'SAZM -- SURFACE AZIMUTH(DEG.)
 2300 'STM --- STANDARD TIME MERIDIAN OF THE LOCATION(DEG)
 2310 'TAU --- TRANSMITTANCE OF THE GLAZING
 2320 'T.FX -- DESIRED FIX TEMPERATURE OF THE ROOM AIR(C)
 2330 'T.GM --- GROUND TEMPERATURE(C)
 2340 'T.H --- TIME IN HOURS
 2350 'T.I --- ASSUMED INITIAL TEMPERATURE FOR ROOM AIR AND SURFACES(C)
 2360 'T.M --- CONDUCTANCE OF WALLS(W/m^2.C)
 2370 'T.V --- VOLUME OF THE ROOM(m^3)
 2380 'XB ---- SPACING BETWEEN ABSORBING PLATE AND THE INSULATION(m)
 2390 'XF ---- SPACING BETWEEN ABSORBING SURFACE AND COVER PLATE(m)
 2400 'X.P --- THICKNESS OF THE ABSORBING PLATE(m)
 2410 'YR% --- YEAR
 2420
 2430 PI# = 3.141593# :SIGMA# = .0000000567# :NS% = 6 :N% = 5
 2440 PI180 = PI#/180# :G = 9.8
 2450 FOR I% = 1 TO NS%
 2460 H(I%) = 11.88
 2470 NEXT I%

```

2480 OPEN "B:DRFILE1.ACT" FOR INPUT AS #1
2490 INPUT #1, BL, BH, BW1, BW2, V, TAU
2500 INPUT #1, CL, CH, XF, XB, XFLR
2510 INPUT #1, LG, LT, STM, CF
2520 INPUT #1, U1(1), U1(2), U1(3), U1(4), U1(5), U1(6)
2530 INPUT #1, S(1), S(2), S(3), S(4), S(5), S(6)
2540 INPUT #1, E(1), E(2), E(3), E(4), E(5)
2550 INPUT #1, E1(1), E1(2), E1(3), E1(4), E1(5), E1(6)
2560 INPUT #1, AB(1), AB(2), AB(3), AB(4), AB(5), AB(6)
2570 INPUT #1, BETA(1), BETA(2), BETA(3), BETA(4), BETA(5), BETA(6)
2580 INPUT #1, X.P, CP.P, RO.P, X.P
2590 FOR IX = 1 TO 2
2600 INPUT #1, SAZM(IX,1), SAZM(IX,2), SAZM(IX,3), SAZM(IX,4), SAZM(IX,5), SAZM(IX,6)
2610 NEXT IX
2620 FOR IX = 1 TO NS%
2630 INPUT #1, F(IX,1), F(IX,2), F(IX,3), F(IX,4), F(IX,5), F(IX,6)
2640 NEXT IX
2650 INPUT #1, NRES%
2660 FOR IX = 0 TO NRES%
2670 INPUT #1, C1(IX), C2(IX), C3(IX)
2680 NEXT IX
2690 INPUT #1, ID%, MON%, YR%
2700 INPUT #1, TG, T.INI, T.FX
2710 INPUT #1, DT, FINTIM, PRTIM, TIM
2720 TR = T.INI :TR0 = TR :T2(0) = TR :T4(0) = TR
2730 TF.M = T2(0) + 5! :TB.M = T4(0) + 5!
2740 CLOSE 1
2750 FOR IX = 0 TO NRES%
2760 TR1(IX) = T.INI
2770 NEXT IX
2780 FOR IX = 1 TO NS%
2790 BETA(IX) = BETA(IX) * PI180
2800 = 1 TO 2
2810 SAZM(J%,IX) = SAZM(J%,IX) * PI180
2820 NI
2830 NI

```

```

2840 FY = BETA(6) :COSFY = COS(FY) :RA.C = 17081/COSFY
2850 FSKY = (1. + COS(BETA(6)))/2! :FGRD = 14 - FSKY
2860 DX = CH/NSUBX :PL = CL/PNL% :DA = DX * PL
2870 A.P = PL * X.P :S.PNL = CH * PL :S.COLL = CSNG(PNL%) * S.PNL
2880 DT.SEC# = CDBL(DT) * 3600#
2890 X.FLR# = .203# :DX.FLR# = X.FLR#/CDBL(NFLR%)
2900 K.FLR# = 1.02# :RO.FLR# = 1280# :CP.FLR# = 927#
2910 ROCP.FLR# = RO.FLR# * CP.FLR#
2920 XC1 = .01905 :XC2 = .01905
2930 H1R# = .27263# :HR1# = H1R#
2940 FOR I% = 2 TO 5
2950 U.A = U.A + U1(I%) * S(I%)
2960 NEXT I%
2970 U.A = U.A + U1(2)*(S(2) - S.COLL) :U.A = U.A + 23.18 * 1.02 'FOUNDATION
2980 VB# = CDBL(V.AIR) :VF# = CDBL(FB)*VB# 'FB = RATIO OF VF TO VB
2990 FLOW = (CSNG(VF#)*XF + CSNG(VB#)*XB) * PL
3000 FOR FIX = 1 TO NFLR%
3010 TFPO#(FIX) = CDBL(TG)
3020 NEXT FIX
3030 PRINT #2, " %%%%%%%%%%%%%%%%%%%%%%%%%%%%%%%%%%%%%%%%%% OUTPUT OF THE SIMULATION RUN %%%%%%%%%%%%%%%%%%%%%%%%%%%%%%%%%%%%%%%%%%"
3040 PRINT #2, :PRINT #2,
3050 PRINT #2, " BUILDING LENGTH -----";BL;"(m)"
3060 PRINT #2, " BUILDING HEIGHT -----";BH;"(m)"
3070 PRINT #2, " BUILDING BOTTOM WIDTH -----";BW1;"(m)"
3080 PRINT #2, " BUILDING TOP WIDTH -----";BW2;"(m)"
3090 PRINT #2, " TOTAL VOLUME OF THE BUILDING -----";V;"(m^3)"
3100 PRINT #2, " COLLECTOR PANEL LENGTH -----";PL;"(m)"
3110 PRINT #2, " COLLECTOR PANEL HEIGHT -----";CH;"(m)"
3120 PRINT #2, " NUMBER OF PANELS USED -----";PNL%
3130 PRINT #2, " FRONT-PASS SPACING -----";XF;"(m)"
3140 PRINT #2, " BACK-PASS SPACING -----";XB;"(m)"
3150 PRINT #2, " TRANSMITTANCE OF COVER GLAZING-----";TAU
3160 PRINT #2, " FLOW RATE PER PANEL -----";FLOW;"(m^3/sec)"
3170 PRINT #2, " NUMBER OF SUBDIVISION -----";NSUB%
3180 PRINT #2, " LENGTH OF EACH SUBREGION-----";DX;"(m)"
3190 PRINT #2, " CLOUDINESS FACTOR -----";CF

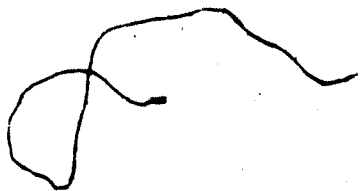
```

'3/4 INCHES FOR SPACING BETWEEN TWO COVERS
:U1(6) = .27263 :U1(1) = .505 :U.A = 0!

```

3200 PRINT #2, " GROUND TEMPERATURE -----";TG;"(C)"
3210 PRINT #2, " INITIAL TEMPERATURE ASSUMED -----";T.INI;"(C)"
3220 PRINT #2, " TOTAL TIME FOR THE RUN -----";FINTIM;"(hrs)"
3230 PRINT #2, " PRINTING INTERVAL -----";PRTIM;"(hrs)"
3240 PRINT #2, " STARTING TIME FOR THE RUN -----";TIM;"(hrs)"
3250 PRINT #2, " TIME INCREMENT -----";DT;"(hrs)"
3260 PRINT #2, ":PRINT #2,
3270 PRINT #2, " INFORMATION ON WALL COMPONENTS"
3280 PRINT #2, "-----"
3290 PRINT #2, " U1(I%) S(I%) E(I%) E1(I%) AB(I%) BETA(I%)"
3300 PRINT #2, " W/(m^2.C) m^2 DEG."
3310 PRINT #2, "-----"
3320 FOR I% = 1 TO 6
3330 PRINT #2,U1(I%), S(I%), E(I%), E1(I%), AB(I%), BETA(I%)/PI180
3340 NEXT I%
3350 PRINT #2, "-----"
3360 PRINT #2, " ANGLE FACTORS OF INTERIOR WALL SURFACES"
3370 PRINT #2, "-----"
3380 PRINT #2, " F(I%,1) F(I%,2) F(I%,3) F(I%,4) F(I%,5) F(I%,6)"
3390 PRINT #2, "-----"
3400 FOR I% = 1 TO NS%
3410 PRINT #2, F(I%,1), F(I%,2), F(I%,3), F(I%,4), F(I%,5), F(I%,6)
3420 NEXT I%
3430 PRINT #2, "-----"
3440 PRINT #2, " SURFACE AZIMUTH"
3450 PRINT #2, "-----"
3460 PRINT #2, " I% SAZM(1,I%) SAZM(2,I%)"
3470 PRINT #2, " DEG."
3480 PRINT #2, "-----"
3490 FOR I%=1 TO 6
3500 PRINT #2, I%, SAZM(1,I%)/PI180, SAZM(2,I%)/PI180
3510 NEXT I% :PRINT #2,
3520 PRINT #2, "-----"
3530 PRINT #2, " RESPONSE FACTORS FOR FLOOR SLAB"
3540 PRINT #2, "-----"
3550 PRINT #2, " I% C1(I%) C2(I%) C3(I%)"

```



```

3560 PRINT #2, "-----"
3570 FOR I% = 0 TO NRES%
3580   PRINT #2, I%, C1(I%), C2(I%), C3(I%)
3590 NEXT I%
3600 PRINT #2, :PRINT #2,
3610 PRINT #2, "-----" :PRINT #2,
3620 RETURN
3630 '*****
3640 ' SUB #2 EFFAB
3650 '*****
3660 'THIS PROGRAM IS USED TO COMPUTE THE ABSORPTANCE, REFLECTANCE AND
3670 'TRANSMITTANCE OF GLASS LAYER IN A MULTILAYER COVER SYSTEM.THE METHOD
3680 'USED HERE IS FROM EDWARDS' ALGORITHM REPORTED IN "SOLAR ENERGY",
3690 'VOL.19, PP.401 - 402, 1977.
3700 'THE CALCULATION IS BASED ON THE ASSUMPTION THAT THE COVERS ARE
3710 'MADE OF THE SAME MATERIAL, I.E., THEY HAVE THE SAME THERMAL
3720 'PROPERTIES. FOR DIFFERENT NUMBER OF COVERS, THE THERMAL
3730 'CONDUCTANCE OF THE COVER SYSTEM IS ESTIMATED ACCORDING TO THE
3740 'VALUES GIVEN BY ASHRAE 1981-FUNDAMENTALS(P.23.28).
3750 'DATE: MARCH 30TH, 1986
3760 'BY: QIQIU ZHAO
3770
3780 'AB(6) -- ABSORPTANCE OF COVER PLATE
3790 'ALFA(1)- ABSORPTANCE OF ABSORBER, OR ROOM BEHIND THE COVER SYSTEM
3800 'NC% ---- NUMBER OF COVER LAYERS
3810 'RL.CV -- REFLECTANCE OF COVER PLATE
3820 'ROU11) - REFLECTANCE OF ABSORBER, OR ROOM BEHIND COVER SYSTEM
3830 'TAU ---- TRANSMITTANCE OF COVER PLATE
3840 'A1(I%) - TOP-OF-THE-STACK ABSORPTANCE
3850 'R(I%) -- OVERALL REFLECTANCE OF THE STACK
3860 'TRANS(I%) -- TOP-OF-THE-STACK TRANSMITTANCE
3870 'AE(I%) - WITHIN-STACK ABSORPTANCE
3880
3890 NC1% = NC% + 1 :I% = 1
3900 FOR I% = 2 TO NC1%.
3910   ROU(I%) = 1-TAU-AB(6) :TAU1(I%) = TAU :ALFA(I%) = AB(6)

```

```

3920 NEXT IX
3930 NC1% = NCX + 1 :IX=1
3940 R(1) = .05 :TRANS(1) = 0# :A1(1) = .95
3950 PRINT #2," TOP-OF-STACK THERMAL PROPERTIES"
3960 PRINT #2," -----"
3970 PRINT #2," # COVERS REFL. TRANSM. ABSORPTANCE"
3980 PRINT #2," (n) (Rn) (Tn) (An)"
3990 PRINT #2," -----"
4000 PRINT #2, IX-1, R(1), TRANS(1), A1(1)
4010 FOR IX = 2 TO NC1%
4020 DEN = 1# - ROU(IX) * R(IX-1)
4030 R(IX) = ROU(IX) + TAU1(IX)^2 * R(IX-1)/DEN
4040 TRANS(IX) = TAU1(IX)/DEN
4050 A1(IX) = ALFA(IX) * R(IX-1) * TAU1(IX)/DEN + ALFA(IX)
4060 PRINT #2, IX-1, R(IX), TRANS(IX), A1(IX)
4070 NEXT IX
4080 PRINT #2," -----" :PRINT #2,
4090 Q(NC1%) = 1#
4100 PRINT #2," WITHIN-STACK ABSORPTANCE"
4110 PRINT #2," -----"
4120 PRINT #2," # COVERS ABSORPTANCE"
4130 PRINT #2," -----"
4140 AE(NC1%) = Q(NC1%) * A1(NC1%)
4150 FOR IX = 2 TO NC1%
4160 J% = NC1% - IX + 1
4170 Q(J%) = TRANS(J%+1) * Q(J%+1)
4180 AE(J%) = A1(J%) * Q(J%)
4190 NEXT IX
4200 FOR IX = 1 TO NC1%
4210 PRINT #2, IX-1, AE(IX)
4220 NEXT IX
4230 PRINT #2," -----" :PRINT #2,
4240 AL.TA = AE(1) :AB.C1=AE(2) :AB.C2=AE(3) :AB.C3=AE(4)
4250 RETURN
4260 '*****
4270 ' SUB #3 COMPUTATION OF HEAT TRANSFER COEFFICIENTS FOR FORCED

```

```

4280 CONVECTION IN THE COLLECTOR CHANNELS
4290 *****
4300 THIS IS FOR THE DETERMINATION OF HEAT TRANSFER COEFFICIENTS BETWEEN
4310 THE WORKING FLUID AND COVER INNER SURFACE, AND THE ABSORBING SURFACE
4320 AS WELL AS BETWEEN THE FLUID AND THE BACK SURFACE OF ABSORBING PLATE,
4330 AND THE SURFACE OF INSULATION LAYER. THE FORMULUS USED ARE FROM THE
4340 REFERENCES AS LISTED IN THE THESIS.
4350
4360 MU.AIR = FNMU.A(TR+273!)
4370 IF (TR+273!)<300! THEN K.AIR=FNK1.A(TR+273!) ELSE K.AIR=FNK2.A(TR+273!)
4380 IF (TR+273!)<260 THEN CP.AIR=FNCP1.A(TR+273!) ELSE CP.AIR=FNCP2.A(TR+273!)
4390 PR = MU.AIR * CP.AIR/K.AIR
4400 RE1#=VF#*CDBL(21*XF*RO.AIR/MU.AIR) :RE2#=VB#*CDBL(2!*XB*RO.AIR/MU.AIR)
4410 IF RE1# < 2300# THEN 4430
4420 NU1# = .0158 * RE1#^.8 :GOTO 4480
4430
4440 'D# = 2# * CDBL(PL*CH)/(1# + CDBL(PL)) 'PL = PANNEL LENGTH(m)
4450 'W# = CDBL(PL)/(RE1# * CDBL(PR) * D#) 'CH = COLLECTOR HEIGHT(m)
4460 'NU1# = 4.9# + .0606# * W#^-1.2/(1# +.08560001# * W#^-0.7)
4470 NU1# = 5.4# 'FOR FULLY DEVELOPED LAMINAR FLOW P.151 OF ANDERSON'S
4480
4490 IF RE2# < 2300# THEN 4510
4500 NU2# = .0158# * RE2#^.8 :GOTO 4560
4510
4520 'D# = 2# * CDBL(PL * CH)/(1# + CDBL(PL))
4530 'W# = CDBL(PL)/(RE2# * CDBL(PR) * D#)
4540 'NU2# = 4.9# + .0606# * W#^-1.2/(1#+.08560001# * W#^-0.7)
4550 NU2# = 5.4#
4560
4570 PRINT #2," === PRANDTL NUMBER CALCULATED IS ";PR
4580 PRINT #2," === AIR VELOCITY IN FRONT IS ";CSNG(VF#);"(m/sec)"
4590 PRINT #2," === AIR VELOCITY IN BACK IS ";CSNG(VB#);"(m/sec)"
4600 PRINT #2," === REYNOLDS NUMBER FOR AIR IN FRONT-PASS IS"; RE1#
4610 PRINT #2," === REYNOLDS NUMBER FOR AIR IN BACK-PASS IS"; RE2#
4620 PRINT #2," === MEAN NUSSELT NUMBER FOR AIR IN FRONT IS "; NU1#
4630 PRINT #2," === MEAN NUSSELT NUMBER FOR AIR IN BACK IS "; NU2#

```

```

4640 PRINT #2, :PRINT #2,
4650 H54# = NU1# * CDBL(K.AIR)/CDBL(2!*XF) :H45#=H54# :H43#=H64# :H34#=H43#
4660 H32# = NU2# * CDBL(K.AIR)/CDBL(2!*XB) :H23#=H32# :H21#=H32# :H12#=H21#
4670 H1R# = .27263# :HR1#=H1R#
4680 QMSS1# = VF# * CDBL(XF * PL * RO.AIR * CP.AIR)
4690 QMSS2# = VB# * CDBL(XB * PL * RO.AIR * CP.AIR)
4700 E5A# = CDBL(E(5)) :E53# = 1#/(1#/CDBL(E(4)) + 1#/CDBL(E(3))) - 1#)
4710 E31# = 1#/(1#/CDBL(E(2)) + 1#/CDBL(E(1))) - 1#) :E13# = E31#
4720 E65# = 1#/(2#/CDBL(E(4)) - 1#) :E56# = E65#
4730 RETURN
4740 *****
4750 SUB #4 SOLAR DATA INPUT *****
4760 *****
4770 *****
4780 DI --- GLOBAL SOLAR RADIATION(W/m^2)
4790 FO --- HEAT TRANSFER COEFFICIENT OF EXTERIOR SURFACES(W/m^2.C)
4800 Q1 --- HEAT TRANSFER HISTORY THROUGH FLOOR(W/m^2)
4810 T1 --- TEMPERATURE HISTORY OF FLOOR SURFACE(C)
4820 T --- TEMPERATURES OF INTERIOR SURFACES(C)
4830 TA --- AMBIENT TEMPERATURE(C)
4840 TRR --- ROOM AIR TEMP FOR THE REAL SITUATION FOR COMPARISON(C)
4850 VWD --- AMBIENT WIND SPEED(M/sec),
4860
4870 IF FLAG2% = 0 THEN 2664
4880 INPUT #1, TIMM, I10, DI, TA, V.A, T.TOP, TRR, ETA.1, VWD, WDIR
4890 IF ETA.1 > 101 THEN ETA.1 = 01
4900 IF VWD < 01 THEN VWD = 01
4910 DI = 400!* SIN(PI#*TIM/FINTIM) :TA = -10 :VWD = 51
4920 PRINT , TIMM,DI,TA,VWD,TRR
4930 RETURN
4940 *****
4950 SUB #5 CALCULATION OF SOLAR ANGLES & RADIATION ON EACH SURFACE
4960 *****
4970 AZM --- SOLAR AZIMUTH MEASURED FROM SOUTH(DEG)
4980 COSV, COSE & COSS --- DIRECTION COSINE OF THE SUN'S POSITION
4990 DELT --- SOLAR DECLINATION ANLGE(DEG)

```

```

5000 'DFF --- DIFFUSE SOLAR RADIATION(W/m^2)
5010 'ET --- EQUATION OF TIME(min..)
5020 'ND% --- DAY OF THE YEAR
5030 'OA --- HOUR ANGLE(DEG)
5040 'SALT --- SOLAR ALTITUDE(DEG)
5050 'SRT --- SUNRISE TIME(HOURS)
5060 'SR --- RADIATION RECEIVED BY WALL(W/m^2)
5070 'SST --- SUNSET TIME(HOURS)
5080
5090 IF FLAG1% = 1 GOTO 5510
5100 FLAG1% = 1
5110 IF MON% = 1 THEN NDX = ID% + 31
5120 IF MON% = 2 THEN NDX = ID% + 59
5130 IF MON% = 3 THEN NDX = ID% + 90
5140 IF MON% = 4 THEN NDX = ID% + 120
5150 IF MON% = 5 THEN NDX = ID% + 151
5160 IF MON% = 6 THEN NDX = ID% + 181
5170 IF MON% = 7 THEN NDX = ID% + 212
5180 IF MON% = 8 THEN NDX = ID% + 243
5190 IF MON% = 9 THEN NDX = ID% + 273
5200 IF MON% = 10 THEN NDX = ID% + 304
5210 IF MON% = 11 THEN NDX = ID% + 334
5220 IF MON% = 12 THEN NDX = ID% + 334
5230
5240 P = .9856 * PI180 * NDX
5250 DELT = .36-22.96*COS(P) - .37*COS(21*P) - .15*COS(31*P) + 41*SIN(P)
5260
5270 IF (NDX>=1) AND (NDX<=106) THEN ET = -14.2*SIN((NDX+7)*PI#/111#)
5280 IF (NDX>=107) AND (NDX<=166) THEN ET = 41*SIN((NDX-106)*PI#/59#)
5290 IF (NDX>=167) AND (NDX<=246) THEN ET = -6.5*SIN((NDX-166)*PI#/80#)
5300 IF (NDX>=247) AND (NDX<=365) THEN ET = 16.4*SIN((NDX-247)*PI#/113#)
5310
5320 LT1 = LT * PI180 : DELT = DELT * PI180
5330 OA1 = FNARCCOS(-TAN(LT1)*TAN(DELT))
5340 Y = OA1 * 12#/PI#
5350 OA1 = OA1/PI180

```

```

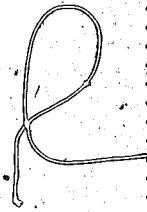
5360 SRT = 121 - ET/60# - (STM - LG + OA1)/151 :SST = SRT + 2!* Y
5370 PRINT #2, :PRINT #2, :PRINT #2, " ===== START OF ONE NEW DAY ====="
5380 PRINT #2, "
5390 PRINT #2, " LOCATION: ";LG;" DEGREE LONGITUDE"
5400 PRINT #2, " ";LT;" DEGREE NORTH LATITUDE"
5410 PRINT #2, " STANDARD TIME MERIDIAN =";STM;" DEGREE"
5420 PRINT #2, " SOLAR DECLINATION(DELTA) =";DELTA/PI180;" DEGREE"
5430 PRINT #2, " EQUATION OF TIME(ET) =";ET;" MINUTES" :PRINT #2,
5440 PRINT #2, " DATE (MON/DAY/YR) : ";MON%;" / ";ID%;" / ";YR%
5450 PRINT #2, " DAY OF THE YEAR: ";ND%
5460 PRINT #2, " SUNRISE TIME: ";SRT;" HOURS"
5470 PRINT #2, " SUNSET TIME : ";SST;" HOURS"
5480 PRINT #2, :PRINT #2,
5490 PRINT #2, "1 2 3 4 5 6 7 8 9"
5500 PRINT #2, "TIM, DI, TA, YRR, TR, T.TOP, T.EXIT, ETA.1, ETA"
5510
5520 OA = 180! - 151* TIM - ET/4! - STM + LG
5530 IF ABS(OA) > ABS(OA1) THEN SHUTDOWN% = 1 ELSE SHUTDOWN% = 0
5540 IF SHUTDOWN% = 1 THEN SR(1,6) = 0! :GOTO 5870
5550 SR(1,6) = DI :GOTO 5870
5560 OA = OA + PI180
5570 COSV = SIN(LT1) * SIN(DELTA) + COS(LT1) * COS(DELTA) * COS(OA)
5580 COSE = COS(DELTA) * SIN(OA)
5590 COSS = COS(DELTA) * COS(OA) * SIN(LT1)
5600 P1 = ABS(COSS)
5610 IF COS(OA) > TAN(DELTA)/TAN(LT1) THEN COSS = P1 ELSE COSS = - P1
5620 SALT = FNARCSIN(COSV) :AZM = FNARCSIN(COSE/COS(SALT))
5630 IF COSS < 0! THEN AZM = CSNG(PI#) - AZM
5640
5650 FOLLOWING ARE THE CALCULATION OF SOLAR RADIATION ON EACH SURFACE
5660
5670 DFF = CF * DI :DI = DI - DFF :SR(1,1) = 0!
5680 FOR JX = 2 TO NS%
5690 GAMA = AZM - SAZM(1,JX)
5700 IF ABS(GAMA) > PI#/2! THEN SR(1,JX) = 0! :GOTO 5760
5710 IF BETA(JX) = 0! THEN COSQ = SIN(SALT) :GOTO 5740

```

```

5720 IF BETA(JX) = PI#2! THEN COSQ = COS(SALT) * COS(GAMA) :GOTO 5740
5730 COSQ = COS(SALT)*COS(GAMA)*SIN(BETA(JX)) - COSV*COS(BETA(JX))
5740
5750 SR(1,JX) = DI * COSQ
5760
5770 SR(1,JX) = SR(1,JX) + DFF
5780 NEXT JX
5790 GOTO 5870
5800
5810 FOR IX = 1 TO 2
5820 FOR JX = 1 TO NSX
5830 SR(IX,JX) = 0!
5840 NEXT JX
5850 NEXT IX
5860 DI = 0!
5870
5880 RETURN

```



```

5890 ***** DETERMINATION OF VARYING HEAT TRANSFER COEFFICIENTS FOR
5900 SUB #6 TWO-PASS & ONE-COVER SYSTEM *****
5910 ***** TWO-PASS & ONE-COVER SYSTEM *****
5920 ***** THE TEMPERATURE-DEPENDENT HEAT TRANSFER COEFFICIENTS SUCH AS THE
5930 RADIANT AND THE WIND HEAT TRANSFER COEFFICIENTS, ARE COMPUTED IN THIS
5940 SUBROUTINE FOR THE ONE-COVER AND TWO-PASS SOLAR COLLECTOR SYSTEM.
5950 THE CALCULATION IS REPEATED FOR EACH TIME STEP.
5960
5970
5980 TSKY = .0552 * (TA + 273!)^1.5
5990 TGRD = TA + 273!
6000 TAM = (FSKY * TSKY ^ 4 + FGRD * TGRD ^ 4) ^ .25
6010 HR.5A# = E5A# * SIGMA# * CDBL((TC+273!)^3 + (TC+273!)^2 * TAM
+ (TC+273!) * TAM^2 + TAM^3)
6020 HR.53# = E53# * SIGMA# * CDBL((TC+273!)^3 + (TC+273!)^2 * (TP+273!)
+ (TC+273!) * (TP+273!)^2 + (TP+273!)^3)
6030 HR.51# = E51# * SIGMA# * CDBL((TP+273!)^3 + (TP+273!)^2 * (TI+273!)
+ (TP+273!) * (TI+273!)^2 + (TI+273!)^3)
6040 HR.55# = HR.5A# :HR.53# = HR.53# :HR.51# = HR.31#

```

:HR.13# = HR.31#

```

6050
6060 IF ABS(WDIR) > 270! THEN 6120
6070 MU.AMB = FNMU.A(TA+273!) : RO.AMB = ENRO.A(TA+273!)
6080 IF (TA+273!) < 300! THEN K.AMB = FNK1.A(TA+273!) ELSE K.AMB = FNK2.A(TA+273!)
6090 IF (TA+273!) < 260 THEN CP.AMB = FNCP1.A(TA+273!) ELSE CP.AMB = FNCP2.A(TA+273!)
6100 LC = 2! * CL*CH/(CL + CH) : RE# = CDBL(VWD * LC * RO.AMB/MU.AMB)
6110 HW# = 8.99 + .86# * CDBL(K.AMB) * RE#^5 * CDBL(PR^5/LC) : GOTO 6150
6120
6130 VC# = .3# + CDBL(.05*VWD)
6140 HW# = 18.625# * VC#^605
6150
6160 RETURN
6170 ***** CALCULATION OF MATRIX COEFFICIENTS FOR TWO-PASS & ONE-COVER *****
6180 SUB #7
6190 SYSTEM
6200 *****
6210 THIS SUBROUTINE IS USED TO COMPUTE THE MATRIX COEFFICIENTS ACCORDING
6220 TO THE HEAT BALANCE EQUATIONS.
6230
6240 A#(1,1) = (HR.31# + H21# + H1R#) * CDBL(DA)
6250 A#(1,5) = 0# : A#(1,4) = 0#
6260 A#(1,3) = -HR.13# * CDBL(DA) : A#(1,2) = -H12# * CDBL(DA)
6270 B#(1) = H1R# * CDBL(DA*TR)
6280
6290 A#(2,2) = (H32# + H12#) * CDBL(DA) + QMSS2#
6300 A#(2,5) = 0# : A#(2,4) = 0#
6310 A#(2,3) = -H23# * CDBL(DA) : A#(2,1) = A#(1,2)
6320 B#(2) = QMSS2# * CDBL(T2(II%-1))
6330
6340 Z1# = CDBL(RO.P * CP.P * X.P * DA) / CDBL(DT*3600!)
6350 Z2# = CDBL(A.P * K.P/DX)
6360 A#(3,3) = CDBL(DA) * (HR.53# + HR.31# + H43# + H23#) + Z1# + CDBL(V1)*Z2#
6370 A#(3,5) = -HR.53# * CDBL(DA) : A#(3,4) = -H43# * CDBL(DA)
6380 A#(3,2) = A#(2,3) : A#(3,1) = A#(1,3)
6390 B#(3) = CDBL(DA * AL.TA * SR(1,6)) + Z1# * CDBL(T3OLD(II%))
6400 B#(3) = B#(3) + Z2# * (T3OLD(II%-1) + T3OLD(II%+1))

```

```

6410
6420 A#(4,4) = H54# + H34#) * CDBL(DA) + QMSS1#
6430 A#(4,5) = -H45# * CDBL(DA) : A#(4,3) = A#(3,4)
6440 A#(4,2) = 0# : A#(4,1) = 0#
6450 B#(4) = QMSS1# * CDBL(T4(I1%-1))
6460
6470 QR5# = CDBL(AB.C1 * DA * SR(1,6)) 'DA = AREA OF SUBREGION(m^2)
6480 A#(5,5) = (HR.53# + H54# + HW# + HR.5A#)*CDBL(DA)
6490 A#(5,4) = A#(4,5) : A#(5,3) = A#(3,5)
6500 A#(5,2) = 0# : A#(5,1) = 0#
6510 B#(5) = QR5# + HW#*CDBL(DA*TA) + HR.5A#*CDBL(DA*(2731))
6520
6530 'FOR J% = 1 TO N%
6540 'PRINT "A'S"; A#(1,J%); A#(2,J%); A#(3,J%), A#(4,J%), A#(5,J%)
6550 'NEXT J% :PRINT
6560 'PRINT "B'S"; B#(1); B#(2); B#(3); B#(4); B#(5) :PRINT
6570 RETURN
6580 '*****
6590 'SUB #8 MATRIX SOLVER
6600 '*****
6610 'THIS IS THE ROUTINE FOR SOLVING THE MATRIX USING GAUSSIAN ELIMINATION
6620 'PROCEDURE.
6630 'A#,B --- MATRIX COEFF. AND RIGHT-SIDE TERMS
6640 'T----- INTERIOR SURFACE TEMPERATURES
6650 'FOR I% = 1 TO N%
6660 'T(I%) = 0!
6670 'NEXT I%
6680 'N1% = N% - 1
6690 'FOR I% = 1 TO N1%
6700 'XK# = A#(I%,I%)
6710 'IF XK# = 0# THEN PRINT "XK("; I%; ") IS ZERO." :STOP
6720 'FOR J% = I% TO N%
6730 'A#(I%,J%) = A#(I%,J%)/XK#
6740 'NEXT J%
6750 'B#(I%) = B#(I%)/XK#
6760 'FOR I1% = I% + 1 TO N%

```

```

6770 FOR J% = I% + 1 TO N%
6780 A#(I1%,J%) = A#(I1%,J%) - A#(I1%,I%) * A#(I%,J%)
6790 NEXT J%
6800 B#(I1%) = B#(I1%) - A#(I1%,I%) * B#(I%)
6810 NEXT I1%
6820 NEXT I%
6830
6840 BACK SUBSTITUTION
6850
6860 IF A#(N%,N%) THEN PRINT "A(";N%";",N%";" I = 0.0" :STOP
6870 T(N%) = CSNG(A#(N%,N%))/A#(N%,N%)
6880 FOR I% = 1 TO N%
6890 I1% = N% - I%
6900 XK# = 0#
6910 FOR J% = I% + 1 TO N%
6920 XK# = A#(I1%,J%) * CDBL(T(J%)) + XK#
6930 NEXT J%
6940 T(I1%) = CSNG(B#(I1%) - XK#)
6950 NEXT I%
6960 PRINT "T's ";T(1);T(2);T(3);T(4);T(5);T(6);T(7) :PRINT
6970 RETURN
6980
6990 SUB #9
7000 *****
7010 ***** CALCULATION OF FLOOR & ROOM TEMPS WITH NUMERICAL METHOD
7020 ***** AND OF HEAT TRANSFER INTO THE BUILDING
7030 *****
7040 ***** HEAT TRANSFER INTO AND THE OUT OF THE BUILDING IS CALCULATED IN THIS
7050 ***** SUBPROGRAM. THE EFFICIENCY OF THE COLLECTOR DURING THE DAYTIME IS
7060 ***** ALSO DETERMINED, SO IS THE ROOM AIR TEMPERATURE. THE PREVISION IS MADE
7070 ***** FOR THE NIGHT TIME HEAT CALCULATION. THE SUBROUTINE INCLUDES A
7080 ***** NUMERICAL PROCEDURE FOR DETERMINATION OF THE FLOOR TEMPERATURE, AS
7090 ***** WELL AS THE ROOM AIR TEMPERATURE. A SCHEME FOR SOLVING A TRIANGLE
7100 ***** MATRIX IS ALSO CODED HERE.
7110 IF SHUTDOWN% = 1 THEN T.EXIT=0!;T2(1)=0! :T2(2)=0! :T2(3)=0! :T2(4)=0!
:T4(1)=0! :T4(2)=0! :T4(3)=0! :T4(4)=0! :GOTO 7120
W1# = VF# * CDBL(PL*XF) : W2# = VB# * CDBL(PL*XB) : W# = W1# + W2#

```

```

7120 T.EXIT = TR + CSNG(W1#*(T(4) - TR)/W#) + CSNG(W2#*(T(2) - TR)/W#)
7130
7140 Q2 = CSNG(PNL%) * Q2 : T.M = (TR + T.EXIT)/2!
7150 IF (T.M+273!) < 260! THEN CP.AIR=FNC1.A(T.M+273!) ELSE CP.AIR=FNC2.A(T.M+273!)
7160 R.C = FNRO.A(T.M+273!) * CP.AIR
7170 IF SHUTDOWN% = 1 THEN ETA = 0! : Q1 = 0! : GOTO 7240
7180 Q1 = CSNG(LL%) * R.C * (CSNG(VF#) * XF + CSNG(VB#) * XB) * PL * (T.EXIT - TR)
7190 SUMI = SR(1,6) * S.COLL
7200 IF SUMI = 0! THEN ETA = 0! : GOTO 7220
7210 ETA = Q1/SUMI
7220
7230 Q.GAIN = Q1 + Q2
7240
7250 TR.NEW = TR0 + (DT*3600!) * (Q.GAIN - Q.LOSS)/(V#)
7260 PRINT " Q.LOSS ="; Q.LOSS; " Q.GAIN ="; Q.GAIN; " TR.NEW = PRINT
7270
7280 TFP#(NFLR%+1) = CDBL(TG)
7290 FAL# = CDBL(U1(1)) : FRMO# = EDBL(R.C*V/S(1))/DT.SEC#
7300 FAT# = CDBL(U.A/S(1))
7310 FB# = FAT#*CDBL(TA) + FRO#*CDBL(TFPO#) + CDBL(Q.GAIN/S(1))
7320 FRM# = FAT# + FRMO# + FAL#
7330 FBB#(1) = FRM# : FCC#(1) = -FAL# : FAA#(1) = 0#
7340 FDD#(1) = FB#
7350 LL% = NFLR%
7360 FOR FIX = 2 TO LL%
7370 IF FIX <> 2 THEN GOTO 7420
7380 FAL# = K.FLR#/DX.FLR# : FAPO# = ROCP.FLR# * DX.FLR#/(2#)
7390 FAU# = CDBL(U1(1)) : FB# = FAPO#*TFPO#(FIX)
7400 FAP# = FAU# + FAL# + FAPO#
7410 GOTO 7540
7420
7430 IF FIX = LL% THEN 7490
7440 FAU# = K.FLR#/DX.FLR# : FAL# = FAU#
7450 FAPO# = ROCP.FLR# * DX.FLR#/DT.SEC#
7460 FB# = FAPO# * TFPO#(FIX)
7470 FAP# = FAU# + FAL# + FAPO#

```

GOTO 7540

FAU# = K.FLR#/DX.FLR# :FAL# = 0#
FAPO# = ROCP.FLR# * DX.FLR#/DT.SEC#
FAP# = FAPO# * TFP#(FIX) + FAU# * TFP#(LL%+1)
FAP# = FAU# + FAU# + FAPO#

FAA#(FIX) = -FAU#
FBB#(FIX) = FAP#
FCC#(FIX) = -FAL#
FDD#(FIX) = FB#

NEXT FIX
FOR FIX = 1 TO LL%

PRINT" AA BB CC DD"

PRINT FAA#(FIX);FBB#(FIX);FCC#(FIX);FDD#(FIX)

NEXT FIX

FOLLOWING IS FOR SOLVING FOR THE TRIANGLE MATRIX

FBETA#(1) = FBB#(1) :FGMA#(1) = FDD#(1)/FBETA#(1)

FOR FIX = 2 TO LL%

FBETA#(FIX) = FBB#(FIX) - FAA#(FIX) * FCC#(FIX - 1) / FBETA#(FIX - 1)
FGMA#(FIX) = (FDD#(FIX) - FAA#(FIX) * FGMA#(FIX - 1)) / FBETA#(FIX)

NEXT FIX

TFP#(LL%) = FGMA#(LL%) :LAST% = LL% - 1

FOR FIX = 1 TO LAST%

FIX% = LL% - FIX

TFP#(FIX) = FGMA#(FIX) - FCC#(FIX) * TFP#(FIX + 1) / FBETA#(FIX)

NEXT FIX

TR0 = CSNG(TFP#(P))

FOR FIX = 1 TO LL%

TFPO#(FIX) = TFP#(FIX)

PRINT" T.FLR(;"FIX;") = ";TFP#(FIX)

NEXT FIX

PRINT" T.FLR(;"FIX;") = ";TFP#(LL%+1)

TR = CSNG(TFP#(1))

RETURN

7480
7490
7500
7510
7520
7530
7540
7550
7560
7570
7580
7590
7600
7610
7620
7630
7640
7650
7660
7670
7680
7690
7700
7710
7720
7730
7740
7750
7760
7770
7780
7790
7800
7810
7820
7830

```

7840 ' SUB #10 OUTPUT OF THE CALCULATED RESULTS
7850 '*****
7860 'THIS IS THE ROUTINE FOR PRINTING OUT THE CALCULATED RESULTS. THE
7870 'PRINT-OUT FOR THE CONVENTIONAL DESIGN IS MADE DIFFERENT FROM THE
7880 'TWO-PASS SYSTEM.
7890
7900 IF FB = 0! THEN 7960
7910 PRINT" OUTPUT IS "
7920 PRINT TIM, DI, TA, TRR, TR :PRINT
7930 WRITE #2, TIM, DI, TA, TRR, TR, T.TOP, T.EXIT, ETA.1, ETA
7950 GOTO 7980
7960
7970 WRITE #2, TIM, DI, TA, TRR, TR, T.TOP, T.EXIT, ETA.1, ETA
7980
7990 RETURN
8000 '*****
8010 ' SUB #11 DETERMINATION OF VARYING HEAT TRANSFER COEFFICIENTS FOR
8020 ' ONE-PASS & ONE-COVER SYSTEM
8030 '*****
8040 'THIS IS FOR THE CONVENTIONAL DESIGN COMPUTATION(i.e. FOR ONE-PASS IN
8050 'BACK OF THE ABSORBING PLATE). ONLY ONE-COVER SYSTEM IS TAKEN CARE
8060 'OF HERE.
8070
8080 TSKY = .0552 * (TA + 273!)^1.5
8090 TGRD = TA + 273!
8100 TAM = (FSKY * TSKY ^4 + FGRD * TGRD ^4)^.25
8110 HR.5A# = E5A#*SIGMA#*CDBL((TC+273!)^3 + (TC+273!)^2*TAM
      + (TC+273!)*TAM^2 + TAM^3)
8120 HR.53# = E53#*SIGMA#*CDBL((TC+273!)^3 + (TC+273!)^2*(TP+273!)
      + (TC+273!)*(TP+273!)^2 + (TP+273!)^3)
8130 HR.31# = E31#*SIGMA#*CDBL((TP+273!)^3 + (TP+273!)^2*(TI+273!)
      + (TP+273!)*(TI+273!)^2 + (TI+273!)^3)
8140 HR.A5# = HR.5A# :HR.35# = HR.53# :HR.13# = HR.31#
8150
8160 MU.AMB = FNMU.A(TA+273!) :RO.AMB = FNRO.A(TA+273!)
8170 IF (TA+273!)<300! THEN K.AMB=FNK}.A(TA+273!) ELSE K.AMB=FNK2.A(TA+273!)

```

```

8180 IF (TA+273!)<260! THEN CP.AMB=FNCP1.A * 1.1 ELSE CP.AMB=FNCP2.A*(TA+273!)
8190 IF ABS(WDIR)>270! THEN 8220
8200 LC = 2!* CL*CH/(CL + CH)
8210 HW# = .86# * CDBL(K.AMB) * RE# * 5 * CDBL(PR * 5/LC)
8220
8230 VC# = -3# + CDBL(.05*VWD)
8240 HW# = 18.625# * VC# ^ .605
8250
8260 T.RA = (TP + TC)/2! : BBB = 1/(T.RA + 273!)
8270 D.RA = MU.AMB * K.AMB/(RO.AMB * 2 * CP.AMB)
8280 RA = G * BBB * (TP - TC) * XF * 3/D.RA
8290 IF RA <= RA.C THEN 8350
8300 RA.COSFY = RA * COSFY
8310 YY1 = 1! - 1708!/RA.COSFY : YY2 = (RA.COSFY/5830!)^(1/3) - 1!
8320 YY1 = (ABS(YY1) + YY1)/2! : YY2 = (ABS(YY2) + YY2)/2!
8330 YY3 = 1! - (SIN(1.8*FY)) ^ 1.6 * 1708!/RA.COSFY
8340 NU.RA = 1! + 1.44 * YY1 * YY3 + YY2 : GOTO 8370
8350
8360 NU.RA = 1!
8370
8380 H34# = CDBL(NU.RA * K.AMB/XF) : H43# = H34#
8390 RETURN
8400 *****
8410 SUB #12 CALCULATION OF MATRIX COEFFICIENTS FOR ONE-PASS &
8420 ONE-COVER SYSTEM
8430 *****
8440 THIS SUBROUTINE IS ASSOCIATED WITH SUB #11. IT IS FOR DETERMINING
8450 THE MATRIX COEFFICIENTS FOR THE CONVENTIONAL DESIGN. THE HEAT
8460 TRANSFER COEFFICIENTS ARE COMPUTED IN THE PREVIOUS SUBPROGRAM.
8470
8480 A#(1,1) = (HR.31# + H21# + H1R#) * CDBL(DA)
8490 A#(1,3) = -HR.13# * CDBL(DA)
8500 B#(1) = H1R# * CDBL(DA*TR)
8510
8520 A#(2,2) = (H32# + H12#) * CDBL(DA) + QMSS2#
8530 A#(2,3) = -H23# * CDBL(DA) : A#(2,1) = A#(1,2) : A#(2,4) = 0#

```

```

8540 B#(2) = QMSS2# * CDBL(T2(II%-1))
8550
8560 Z1# = CDBL(RO.P * CP.P * X.P * DA) / CDBL(DT*3600!)
8570 Z2# = CDBL(A.P * K.P / DX)
8580 A#(3,3) = CDBL(DA) * (HR.53# + HR.31# + H43# + H23#) + Z1# + CDBL(V1) * Z2#
8590 A#(3,4) = -(HR.53# + H43#) * CDBL(DA)
8600 A#(3,2) = A#(2,3)
8610 B#(3) = CDBL(DA * AL.TA * SR(1,6)) + Z1# * CDBL(T3OLD(II%))
8620 B#(3) = B#(3) + Z2# * (T3OLD(II%-1) + T3OLD(II%+1))
8630
8640 QR5# = CDBL(AB.C1 * DA * SR(1,6)) 'DA = AREA OF SUBREGION(m^2)
8650 A#(4,4) = (HR.53# + HR.4# + HW# + HR.5A#) * CDBL(DA)
8660 A#(4,3) = A#(3,4) : A#(4,2) = 0# : A#(4,1) = 0#
8670 B#(4) = QR5# + HW# * CDBL(DA * TA) + HR.5A# * CDBL(DA * (TAM-273!))
8680
8690 'FOR JX = 1 TO NX
8700 'PRINT "A'S"; A#(1,JX); A#(2,JX); A#(3,JX), A#(4,JX)
8710 'NEXT JX :PRINT
8720 'PRINT "B'S"; B#(1); B#(2); B#(3); B#(4) :PRINT
8730 RETURN
8740 '*****
8750 'SUB #13 DETERMINATION OF VARYING HEAT TRANSFER COEFFICIENTS FOR
8760 'TWO-PASS & TWO-COVER SYSTEM
8770 '*****
8780 'TWO-COVER-TWO-PASS SYSTEM IS DEALT WITH IN THIS SUBROUTINE AND NEXT
8790 'SUBROUTINE. THE SIMILAR CALCULATION STEPS ARE TAKEN.
8800
8810 TSKY = .0552 * (TA + 273!) ^ 1.5
8820 TGRD = TA + 273!
8830 TAM = (FSKY * TSKY ^ 4 + FGRD * TGRD ^ 4) ^ .25
8840 HR.6A# = E5A# * SIGMA# * CDBL((TC2+273!) ^ 3 + (TC2+273!) ^ 2 * TAM
+ (TC2+273!) * TAM ^ 2 + TAM ^ 3)
8850 HR.65# = E65# * SIGMA# * CDBL((TC1+273!) ^ 3 + (TC1+273!) ^ 2 * (TC2+273!)
+ (TC1+273!) * (TC2+273!) ^ 2 + (TC2+273!) ^ 3)
8860 HR.53# = E53# * SIGMA# * CDBL((TC1+273!) ^ 3 + (TC1+273!) ^ 2 * (TP+273!)
+ (TC1+273!) * (TP+273!) ^ 2 + (TP+273!) ^ 3)

```

```

8870 HR.31# = E31#*SIGMA#CDBL((TP+273!)^3 + (TP+273!)^2*(TI+273!)
+ (TP+273!)*(TI+273!)^2 + (TI+273!)^3)
8880 HR.A6# = HR.6A# :HR.56# = HR.65# :HR.35# = HR.53# :HR.13# = HR.31#
8890
8900 MU.AMB = FNMU.A(TA+273!) :RO.AMB = FNRO.A(TA+273!)
8910 IF (TA+273!)<300! THEN K.AMB=FNK1.A(TA+273!) ELSE K.AMB=FNK2.A(TA+273!)
8920 IF (TA+273!)<260 THEN CP.AMB=FNCP1.A(TA+273!) ELSE CP.AMB=FNCP2.A(TA+273!)
8930 IF ABS(WD) > 270! THEN 8960
8940 LC = 2! * CL / (CL + CH) :RE# = CDBL(VWD * LC * RO.AMB/MU.AMB)
8950 HW# = .86#*CDBL(K.AMB)*RE#*.5*CDBL(PR^.5/LC) :GOTO 8990
8960
8970 VC# = .3# * CDBL(.05*VWD)
8980 HW# = 18.625# * VC#^.605
8990
9000 T.RA = (TC1 + TC2)/2 :BBB = 1/(T.RA + 273!)
9010 D.RA = MU.AMB * K.AMB/(RO.AMB^2 * CP.AMB)
9020 RA = G * BBB * (TC1 - TC2) * XC1^3/D.RA
9030 IF RA <= RA.C THEN 9090
9040 RA.COSFY = RA * COSFY
9050 YY1 = 1! - 1708!/RA.COSFY :YY2 = (RA.COSFY/5830!)^(1/3) - 1!
9060 YY1 = (ABS(YY1) + YY1)/2! :YY2 = (ABS(YY2) + YY2)/2!
9070 YY3 = 1! - (SIN(1.8*FY))*.1.6*1708!/RA.COSFY
9080 NU.RA = 1! + 1.44 * YY1 * YY2 + YY3 :GOTO 9110
9090
9100 NU.RA = 1!
9110
9120 H65# = CDBL(NU.RA * K.AMB/XC1) :H56# = H65#
9130 RETURN
9140 *****
9150 SUB #14 CALCULATION OF MATRIX COEFFICIENTS FOR TWO-PASS AND
9160 TWO-COVER SYSTEM
9170 *****
9180 THIS IS FOR TWO-COVER AND TWO-PASS SYSTEMS AS INDICATED IN SUB #13.
9190
9200 A#(1,1) = (HR.31# + H21# + H1R#) * CDBL(DA)
9210 A#(1,6) = 0# :A#(1,5) = 0# :A#(1,4) = 0#

```

```

9220 A#(1,3) = -HR.13# * CDBL(DA) :A#(1,2) = -H12# * CDBL(DA)
9230 B#(1) = H1R# * CDBL(DA*TR)
9240
9250 A#(2,2) = (H32# + H12#) * CDBL(DA) + QMSS2#
9260 A#(2,6) = 0# :A#(2,5) = 0# :A#(2,4) = 0#
9270 A#(2,3) = -H23# * CDBL(DA) :A#(2,1) = A#(1,2)
9280 B#(2) = QMSS2# * CDBL(T2(II%-1))
9290
9300 Z1# = CDBL(RQ.P * CP.P * X.P * DA) / CDBL(DT*3600!)
9310 Z2# = CDBL(A.P * K.P / DX)
9320 A#(3,3) = CDBL(DA) * (HR.53# + HR.31# + H43# + H23#) + Z1# + CDBL(V1)*Z2#
9330 A#(3,5) = -HR.53# * CDBL(DA) :A#(3,4) = -H43# * CDBL(DA)
9340 A#(3,2) = A#(2,3) :A#(3,1) = A#(1,3) :A#(3,6) = 0#
9350 B#(3) = CDBL(DA * AL.TA * SR(1,6)) + Z1# * CDBL(T3OLD(II%))
9360 B#(3) = B#(3) + Z2# * (T3OLD(II%-1) + T3OLD(II%+1))
9370
9380 A#(4,4) = (H54# + H34#) * CDBL(DA) + QMSS1#
9390 A#(4,5) = -H45# * CDBL(DA) :A#(4,3) = A#(3,4)
9400 A#(4,6) = 0# :A#(4,2) = 0# :A#(4,1) = 0#
9410 B#(4) = QMSS1# * CDBL(T4(II%-1))
9420
9430 QR5# = CDBL(AB.C1 * DA * SR(1,6))
9440 A#(5,5) = (HR.53# + H54# + H65# + HR.65#) * CDBL(DA)
9450 A#(5,6) = -(H65# + HR.65#) * CDBL(DA)
9460 A#(5,4) = A#(4,5) :A#(5,3) = A#(3,5)
9470 A#(5,2) = 0# :A#(5,1) = 0#
9480 B#(5) = QR5#
9490
9500 QR6# = CDBL(AB.C2 * DA * SR(1,6))
9510 A#(6,6) = (HR.56# + H56# + HW# + HR.6A#) * CDBL(DA)
9520 A#(6,5) = A#(5,6) :A#(6,4) = 0# :A#(6,3) = 0# :A#(6,2) = 0# :A#(6,1) = 0#
9530 B#(6) = QR6# + HW# * CDBL(DA*TA) + HR.6A# * CDBL(DA*(TAM-273!))
9540
9550 'FOR JX = 1 TO N
9560 ' PRINT A#(1,JX);A#(2,JX);A#(3,JX);A#(4,JX);A#(5,JX);A#(6,JX)
9570 'NEXT JX

```

```

9580 'PRINT' B'S'; B#(1); B#(2); B#(3); B#(4); B#(5); B#(6) :PRINT
9590 RETURN
9600 *****
9610 'SUB #15 DETERMINATION OF VARYING HEAT TRANSFER COEFFICIENTS FOR
9620 TWO-PASS AND THREE-COVER SYSTEM
9630 *****
9640 'THIS AND NEXT SUBROUTINES ARE DEALING WITH THREE-COVER AND TWO-PASS
9650 SYSTEMS. TIME NEEDED FOR THE CALCULATION IS LONGER WHEN MORE COVERS
9660 ARE PUT ON. THE COVERS ARE ASSUMED MADE OF SAME MATERIAL.
9670 *****
9680 TSKY = .0552 * (TA + 2731) ^ 1.5
9690 TGRD = TA + 2731
9700 TAM = (FSKY * TSKY ^ 4 + FGRD * TGRD ^ 4) ^ .25
9710 HR.7A# = E5A# * SIGMA# * CDBL((TC3+2731) ^ 3 * (TC3+2731) ^ 2 * TAM
+ (TC3+2731) * TAM ^ 2 + TAM ^ 3)
9720 HR.76# = E65# * SIGMA# * CDBL((TC2+2731) ^ 3 + (TC2+2731) ^ 2 * (TC3+2731)
+ (TC2+2731) * (TC3+2731) ^ 2 + (TC3+2731) ^ 3)
9730 HR.65# = E65# * SIGMA# * CDBL((TC1+2731) ^ 3 + (TC1+2731) ^ 2 * (TC2+2731)
+ (TC1+2731) * (TC2+2731) ^ 2 + (TC2+2731) ^ 3)
9740 HR.53# = E53# * SIGMA# * CDBL((TC1+2731) ^ 3 + (TC1+2731) ^ 2 * (TP+2731)
+ (TC1+2731) * (TP+2731) ^ 2 + (TP+2731) ^ 3)
9750 HR.31# = E31# * SIGMA# * CDBL((TP+2731) ^ 3 + (TP+2731) ^ 2 * (TI+2731)
+ (TP+2731) * (TI+2731) ^ 2 + (TI+2731) ^ 3)
9760 HR.A7# = HR.7A# : HR.67# = HR.76# : HR.56# = HR.65# : HR.35# = HR.53# : HR.13# = HR.31#
9770
9780 MU.AMB = FNMU.A(TA+2731) : RO.AMB = FNRO.A(TA+2731)
9790 IF (TA+2731) < 3001 THEN K.AMB = FNK1.A(TA+2731) ELSE K.AMB = FNK2.A(TA+2731)
9800 IF (TA+2731) < 260 THEN CP.AMB = FNCPI.A(TA+2731) ELSE CP.AMB = FNCPI.A(TA+2731)
9810 IF ABS(WDIR) > 270 THEN 9840
9820 LC = 21 * CL * CH / (CL + CH) : RE# = CDBL(VWD * LC * RO.AMB / MU.AMB)
9830 HW# = .86# * CDBL(K.AMB) * RE# ^ .5 * CDBL(PR ^ .5 / LC) : GOTO 9870
9840
9850 VC# = .3# + CDBL(.05 * VWD)
9860 HW# = 18.625# * VC# ^ .605
9870
9880 T.RA = (TC1 + TC2) / 21 : BBB = 1 / (T.RA + 2731)

```

```

9890 D.RA = MU.AMB * K.AMB / (RO.AMB ^ 2 * CP.AMB)
9900 RA = G * BBB * (TC1 - TC2) * XC1 ^ 3 / D.RA
9910 IF RA <= RA.C THEN 9970
9920 RA.COSFY = RA * COSFY
9930 YY1 = 1! - 1708! / RA.COSFY : YY2 = (RA.COSFY / 5830!) ^ (1/3) - 1!
9940 YY1 = (ABS(YY1) + YY1) / 2! : YY2 = (ABS(YY2) + YY2) / 2!
9950 YY3 = 1! - (SIN(1.8 * FY)) ^ 1.6 * 1708! / RA.COSFY
9960 NU.RA = 1! + 1.44 * YY1 * YY3 + YY2 : GOTO 9990
9970
9980 NU.RA = 1!
9990

```

```

10000 H65# = CDBL(NU.RA * K.AMB / XC1) : H56# = H65#
10010 T.RA = (TC2 + TC3) / 2! : BBB = 1 / (T.RA + 273!)
10020 D.RA = MU.AMB * K.AMB / (RO.AMB ^ 2 * CP.AMB)
10030 RA = G * BBB * (TC2 - TC3) * XC1 ^ 3 / D.RA
10040 IF RA <= RA.C THEN 10100
10050 RA.COSFY = RA * COSFY
10060 YY1 = 1! - 1708! / RA.COSFY : YY2 = (RA.COSFY / 5830!) ^ (1/3) - 1!
10070 YY1 = (ABS(YY1) + YY1) / 2! : YY2 = (ABS(YY2) + YY2) / 2!
10080 YY3 = 1! - (SIN(1.8 * FY)) ^ 1.6 * 1708! / RA.COSFY
10090 NU.RA = 1! + 1.44 * YY1 * YY3 + YY2 : GOTO 10120
10100

```

```

10110 NU.RA = 1!
10120
10130 H76# = CDBL(NU.RA * K.AMB / XC2) : H67# = H76#
10140 RETURN
10150 *****
10160 SUB #16 CALCULATION OF MATRIX COEFFICIENTS FOR TWO-PASS AND
10170 THREE-COVER SYSTEM
10180 *****
10190 THIS IS FOR THREE-COVER AND TWO-PASS SYSTEMS.
10200

```

```

10210 A#(1,1) = (HR.31# + H2.1# + H1R#) * CDBL(DA)
10220 A#(1,7) = 0# : A#(1,6) = 0# : A#(1,5) = 0# : A#(1,4) = 0#
10230 A#(1,3) = -HR.13# * CDBL(DA) : A#(1,2) = -H12# * CDBL(DA)
10240 B#(1) = H1R# * CDBL(DA * TR)

```

10250 A#(2,2) = (H32# + H12#) * CDBL(DA) + QMSS2#
 10260 A#(2,7) = 0# :A#(2,6) = 0# :A#(2,5) = 0# :A#(2,4) = 0#
 10270 A#(2,3) = -H23# * CDBL(DA) :A#(2,1) = A#(1,2)
 10280 B#(2) = QMSS2# * CDBL(T2(II%-1))
 10300
 10310 Z1# CDBL(RO.P * CP.P * X.P * DA) / CDBL(DT*3600!)
 10320 Z2# = CDBL(A.P * K.P / DX)
 10330 A#(3,3) = CDBL(DA) * (HR.53# + HR.31# + H43# + H23#) * Z1# + CDBL(V1) * Z2#
 10340 A#(3,5) = -HR.53# * CDBL(DA) :A#(3,4) = -H43# * CDBL(DA)
 10350 A#(3,2) = A#(2,3) :A#(3,1) = A#(1,3) :A#(3,6) = 0# :A#(3,7) = 0#
 10360 B#(3) = CDBL(DA * AL.TA * SR(1,6)) + Z1# * CDBL(T3OLD(II%))
 10370 B#(3) = B#(3) + Z2# * (T3OLD(II%-1) + T3OLD(II%+1))
 10380
 10390 A#(4,4) = (H54# + H34#) * CDBL(DA) + QMSS1#
 10400 A#(4,5) = -H45# * CDBL(DA) :A#(4,3) = A#(3,4)
 10410 A#(4,7) = 0# :A#(4,6) = 0# :A#(4,2) = 0# :A#(4,1) = 0#
 10420 B#(4) = QMSS1# * CDBL(T4(II%-1))
 10430
 10440 QR5# = CDBL(AB.C1 * DA * SR(1,6))
 10450 A#(5,5) = (HR.53# + H54# + H65# + HR.65#) * CDBL(DA)
 10460 A#(5,6) = -(H65# + HR.65#) * CDBL(DA)
 10470 A#(5,4) = A#(4,5) :A#(5,3) = A#(3,5)
 10480 A#(5,2) = 0# :A#(5,1) = 0# :A#(5,7) = 0#
 10490 B#(5) = QR5#
 10500
 10510 QR6# = CDBL(AB.C2 * DA * SR(1,6))
 10520 A#(6,6) = (HR.56# + H56# + H76# + HR.76#) * CDBL(DA)
 10530 A#(6,5) = A#(5,6) :A#(6,7) = -(H76# + HR.67#) * CDBL(DA)
 10540 A#(6,4) = 0# :A#(6,3) = 0# :A#(6,2) = 0# :A#(6,1) = 0#
 10550 B#(6) = QR6#
 10560
 10570 QR7# = CDBL(AB.C3 * DA * SR(1,6))
 10580 A#(7,7) = (HR.76# + H76# + HW# + HR.7A#) * CDBL(DA)
 10590 A#(7,6) = A#(6,7) :A#(7,5) = 0# :A#(7,4) = 0# :A#(7,3) = 0#
 10600 A#(7,2) = 0# :A#(7,1) = 0#

```
10610 B#(7) = QR7# + HW#*CDBL(DA*TA) + HR.7A#*CDBL(DA*(TAM-273!))
10620
10630 'FOR J% = 1 TO N%
10640 ' PRINT"A'S";A#(1,J%);A#(2,J%);A#(3,J%);A#(4,J%);A#(5,J%);A#(6,J%);A#(7,J%)
10650 'NEXT J% :PRINT
10660 'PRINT"B'S"; B#(1); B#(2); B#(3); B#(4); B#(5); B#(6); B#(7) :PRINT
10670 RETURN
```

APPENDIX B.3: FORMAT OF INPUT FILE #1 FOR THE ACTIVE SYSTEM MODEL

BL (m)	BH (m)	BW1 (m)	BW2 (m)	V _z (m ³)	TAU
14.64	4.88	9.76	5.62	549.3	0.85
CL (m)	CH (m)	XF (m)	XB (m)	XFLR	
13.42	4.27	0.0635	0.0508	0.203	
LG (deg.)	LT (deg.)	STM (deg.)	CF		
113.5	53.4	105	0.1		
U(1)	U(2)	U(3)	U(4)	U(5)	U(6)
0.0	0.280	0.133	0.255	0.278	12.5
S(1)	S(2)	S(3)	S(4)	S(5)	S(6)
142.89	70.34	21.48	83.00	73.78	70.34
E(1)	E(2)	E(3)	E(4)	E(5)	
0.60	0.70	0.95	0.63	0.63	
E1(1)	E1(2)	E1(3)	E1(4)	E1(5)	E1(6)
0.80	0.80	0.80	0.80	0.80	0.80
AB(1)	AB(2)	AB(3)	AB(4)	AB(5)	AB(6)
0.85	0.85	0.85	0.85	0.85	0.02
BETA(1)	BETA(2)	BETA(3)	BETA(4)	BETA(5)	BETA(6)
0.0	113.0	90.0	0.0	90.0	67.0
K.P	CP.P	RO.P	X.P		
221.44	896.0	2739.4	0.003		
SAZM(1,1)	SAZM(1,2)	SAZM(1,3)	SAZM(1,4)	SAZM(1,5)	SAZM(1,6)
0.0	180.0	-90.0	0.0	90.0	0.0

SAZM(2,1)	SAZM(2,2)	SAZM(2,3)	SAZM(2,4)	SAZM(2,5)	SAZM(2,6)
0.0	0.0	0.0	0.0	-90.0	180.0
F(1,1)	F(1,2)	F(1,3)	F(1,4)	F(1,5)	F(1,6)
0.0	0.3	0.11	0.18	.11	0.3
F(2,1)	F(2,2)	F(2,3)	F(2,4)	F(2,5)	F(2,6)
0.522	0.0	0.075	0.216	0.075	0.138
F(3,1)	F(3,2)	F(3,3)	F(3,4)	F(3,5)	F(3,6)
0.33	0.195	0.0	0.21	0.07	0.195
F(4,1)	F(4,2)	F(4,3)	F(4,4)	F(4,5)	F(4,6)
0.313	0.204	0.14	0.0	0.14	0.204
F(5,1)	F(5,2)	F(5,3)	F(5,4)	F(5,5)	F(5,6)
0.33	0.195	0.075	0.21	0.0	0.195
F(6,1)	F(6,2)	F(6,3)	F(6,4)	F(6,5)	F(6,6)
0.522	0.138	0.075	0.216	0.075	0.0

NR
7

C1(0)	C2(0)	C3(0)
0.000000	0.555389	1.000000
C1(1)	C2(1)	C3(1)
0.000008	-1.346055	-2.414203
C1(2)	C2(2)	C3(2)
0.000203	1.136764	2.030093
C1(3)	C2(3)	C3(3)
0.000607	-0.394896	-0.701659

C1(4)	0.000381	C2(4)	0.052085	C3(4)	0.091903
C1(5)	0.000056	C2(5)	-0.002047	C3(5)	-0.003565
C1(6)	0.000002	C2(6)	0.000017	C3(6)	0.000028
C1(7)	0.000000	C2(7)	-0.000000	C3(7)	-0.000000

DD 21 MM 12 YY 1985

TG 5.0 T.INI 0.0 T.FX 10.0

DT 0.25 FINTIM 48.0 PRTIM 0.25 TIM 0.0

APPENDIX B.4: A SAMPLE OF OUTPUT FILE FROM THE ACTIVE SYSTEM MODEL

XXXXXXXXXXXXXXXXX OUTPUT OF THE SIMULATION RUN XXXXXXXXXXXXXXXXXXXXXXXX

BUILDING LENGTH ----- 14.64 (m)
 BUILDING HEIGHT ----- 4.88 (m)
 BUILDING BOTTOM WIDTH ----- 9.76 (m)
 BUILDING TOP WIDTH ----- 5.62 (m)
 TOTAL VOLUME OF THE BUILDING -- 549.3 (m^3)
 COLLECTOR PANEL LENGTH ----- .61 (m)
 COLLECTOR PANEL HEIGHT ----- 4.27 (m)
 NUMBER OF PANELS USED ----- 22
 FRONT-PASS SPACING ----- .0635 (m)
 BACK-PASS SPACING ----- .0508 (m)
 TRANSMITTANCE OF COVER GLAZING ----- .946
 FLOW RATE PER PANEL ----- .054229 (m^3/sec)
 NUMBER OF SUBDIVISION ----- 4
 LENGTH OF EACH SUBREGION ----- 1.0675 (m)
 CLOUDINESS FACTOR ----- .1
 GROUND TEMPERATURE ----- 5 (C)
 INITIAL TEMPERATURE ASSUMED ----- 5 (C)
 TOTAL TIME FOR THE RUN ----- 96 (hrs)
 PRINTING INTERVAL ----- .25 (hrs)
 STARTING TIME FOR THE RUN ----- 0 (hrs)
 TIME INCREMENT ----- .25 (hrs)

INFORMATION ON WALL COMPONENTS

U1(I%) W/(m^2.C)	S(I%) m^2	E(I%) E(I%)	E1(I%)	AB(I%)	BETA(I%) DEG.
.505	142.89	.6	.8	.85	0
.28	70.34	.7	.8	.85	113

.133	21.48	.95	.8	.85	90
.255	83	.63	.8	.85	0
.278	73.78	.63	.8	.85	90
.27263	70.34	0	.8	.02	67

ANGLE FACTORS OF INTERIOR WALL SURFACES

F(I%,1)	F(I%,2)	F(I%,3)	F(I%,4)	F(I%,5)	F(I%,6)
0	.3	.11	.18	.11	.3
.522	0	.075	.216	.075	.138
.33	.195	0	.21	.07	.195
.313	.204	.14	0	.14	.204
.33	.195	.075	.21	0	.195
.522	.138	.075	.216	.075	0

SURFACE AZIMUTH

I%	SAZM(1,I%) DEG.	SAZM(2,I%) DEG.
1	0	0
2	180	0
3	-90	90
4	0	0
5	90	-90
6	0	180

RESPONSE FACTORS FOR FLOOR SLAB

--

IX	C1(IX)	C2(IX)	C3(IX)
0	0	.55389	1
1	.000008	-1.346055	-2.414203
2	.000203	1.136764	2.030093
3	.000607	-.394896	-.701659
4	.000381	.052085	.091903
5	.000056	-.002047	-.003565
6	.000002	.000017	.000028
7	0	0	0

TOP-OF-STACK THERMAL PROPERTIES

# COVERS (n)	REFL. (Rn)	TRANSM. (Tn)	ABSORPTANCE (An)
0	.05	0	.95
1	7.8803E-02	.9476109	2.094761E-02

WITHIN-STACK ABSORPTANCE

# COVERS	ABSORPTANCE
0	.9002304
1	2.094761E-02

=== PRANDTL NUMBER CALCULATED IS .7155308
 === AIR VELOCITY IN FRONT IS .6 (m/sec)
 === AIR VELOCITY IN BACK IS 1 (m/sec)
 === REYNOLDS NUMBER FOR AIR IN FRONT-PASS IS 5547.301392304944

=== REYNOLDS NUMBER FOR AIR IN BACK-PASS IS 7396.4013671875
=== MEAN NUSSELT NUMBER FOR AIR IN FRONT IS 15.62868796965546
=== MEAN NUSSELT NUMBER FOR AIR IN BACK IS 19.67313214987617

===== START OF ONE NEW DAY =====

LOCATION: 113.5 DEGREE LONGITUDE
53.4 DEGREE NORTH LATITUDE
STANDARD TIME MERIDIAN = 105 DEGREE
SOLAR DECLINATION(DELTA) = -23.42229 DEGREE
EQUATION OF TIME(ET) = 2.272399 MINUTES

@@@ DATE (MON/DAY/YR): 12 / 21 / 1985.

DAY OF THE YEAR: 355

SUNRISE TIME: 8.907685 HOURS

SUNSET TIME : 16.1499 HOURS

	1	2	3	4	5	6	7	8	9					
TIM, DI, TA, TRR, TR, T.TOP, T.EXIT, ETA.1, ETA	0,0,5.596,3.9595,5,4.7515,0,0,0	.25,0,5.477,3.925,.9050495,4.741,0,0,0	.5,0,5.626,3.9865,.9116064,4.677,0,0,0	.75,0,5.709,3.948,.9179779,4.752,0,0,0	1,0,6.109,3.9545,.9550841,4.7455,0,0,0	1.25,0,5.583,4.0315,.9035384,4.7205,0,0,0	1.5,0,5.491,3.888,.8936274,4.6655,0,0,0	1.75,0,5.76,3.8465,.9185212,4.608,0,0,0	2,0,5.36,3.9255,.8793339,4.588,0,0,0	2.25,0,4.658,3.784,.8111135,4.5475,0,0,0	2.5,0,4.313,3.6635,.7771574,4.408,0,0,0	2.75,0,4.429,3.67,.787535,4.3585,0,0,0	3,0,5.718,3.6285,.9106087,4.349,0,0,0	3.25,0,5.955,3.7105,.9329844,4.3535,0,0,0

1.25,0,3.376,3.86,.6810907,4.541,0,0,0
 1.5,0,3.182,3.8205,.6621175,4.377,0,0,0
 1.75,0,2.942,3.7725,.6387222,4.367501,0,0,0
 2,0,2.91,3.609,.6352947,4.283,0,0,0
 . . .
 . . .
 . . .

===== TERMINATION OF THIS RUN =====

U

h

**APPENDIX C.1: SPECIFICATIONS OF TWO FLAT-PLATE COLLECTORS
BUILT BY ALBERTA AGRICULTURE**

absorber	0.475 mm (28 ga.) galvanized sheet metal primed and painted flat black
glazing	Tedlar 400 SE film
insulation	back and sides: 25.4 mm Thermax with RSI=1.4104
dimension	1.22 m x 2.44 m x 0.267 m
spacing of air channel	19 mm
installation inclination	70° from horizontal
air flow pattern	below the absorbing plate

The two collectors were made of the same materials with the same dimensions. For the double-glazed collector, the spacing between the two covers is 19 mm, and air is to flow below the absorbing plate as well.